

**Characterisation of *Plasmodium falciparum*
merozoite Apical Membrane Antigen-1 protein
changes prior to erythrocyte invasion**

By
Sarita Louise Downing

A dissertation submitted in fulfilment of the requirements for the degree

Magister Scientiae

in

Pharmacology

in the

Faculty of Health Sciences at the University of Pretoria

Supervisor

Prof AD Cromarty

Co-supervisor

Dr. S Stoychev

2016



UNIVERSITEIT VAN PRETORIA
UNIVERSITY OF PRETORIA
YUNIBESITHI YA PRETORIA

Acknowledgements

I would like to thank my supervisors, Prof. Duncan Cromarty and Dr. Stoyan Stoychev. I am sincerely grateful for all your guidance and support throughout this project.

To Prof. Robin Anders of La Trobe University Australia, thank you for your generous donation of the *PfAMA-1* antibody.

To Prof. Lynn-Marie Birkholtz and all the students of the Biochemistry Department of the University of Pretoria, thank you for welcoming me into your lab. I am truly grateful for the use of your labs and for all the kindness and patience you all showed me when assisting me in the lab.

A kind thank you to Alan Hall and Antoinette Buys for their assistance on the Confocal and TEM microscopes, and to all the staff at the Laboratory of Microscopy and Microanalysis of the University of Pretoria, thank you for always being so friendly.

To the staff and students of the Pharmacology Department of the University of Pretoria and the Biosciences Department of the CSIR, thank you for all the support along the way.

To my family, at home and across the globe, thank you for all the love and support. Daddy and Mammy, I cannot thank you enough for all the loving encouragement and support you have both given me.

To my friends, thank you all so much for all the love and support. I truly appreciate each prayer and hug throughout. To my dearest and wisest friend, Veronica, thank you for all the wise advice and your sincere prayers.

Thank you God for this incredible experience and each person I have learnt from. For Your faithfulness and steadfast love.

‘With God all things are possible.’

Matthew 19:26

Table of contents

Declaration	vi
Abstract	vii
List of Figures	ix
List of Tables	xv
Abbreviations	xvi
Chapter 1: Literature Review	1
1.1 Introduction	1
1.1.1 <i>What is Malaria?</i>	1
1.1.2 <i>Areas of Infection and Populations Affected</i>	2
1.1.3 <i>Clinical Manifestations</i>	3
1.1.4 <i>The Life Cycle</i>	3
1.1.5 <i>Treatment Regime</i>	5
1.2 The Merozoite and Apical Membrane Antigen-1 Protein	7
1.2.1 <i>Merozoite egression from the Erythrocyte</i>	7
1.2.2 <i>Merozoite Invasion of the Erythrocyte</i>	9
1.2.3 <i>The Apical Membrane Antigen-1 Protein</i>	10
(a) <i>Function, Importance and Future of PfAMA-1</i>	10
(b) <i>Type of Protein and Structure</i>	11
(c) <i>Proteolytic Processing</i>	12
1.3 Methods Used for Visualisation of Merozoites and Identification and Isolation of PfAMA-1	13
1.3.1 <i>Visualisation Methods</i>	13
1.3.2 <i>Protein Identification and Isolation Methods</i>	15
1.4 Study Outline	19
1.4.1 <i>Aim</i>	19
1.4.2 <i>Objectives</i>	19
Chapter 2: Materials and Methods	20
2.1 Culturing of Plasmodium falciparum parasites	20
2.1.1 <i>Erythrocytes and Strain of P. falciparum</i>	20
2.1.2 <i>In vitro Conditions</i>	20



2.1.3	<i>Parasitemia</i>	21
2.1.4	<i>Washing of Erythrocytes</i>	22
2.1.5	<i>Working Sterile</i>	22
2.1.6	<i>Sorbitol Synchronisation of a Non-Homogeneous 3D7 Culture</i>	23
2.1.7	<i>Isolation of Synchronised Cultures</i>	23
	(a) <i>Preparation of the MAC Column</i>	23
	(b) <i>Isolation of Late Stage Trophozoites</i>	24
	(c) <i>Isolation of Merozoites</i>	25
2.2	<i>Visualisation of Merozoite Maturation and Merozoite-Erythrocyte Invasion Sequence</i>	26
2.2.1	<i>Isolation of Schizonts and Merozoites</i>	26
2.2.2	<i>Fixation of Merozoites Invading Erythrocytes</i>	26
2.2.3	<i>Dehydration</i>	27
2.2.4	<i>Polymerisation</i>	27
2.2.5	<i>Preparation of the Copper Disc</i>	27
2.2.6	<i>Visualisation</i>	27
2.3	<i>Visualisation of Fluorescently Labelled PfAMA-1 of Merozoites</i>	28
2.3.1	<i>Fluorescent Labelling of PfAMA-1 Antibody</i>	28
2.3.2	<i>Fluorescent Labelling of Merozoites</i>	28
	(a) <i>Isolation of Merozoites</i>	28
	(b) <i>Preparation of Cover Slips for Confocal Microscopy</i>	28
	(i) <i>Acid wash</i>	28
	(ii) <i>Lysine Coating</i>	28
	(iii) <i>Fixation</i>	29
	(iv) <i>Blocking and Ab Labelling</i>	29
	(v) <i>DAPI Staining</i>	29
	(vi) <i>Visualisation</i>	29
2.4	<i>Proteomic Analysis of 3D7 Merozoites</i>	30
2.4.1	<i>SDS-PAGE</i>	30
2.4.2	<i>Western Blotting</i>	31
	(a) <i>Protein Transfer</i>	31
	(b) <i>Blocking of Membrane</i>	31
	(c) <i>Binding of Ab</i>	31



(d) <i>Visualisation</i>	32
2.4.3 <i>In-gel Digestion</i>	32
(a) <i>De-staining of Bands</i>	32
(b) <i>Reduction and Alkylation</i>	33
(c) <i>Trypsin Digestion</i>	33
(d) <i>Extraction of Peptides</i>	33
2.4.4 <i>In-solution Digestion</i>	34
(a) <i>Acetone Precipitation</i>	34
(b) <i>Reduction and Alkylation</i>	34
(c) <i>Trypsin Digestion</i>	35
(d) <i>C18 Digest Sample Clean-up</i>	35
2.4.5 <i>LC-MS/MS</i>	36
Chapter 3: Results and Discussion	38
3.1 <i>Isolation of Highly Synchronised Parasite Cultures</i>	38
3.1.1 <i>Culturing Parameters for Synchronised Cultures of 3D7s</i>	38
3.1.2 <i>Isolation of Merozoites</i>	43
3.2 <i>Visualisation of Plasmodium falciparum Merozoites</i>	47
3.2.1 <i>TEM of Merozoite Maturation and Merozoite-Erythrocyte Invasion Sequence</i>	47
3.2.2 <i>Confocal Microscopy of Fluorescently Labelled PfAMA-1 of Merozoites</i>	55
3.3 <i>Proteomic Analysis of 3D7 Merozoites</i>	58
Chapter 4: Conclusion	80
Chapter 5: References	83
Appendices	91
Appendix I	91
Appendix II	93
Appendix III	97
Appendix IV	102

Declaration

University of Pretoria

Faculty of Health Sciences

Department of Pharmacology

I, Sarita Louise Downing,

Student number: 24051129

Subject of the work: Characterisation of *Plasmodium falciparum* merozoite apical membrane antigen-1 protein changes prior to erythrocyte invasion.

1. I understand what plagiarism entails and am aware of the University's policy in this regard.
2. I declare that this dissertation is my own original work. Where someone else's work was used (whether from a printed source, the internet or any other source) due acknowledgement was given and reference was made according to departmental requirements.
3. I did not make use of another student's previous work and submitted it as my own.
4. I did not allow and will not allow anyone to copy my work with the intention of presenting it as his or her own work.

Signature: _____

Date: _____

Abstract

Malaria is a global pandemic that affects millions of people each year. It is a parasitic infection caused by the *Plasmodium* family, with *Plasmodium falciparum* being the most virulent strain. Malaria is transmitted to humans by the female *Anopheles* mosquito. The parasite undergoes two different cycles of its life cycle within the human host: the liver and intraerythrocytic life cycle. The latter consists of an asexual and sexual cycle. The intraerythrocytic cycle is perhaps the most important stage of the parasite's life cycle as it promotes the spread of the disease within and between hosts. The focus of this investigation was aimed at the invasion process of the merozoites into the erythrocytes. The *Plasmodium* merozoite utilises a cascade of proteins during the erythrocyte invasion process, which is a swift action that takes place in approximately 30 seconds. A number of surface proteins are expressed during merozoite development and are distributed along the merozoite surfaces to assist with attachment and invasion, the most crucial being MSP-1, AMA-1 and RON-2. MSP-1 and AMA-1 are vital targets for the development of malaria vaccines.

AMA-1 is the central target protein of this investigation as it plays an essential role in the invasion process. AMA-1 commits the merozoite to invade the erythrocyte, as it assists the RON proteins in the formation of an irreversible tight-junction with the membrane of the erythrocyte. Antibodies, specific to AMA-1, bind to the protein, which prevents the formation of the tight junction and inhibits the invasion of the merozoite into the erythrocyte, therefore preventing the spread of the disease.

However, before invasion, AMA-1 undergoes a number of proteolytic processes. It is synthesized as an 83 kDa (AMA-1₈₃) precursor protein in the apical organelle of the merozoite. This is then cleaved at the N-terminus to give rise to a 66 kDa (AMA-1₆₆) fragment, which is secreted onto the surface of the merozoite. The AMA-1₆₆ fragment is then cleaved into either a 48 kDa (AMA-1₄₈) or 44 kDa (AMA-1₄₄) fragment. One of these three fragments is then used by the merozoite for erythrocyte invasion.

The aim of this investigation was to isolate and characterise each of the fragments of the *Plasmodium falciparum* AMA-1 (*Pf*AMA-1) protein using the 3D7 lab strain of *P.*

falciparum and to visualise the merozoite-erythrocyte invasion process, to possibly identify which of the AMA-1 fragments are involved in the invasion process. In order to achieve this large clusters of merozoites from sorbitol-synchronised cultures were isolated. Schizonts were isolated from culture by magnetic separation and incubated with E64 to prevent the release of merozoites. Merozoites that were required for the isolation of PfAMA-1 were harvested from the schizonts by saponin lysis, then homogenised, separated by SDS-PAGE and digested for LC-MS/MS analysis. Merozoites that were required for the visualisation procedures were not incubated with E64, to allow natural egression from the erythrocyte.

The transmission electron microscopy results produced clear images of the merozoite-erythrocyte invasion process and the positioning of PfAMA-1 on the merozoite, before and after schizont rupture, was visualised from results obtained from confocal microscopy. Then PfAMA-1 was identified in isolated merozoite samples by LC-MS/MS analysis. However, due to its low abundance, isolation of high enough concentrations of PfAMA-1 to characterise its different fragments was not achieved.

Further investigation into the development of the culturing and isolating methods could help in future projects aimed at isolating higher concentrations of merozoite proteins from synchronised cultures with a lower merozoite egression window period, in order to accomplish detailed analysis on invading proteins for the future development of treatments against malaria.

Keywords: Malaria, *Plasmodium falciparum*, merozoite, erythrocyte, invasion process, AMA-1.

List of Figures

Chapter 1

- Figure 1.1** The *Anopheles* female mosquito. 1
- Figure 1.2** Global distribution of malaria. Africa still remains the continent with the highest number of reported cases in the world. Image is from the WHO World Malaria Report of 2014. 2
- Figure 1.3** The complete life cycle of the malaria parasite. 1) Liver stage 2) Intraerythrocytic stage 3) Mosquito stage. The erythrocytes are indicated as RBCs. Image from Bousema *et al.* (2011) with permission. 3
- Figure 1.4** The morphological forms of the intraerythrocytic asexual and sexual life cycle. Figure was hand-drawn from microscopic images. 5
- Figure 1.5** Merozoite egression models. **A** represents the ‘Membrane fusion’ model by Winograd *et al.* (1999). **B** represents the ‘Explosive-rupture’ model by Glushakova *et al.* (2005). **C** represents the ‘Inside-out’ model by Wickham *et al.* (2003). **D** represents the ‘Outside-in’ model by Salmon *et al.* (2001) and Soni *et al.* (2005). This image is from Michael Blackman (2008) with permission. 8
- Figure 1.6** The characteristic structure of a *Plasmodium* merozoite. Image from Cowman *et al.* (2006). 9
- Figure 1.7** Merozoite invasion model. **A**: Attachment. **B**: Reorientation. **C**: Tight-junction formation. **D**: PV membrane formation. **E**: Completely invaded merozoite. From Srinivasan *et al.* (2011) with permission. 10
- Figure 1.8** Types of protein-membrane associations. **A** indicates the lipid bilayer of the membrane. The types of proteins are represented from 1 to 4, with integral proteins represented as 1, 2 and 3. While 4 represents a peripheral protein. Protein 1: lies entirely within the membrane. Protein 2: transverses the membrane, Protein 3: projects into the membrane. Protein 4: associates with the membrane surface. 11
- Figure 1.9** The proteolytic processing of *PfAMA-1*. The left side of the figure depicts the normal processing of *PfAMA-1* from the micronemes. The right side depicts the inhibition effect of *PfAMA-1* antibodies on the proteolytic processing. Image from Dutta *et al.* (2003) with permission. 12
- Figure 1.10** Transmission Electron Microscope. The Joel JEM 2100F Field Emission Electron Microscope of the Laboratory of Microscopy and Microanalysis of the University of Pretoria. Photograph: Tanya Marie Downing. 14
- Figure 1.11** Confocal Microscope Zeiss 510 META model of the Laboratory of Microscopy and Microanalysis of the University of Pretoria. Photograph: Tanya Marie Downing. 14

Figure 1.12 SDS-PAGE. **A** illustrates protein separation according to charge by using isoelectric focusing. **B** is separation according to MW. **C** is a 2-D gel with separation first by charge and then MW. 16

Figure 1.13 Western blotting. **A** represents proteins separated on a gel. **B** represents a western blot membrane with target proteins visible. 16

Figure 1.14 A Flow diagram of the different analytical methods of protein mixtures for MS. **A** and **B** represent the electrophoresis methods and **C** represents the non-electrophoresis method. **B** represents the procedure for protein analysis for this investigation of *PfAMA-1*. 18

Chapter 2

Figure 2.1 Set up of the VarioMACS magnetic separator. Late stage parasites (iRBCs) become paramagnetic and are captured by the column, while in a magnetic field, while the uninfected erythrocytes (RBCs) are eluted from the column. This image is an adaptation from Mata-Cantero *et al.* (2014) with permission. 25

Chapter 3

Figure 3.1 Unsynchronised culture. The heterogeneous stages of *Plasmodium falciparum* asexual intraerythrocytic life cycle. The black arrows indicate the Ring stages. The orange arrows indicate the Trophozoite stages. The red arrow indicates the merozoites bursting from a schizont. Image was taken at 100X magnification with 20 µm scale bar. 40

Figure 3.2 Synchronisation. **A** represents the unsynchronised culture before the first synchronisation: the white arrows indicate young rings ~3-4 hpi. The black arrows indicate late stage trophozoites ~30-34 hpi. **B** shows the culture after sorbitol lysis, where the green arrow indicates a lysed trophozoite containing erythrocyte. **C** represents the culture before the second synchronisation, where the white arrows indicate late rings ~18-22 hpi. The black arrows indicate early stage trophozoites ~26-30 hpi. Images were taken at 100X magnification with 20 µm scale bar. 41

Figure 3.3 Response of erythrocytes to different osmotic pressures. **A** illustrates when an erythrocyte is placed in a hypertonic solution, water molecules move out of the cell and it shrinks. **B** illustrates the effects an isotonic solution has on an erythrocyte, no net movement of water molecules. **C** illustrates when an erythrocyte is placed in a hypotonic solution, water molecules move into the cell; it swells and bursts. **C** illustrates the effect of sorbitol on infected erythrocytes. 42

Figure 3.4 After magnetic isolation. Late trophozoites (~34-38 hpi) were isolated from uninfected erythrocytes. 44

Figure 3.5 The eluted sample fractions showing the low numbers of parasitised erythrocytes that were not retained by the column. **A** represents the FT₁ of the eluted culture where a small percentage of the parasites (black arrow) escape the column. **B** represents FT₂ once the culture has been eluted through the column a second time, with uninfected erythrocytes (red arrow) remaining and ~0,1% of infected erythrocytes. Images were taken at 100X magnification with 20 µm scale bar. 44

Figure 3.6 After incubation with 10 µM E64. A mature schizont where merozoites are clearly visible as indicated by the blue arrow. Image was taken at 100X magnification with 20 µm scale bar. 45

Figure 3.7 Incubation with 20 µM of E64. Parasites die within the erythrocyte and cellular contents condenses. Image was taken at 100X magnification with 20 µm scale bar. 46

Figure 3.8 Merozoite-erythrocyte invasion sequence as seen under a light microscope after Giemsa staining. **A:** Free merozoite (mz); where the green arrow indicates a mz cluster from a burst schizont and the white arrow indicates a single free mz opposite an erythrocyte, indicated by the red arrow. **B:** The white arrow indicates the attached mz just on the surface of the erythrocyte membrane. **C:** A mz clearly invading an erythrocyte, as indentations in the erythrocyte membrane are indicated with a yellow arrow. **D:** A completely invaded mz indicated by a white arrow. Images were taken at 100X magnification with 20 µm scale bar. 49

Figure 3.9 TEM images of developing merozoites in schizonts. **A:** A schizont between ~44 to 45 hpi. Separate merozoites can be seen developing as indicated by the white arrows. The blue arrow indicates the hemozoin crystals. **B:** ~46 hpi schizont with a number of the merozoites developing organelles, the orange arrows indicates the rhoptries, the red arrow indicates the micronemes and the blue arrows indicate the dense granules. Scale bar = 2 µm.. 50

Figure 3.10 Mature schizonts at the 48th hour of life cycle with matured mz completely filling the erythrocyte. The black arrow indicates a mature mz. Scale bar = 2 µm. 50

Figure 3.11 Egression of merozoites. The erythrocyte membrane has dissociated, releasing its cytoplasmic contents and the mature mz. The white arrow indicates the dissociated PV membrane. (RBC) indicates the uninfected erythrocyte. Scale bar = 2 µm. 51

Figure 3.12 Merozoites. **A**: A number of free merozoites. With a 2 μm scale bar. **B**: Merozoite structure. 4X magnification of a single merozoite along side an erythrocyte. The white arrow indicates the nucleus, the orange arrows indicate the rhoptry organelles and the yellow arrow indicates the microneme organelles. Scale bar = 500 nm. 52

Figure 3.13 Merozoite attachment. **A** indicates the attachment phase of the merozoite invasion process; the square indicates the merozoite attaching to the erythrocyte (indicated as RBC). **B** is a 4X increased magnification of **A**, where RBC indicates the erythrocyte and the blue arrows indicate to the surface protein attachments of the mz. **A** has a 2 μm scale bar and **B** a 500 nm scale bar. 53

Figure 3.14 Merozoite orientation and tight-junction formation. The mz that has orientated itself for invasion and beginning to form the tight-junction, as indicated with a white arrow. A 2 μm scale bar. 54

Figure 3.15 Merozoite invaded erythrocyte. **A** represents an invaded erythrocyte (RBC) by a mz as indicated within the blue box. A 2 μm scale bar. **B** is a 4X magnification of **A** with a scale bar of 500 nm. The PV membrane, a distinct white lining around the mz, which is indicated by the yellow arrow, surrounds the completely invaded mz. 54

Figure 3.16 Localisation of *Pf*AMA-1 in mature schizonts (~48 hpi). **A** is the DAPI (blue) stain only. **B** is the Cy3-*Pf*AMA-1 (yellow) stain only. **C** is the overlay of **A** and **B**. The blue arrows indicate an intact mature schizont with merozoites. The green arrows indicate an erupted schizont with merozoites egressing. Scale bar = 5 μm . 56

Figure 3.17 Localisation of *Pf*AMA-1 in free merozoites. **A** is the DAPI (blue) stain only. **B** is the Cy3-*Pf*AMA-1 (yellow) stain only. **C** is the overlay of **A** and **B**. The white arrows indicate the apical localisation of labelled *Pf*AMA-1. Scale bar = 5 μm . **D** is an enhanced overlay image of **C** that shows the apical localisation of *Pf*AMA-1. Scale bar 10 μm . 57

Figure 3.18 A SDS-PAGE of isolated *Pf*merozoite proteins from **A** single 30 mL synchronised culture of 3-5% parasitemia with 3-5% Hct and **B** a collective sample of 7-8 synchronised cultures of similar culture parameters as **A**. **C** is the western blot of **B** where the white band at ~60 kDa indicates non-specific binding of the 1F9 antibody and was identified as Albumin by gel digestion and LC-MS analysis. 59

Figure 3.19 SDS-PAGE of *Pf*merozoite proteins. Samples were prepared from the same protein extract and prepared under **A**: Non-reducing conditions **B**: Reducing conditions. There were clear differences in band intensities between the two conditions of sample preparation. The blue arrows indicate protein bands with the same mass that were found in both lanes while the orange arrows indicate the difference of band intensity between both conditions. 60

Figure 3.20 Western blot membrane blocked with 2% BSA. **A** represents molecular weight standards. Samples **1B-D** were run under reduced conditions and **2B-D** under non-reduced conditions. **B**: *Pf*AMA-1 antibody (1F9), **C**: BSA standard, **D**: Isolated *Pf*merozoite sample. The dark bands indicate binding of the 1F9 antibody and the white bands indicate quenching of the substrate. 62

Figure 3.21 Western blot membrane blocked with 2% milk. **A** represents MW standards. Samples **1B-D** were run under reduced conditions and **2B-D** under non-reduced conditions. **B**: *Pf*AMA-1 antibody (1F9), **C**: BSA standard, **D**: Isolated *Pf*merozoite sample. The dark bands indicate binding of the 1F9 antibody and the white bands indicate quenching of the substrate. 62

Figure 3.22 The amino acid sequence of *Pf*AMA-1. The yellow highlights represent the trypsin cleavage sites. The green highlights represent the peptides identified by LC-MS/MS. 70

Figure 3.23 The overview display of the Peptideshaker data of the protease inhibitor treated merozoite sample. The highlighted protein, PF3D7_1133400, is *Pf*AMA-1. Box **A** displays the identified proteins. Box **B** displays the selected protein's identified peptides with their respective PSM in Box **C**. Box **D** displays the spectrum of the selected peptide and Box **E** displays the coverage percentage of the protein from the identified peptides. 72

Figure 3.24 The overview display of the Peptideshaker data of the untreated merozoite sample. AMA-1 is the highlighted protein with the accession number of PF3D7_1133400. Box **A** displays the identified proteins. Box **B** displays the selected protein's identified peptides with their respective PSM in Box **C**. Box **D** displays the spectrum of the selected peptide and Box **E** displays the coverage percentage of the protein from the identified peptides. 73

Figure 3.25 The protein BLAST results of YDIEEVHGSGIR: The graphical summary. 75

Figure 3.26 The protein BLAST results of YDIEEVHGSGIR. **A** indicates to the protein descriptions. **B** indicates the alignment sequence of AMA-1 and **C** indicates the sequence of the human protein. 76

Figure 3.27 *Pf*AMA-1 peptide spectra. The y-axis represents the ion intensity (cps) and the x-axis represents the mass to charge ratio (m/z) of each peak. **A** is the MS spectrum of YDIEEVHGSGIR with an ion intensity of less than 3 cps. **B** is the spectrum of SAFLPTGAFK with an intensity of 7 cps. **C** is the spectrum of LVFELSASDQPK with the highest intensity (and relative abundance) of 12 cps. 77

Figure 3.28 The *de novo* sequence of peptide LVFELSASDQPK. The red columns indicate the amino acids identified from the y-ions and the blue columns indicate the amino acids identified from the b-ions. The y-ions sequence the peptide in reverse order (right to left). 78

Figure 3.29 Peptide fragment ions. A illustrates all the possible ions that form from peptide fragmentation during ESI along the peptide bonds: a- and x-ions, b- and y-ions and c- and z-ions. B illustrates a peptide that can be fragmented into its different b-ions (left to right) and y-ions (from right to left). The b- and y-ion set of ions are the most commonly formed from peptide fragmentation. 78

List of Tables

Chapter 1

Table 1.1 Summary of Antimalarial Drug Treatments	6
--	---

Chapter 3

Table 3.1 Proteomic Profile of Gel Digestion	64
---	----

Table 3.2 A List of Common Surface Proteins	64
--	----

Table 3.3 Protein Comparisons of Gel Digestion ^a and In-solution Digestion	66
--	----

Table 3.4 Comparison of Merozoite Surface Proteins Identified from an In-gel and In-solution Trypsin Digestion	67
---	----

Table 3.5 In-solution Digestion Method: A Proteomic Comparison of a Protease Inhibitor Cocktail (PIC) Treated Sample ^a versus a Non Protease Inhibitor (NPI) Treated Sample	69
---	----

Table 3.6 Comparison of Merozoite Surface Proteins Identified from the Protease Inhibitor Cocktail (PIC) Treated Sample ^a versus a Non Protease Inhibitor (NPI) Treated Sample	69
--	----

Table 3.7 The LC-MS/MS Results of Identified <i>Pf</i> AMA-1 Peptides	71
--	----

Appendix IV

Table A1 Summary of Fixing and Blocking Methods for Confocal Microscopy	102
--	-----

Table A2 Examples of Types of Proteins Identified	104
--	-----

Abbreviations

1F9 antibody	Rabbit polyclonal anti-AMA-1 antibody
1-D	One dimensional
2-D	Two dimensional
Ab	Antibody (ies)
ABRA	Acid basic repeat antigen
ACN	Acetonitrile
ACM	AlbuMax-II culture medium
ACT	Artemisinin combination therapy
AMA-1	Apical membrane antigen 1
Arg	Arginine
Bar	Unit of pressure
BCA	Bicinchoninic acid disodium salt hydrate
BNF	British National Formulary
BPU	Blood pack unit
BSA	Bovine serum albumin
°C	Degrees centigrade
CLAG	Cytoadherence-linked asexual protein
cm ²	Centimetre squared
CM	Confocal microscopy
CPDA-1	Citrate phosphate dextrose (anticoagulant)
CSP	Circumsporozoite protein
cps	Characters per second
C-terminal	Free carboxyl (COO ⁻) group of an amino acid chain
CuSO ₄ .5H ₂ O	Cupric Sulphate
Cy3	Cyanine 3
Cy3-Ab	Cy3 labelled antibody
Cys	Cysteine
Da	Dalton
kDa	Kilo-Dalton
DAPI	4',6-diamidino-2-phenylindole
DBL	Duffy binding-like
DDSA	Dodecenyl succinic anhydride
ddH ₂ O	Double distilled water
dddH ₂ O	Double distilled deionised water
DNA	Deoxyribonucleic acid
DTT	Dithiothreitol
E64	N- [N- (L-3- transcarboxyirane-2-carbonyl)-L-Leucyl]-agmatine2 (Protease inhibitor)



EBA	Erythrocyte binding antigen
EDTA	Ethylenediaminetetraacetic acid
EtOH	Ethanol
FA	Formaldehyde
FDR	False discovery rate
FT _{1/2}	Flow through 1 or 2
<i>g</i>	Centrifugal force
GAMA	GPI anchored micronemal antigen
GPI	Glycosylphosphatidyl inositol
H ₂ O	Water
h	Hour(s)
HCl	Hydrochloric acid
Hct	Haematocrit
HEPES	2-[4-(2-hydroxyethyl) piperazin-1-yl] ethane sulfonic acid
hpi	Hours post infection
IAA	Iodoacetamide
ICM	Incomplete medium
IMET	Initial mass error tolerance
K	Lysine
KCl	Potassium chloride
kV	Kilo-volts
L	Litre
LCMS	Liquid chromatography mass spectrometry
Lys	Lysine
M	Molarity (unit: mole)
mbar	Millibar
MCP	Merozoite cap protein
MeOH	Methanol
min	Minute(s)
milliQ-H ₂ O	Mas Spectrometry grade water
mg	Milligrams
mL	Millilitres
mM	Millimolar
mm	Millimetre
µg	Microgram
µL	Microlitre
µm	Micrometre
mOs/kg	Osmolality



μM	Micromolar
MR	Modifier reagent
MSP	Merozoite surface proteins
ms	Milliseconds
MW	Molecular weight
mz	Merozoites
m/z	Mass to charge ratio
NaCl	Sodium chloride
Na_2CO_3	Sodium carbonate
NaHCO_3	Sodium bicarbonate
NaOH	Sodium hydroxide
ng	Nanograms
NH_4HCO_3	Ammonium bicarbonate
NMA	Nadic methyl anhydride
N-terminal	Free amino (NH_2) group of an amino acid chain
PAGE	Polyacrylamide gel electrophoresis
PAN	Plasminogen Apple Nematode
PBS	Phosphate buffered saline
PBS-T	Phosphate buffered saline – Tween-20
<i>Pf</i>	<i>Plasmodium falciparum</i>
pI	Isoelectric pH
PMSF	Phenylmethylsulfonyl fluoride
PV	Parasite vacuole
PVDF	Polyvinilidene fluoride
Q2	Quadrapole Two
QR	Quencher reagent
R	single character denotation for Arginine
RAMA	Rhoptry associated membrane antigen
RAP	Rhoptry-associated protein
RBCs	Red blood cells
iRBCs	Infected red blood cells
RESA	Ring-infected erythrocyte surface antigen
RH	Reticulocyte binding protein homologues
RhopH	High molecular weight rhoptry protein
RhopL	Low molecular weight rhoptry protein
RNA	Ribonucleic acid
rpm	Rotations per minute
RPMI	Roswell Park Memorial Institution
RON	Rhoptry neck protein
RT	Room temperature
S1	Benyldimethylamide
s	Seconds
SDS	Sodium dodecyl sulphate

SDS-PAGE	Sodium dodecyl sulphate polyacrylamide gel electrophoresis
SERA	Serine repeat antigen
SUB	Subtilisin-like serine protease
TEM	Transmission Electron Microscopy
TBS-T	Tris base solution with Tween-20
V	Volts
v/v	Volume to volume percentage
WHO	World Health Organisation
w/v	Weight to volume percentage
X	Times

Chapter 1

1. Literature Review

1.1 Introduction

1.1.1 What is Malaria?

Malaria is a heamosporidian (1) parasitic infection caused by the genus *Plasmodium*, which belongs to the phylum Apicomplexa (2). This phylum is classified according to the ‘apical complex’ organelles that are characteristic of this unicellular parasite (3), which has an intricate life cycle with differential ‘cell-invasive’ stages that require these apical organelles and their content to invade specific cells of each of their hosts (4).

The *Plasmodium* parasite is transmitted by the *Anopheles* mosquito, Figure 1.1, and can infect both humans and animals. *Plasmodium falciparum*, *P. vivax*, *P. ovale*, *P. knowlesi* and *P. malariae* are the five species of *Plasmodium* that commonly cause malaria in humans, with *P. falciparum* being the most pernicious strain of malaria. Genetically, each of the *Plasmodium* strains are distantly related to one another and it is proposed that their adaptation to humans occurred independently (5). Krief *et al.* (2010) suggested that *P. falciparum* originated from the great apes and was transmitted to humans about 30 000 years ago (6).



Figure 1.1 The *Anopheles* female mosquito. (<http://www.cdc.gov/malaria/about/biology/mosquitoes/>)

1.1.2 Areas of Infection and Populations Affected

Globally, malaria infects 100 to 300 million people each year. In 2015, the World Health Organisation (WHO) reported that 106 countries and territories had been affected by malaria since the year 2000. However 16 of these countries were reported to have no indigenous cases in 2014 (7). Figure 1.2 indicates the global distribution of malaria in 2013, from the 2014 WHO World Malaria Report (8). The mortality rate of malaria for 2015 was reported between 200 000 to 635 000 deaths, with nearly 500 000 deaths in children under the age of 5 years, and 90% of all malaria related deaths occurring in Africa alone (7).

P. falciparum contributes to an estimated 85% of all recorded cases of malaria (9), causing ~25% of the global infections in the region of Southeast Asia and as many as 70 to 80% of cases found in Africa (10). This is due to the warmer climates of the tropical and sub-tropical areas, in which the parasite thrives. In fact, malaria derived its name from the Italian ‘mal’ – ‘aria’ which means bad or poisonous air, as it was believed to have originated from breathing in the vapours of marshlands (11).

Despite the overwhelming number of reported cases and deaths that occurred from malaria in 2015, the WHO reported a 48% decrease in deaths in the last 15 years and have begun a new global control and eradication campaign, the Global Technical Strategy for Malaria, for 2016 to 2030 (7).

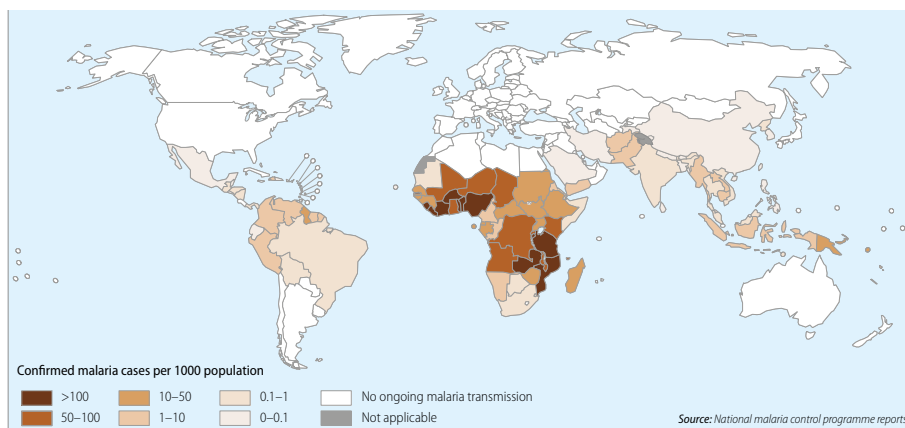


Figure 1.2 Global distribution of malaria. Africa still remains the continent with the highest number of reported cases in the world. Image is from the WHO World Malaria Report of 2014.

1.1.3 Clinical Manifestations

Once a *Plasmodium* infected mosquito has bitten and transmitted the parasite to the human host, the infected person will begin to present with symptoms between 7 to 14 days after transmission. Malaria causes sequential high fevers, chills and shivering, accompanied by joint and muscle pain, orthostatic hypotension, and headaches and vomiting. If left untreated, the disease will lead to severe, life threatening illnesses such as anaemia, metabolic acidosis, hypoglycaemia, acute renal failure, pulmonary oedema and cerebral malaria, all of which can lead to coma and death (11–15).

1.1.4 The Life Cycle

The general life cycle of the *Plasmodium* parasite is a complex one that involves both an invertebrate and a vertebrate host (16). It has a sexual and an asexual cycle, as shown in Figure 1.3. The sexual life cycle begins in a select parasite subpopulation, called gametocytes, in the erythrocytes of the human host. After the gametocytes are taken up by the mosquito, several stages of development result in sporozoites, which then reside in its salivary glands before the next feed. The asexual life cycle begins with the transmission of the parasite's sporozoites from the mosquito back to the human host. Within the human host the parasite's life cycle undergoes two developmental stages: the hepatic and intraerythrocytic stages. The length of each stage or cycle may differ between the *Plasmodium* strains.

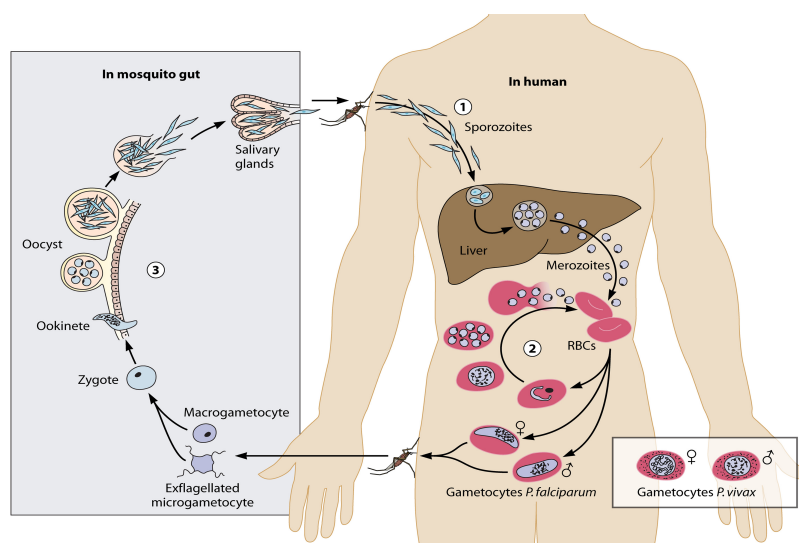


Figure 1.3 The complete life cycle of the malaria parasite. 1) Liver stage 2) Intraerythrocytic stage 3) Mosquito stage. The erythrocytes are indicated as RBCs. Image from Bousema *et al.* (2011) (17) with permission.

For the *P. falciparum* strain, once the female *Anopheles* mosquito has ingested the sexually distinct gametocytes from the blood of the human host, the sexual cycle begins within the midgut (18). The macrogamete (female gamete) is fertilised by the exflagellated microgamete (male gamete) to form a zygote. Within 24 to 72 hours of ingesting the gametocytes, the zygote will develop into a motile ookinete that will penetrate the epithelium of the midgut and reside beneath the basal lamina of the outer gut wall and mature into an oocyst. During a 7 day period, the oocyst will develop into hundreds of sporozoites that will be released into the haemocoelomic space of the insect and migrate to the salivary glands. From there the sporozoites will be injected into the vertebrate host and begin the asexual cycle, from which a small percentage (0.2-1%) will develop into gametocytes (19–23).

When the sporozoites enter the blood stream of a human host, they migrate to the liver where they invade the hepatocyte cells. This is an asymptomatic stage, where the intrahepatic parasites develop and mature into schizonts within approximately 7 days. A single schizont contains a number of merozoites that are released once the hepatocyte ruptures (24). The merozoites enter the blood system as aggregate vesicles known as merozoites, which rupture and release the merozoites, allowing them to infect the erythrocytes (25).

The parasite now enters the intraerythrocytic stage. During this cycle the parasite develops into either merozoites (asexual) or gametocytes (sexual) (26). The mosquito will take up the latter during its next feed, whereas the merozoites invade new erythrocytes and replicate again. The intraerythrocytic asexual cycle of *P. falciparum* is roughly 48 hours in length. The parasite undergoes three distinct morphological developmental stages over a 48-hour period, which is clearly illustrated in Figure 1.4.

Within the first few hours of erythrocyte invasion, the merozoite will flatten and take the form of a ‘ring’ as it begins to develop. This stage is aptly named the ring stage and is ~ 20 hours long. From approximately the 20th to 38th hour of the cycle, the parasite matures into the trophozoite stage, where it expands and begins to occupy most of the erythrocyte cytosol. During the late trophozoite and into the early schizont stage the parasite undergoes a number of nuclear mitotic divisions to produce immature

merozoites that will mature, during the late schizont stage, into functional invasive merozoites, from the 38th to 48th hour of the intraerythrocytic cycle (27).

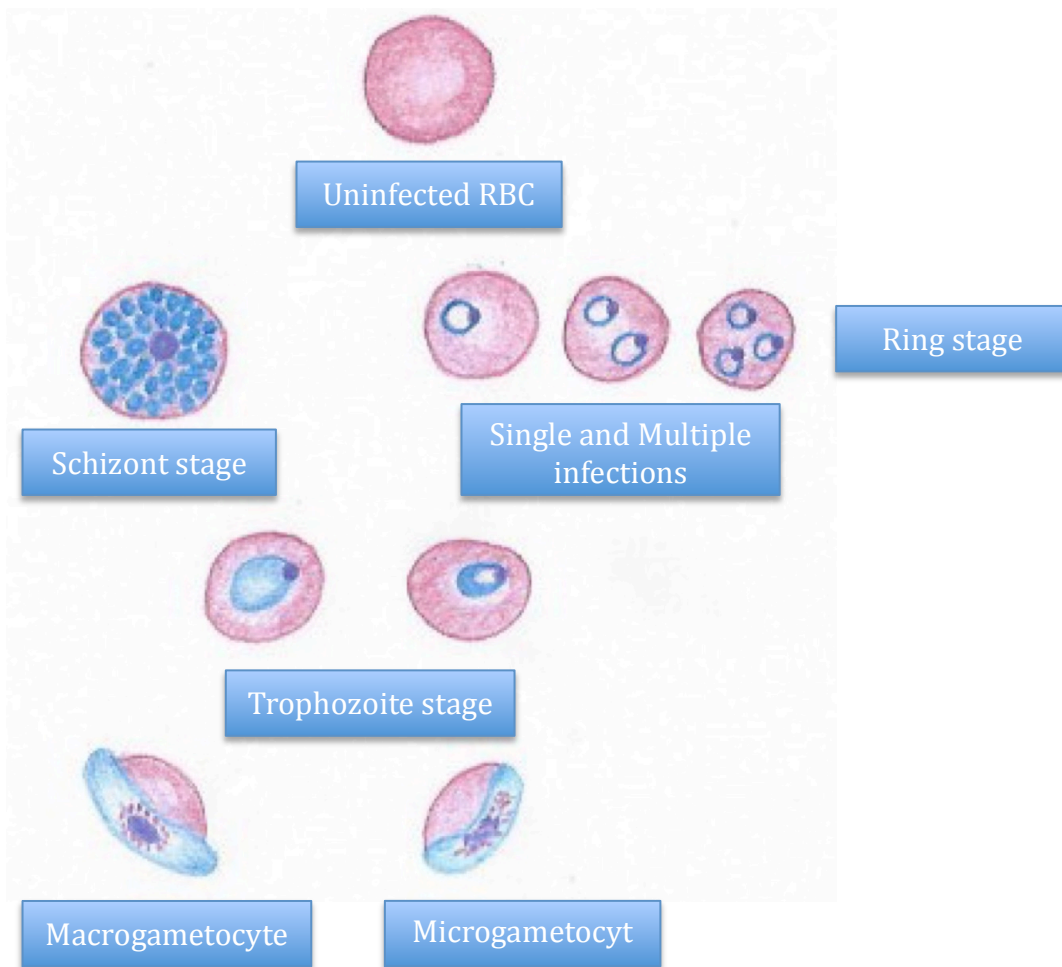


Figure 1.4 The morphological forms of the intraerythrocytic asexual and sexual life cycle. Figure was hand-drawn from microscopic images.

1.1.5 Treatment Regime

There are a number of treatment regimes that target the different phases of both the liver and the erythrocytic stages. ‘Tissue schizonticidal agents’ are classified as the 8-aminoquinolines and include drugs such as primaquine and tafenoquine. These drugs act on the liver stages, which decreases the transmission of the disease between hosts. The ‘blood schizonticidal agents’ are classified into different groups: the quinoline-methanols (Quinine) and 4-aminoquinolines (Chloroquine), the phenanthrene-methanols (Halofantrine) and antifolates (Sulfones and pyrimethamine). Some antibiotics, such as doxycycline, and sesquiterpene lactones like artemisinin-derived compounds are also

prescribed to treat malaria (11). However, these blood stage drugs have become ineffective in treating acute attacks of malaria due to resistance.

Currently, combination drug treatments, such as the artemisinin combination therapy or ACT provide the best treatment, as they combat against the parasite over a wider scope of its life cycle. Artemetherlumefantrine or dihydroartemisinin-piperaquine are the two most commonly used drugs of ACT. Combination drug treatments are also available for prophylaxis, which are known as the ‘Chemoprophylactic agents’, an example of this would be an oral chloroquine with doxycycline. Table 1.1 gives a simple summary of the antimalarial drug treatments according to the South African guidelines of 2015 and the United Kingdom guidelines of 2016 (28,29).

Table 1.1 Summary of Antimalarial Drug Treatments^a

	Drug Treatment	
	South Africa	United Kingdom
Uncomplicated Malaria	Artemether-lumefantrine with paracetamol or oral quinine with doxycycline	Artemisinin combination therapy (ACT) ² or oral atovaquone-proguanil (Malarone) or quinine/ oral quinine sulphate with doxycycline
Severe Malaria	Intravenous artesunate or intravenous quinine Both followed by a complete course of artemether- lumefantrine	Intravenous artesunate or intravenous quinine Both followed by a complete course of ACT or quinine with doxycycline or atovaquone-proguanil (Malarone)
Pregnancy	Oral quinine with clindamycin or Mefloquine ¹	Oral quinine and clindamycin
Children	Oral quinine with clindamycin or Mefloquine or atovaquone-proguanil	ACTs or oral quinine or atovaquone-proguanil
Prophylaxis	Mefloquine or doxycycline or atovaquone-proguanil	Chloroquine and/ or proguanil or doxycycline or Mefloquine or atovaquone-proguanil
With HIV	Doxycycline	No recommendations
1: Lariam, Mefliam 2: Artemether-lumefantrine or dihydroartemisinin- piperaquine		

The asexual development in the erythrocytic stage is the most noticeable phase of the malaria life cycle as the clinical symptoms of the disease arise here (30). Although, there are a number of different drug therapies targeting specific stages of the life cycle, the drugs are becoming less effective due to the increasing resistance of the parasite. Therefore, a vaccine, as a single treatment or in conjunction with current treatments, would be a more effective means of eradicating the disease in humans. Researchers have evaluated several specific protein targets of the parasite for vaccine candidates, from the merozoite, such as merozoite surface protein 1 (MSP-1) and apical membrane antigen 1 (AMA-1) (31–35), as well as from the sporozoites. The RTS,S/AS02A vaccine was developed from the circumsporozoite protein (CSP) and has been through the third phase of clinical trials, where it has been tested in seven malaria endemic Africa countries. The vaccine reported, according to the authors, to have ‘a significant efficacy of 40 - 77% against malaria in young children’. However, there was no significant difference in the efficacy of the vaccine between the control and treatment group of the infants, but the vaccine was said to have ‘prevented many cases of clinical and severe malaria over the 18 months after vaccine dose 3’ and ‘could be an important addition to current malaria control in Africa’ (36,37).

Understanding the detailed physiological processes and functional proteins of the various stages of the parasites life cycle, specifically those of the merozoite invasion of the erythrocytes, could lead to the future development of safe and effective vaccines from targeted malaria proteins.

1.2 *The Merozoite and Apical Membrane Antigen-1 Protein*

1.2.1 *Merozoite egression from the Erythrocyte*

A number of different models of merozoite egression have been proposed by a number of researchers, according to the review of Michael Blackman in 2008 (38), that explain the possible dispersal patterns of the merozoites within the bloodstream, which may contribute to the efficiency of the merozoites invasion of the erythrocytes.

The ‘Membrane fusion’ was the first model proposed, indicated as pathway A in Figure 1.5, where the erythrocyte and PV membranes fuse and form a ‘duct-like’ structure within the membrane to release the merozoites; which are released as a cluster still

attached to the hemozoid crystal (39,40). In 2005 Glushkova *et al.* (41) described merozoite egression as an ‘explosive rupture’ of both membranes, causing a radial dispersion of individual merozoites, this is indicated as pathway B in Figure 1.5. The last two models of merozoite egression have similar membrane dissociation patterns, in which the erythrocyte and PV membranes dissociate individually. The ‘Inside-out’ model, indicated as pathway C in Figure 1.5, was reported, in 2003 by Wickham *et al.* (42), as a two-step process that involved dissociation of the PV membrane first, thereby releasing the merozoites within the erythrocyte cytosol, followed by the breakdown of the erythrocytic membrane, liberating the merozoites to begin a new asexual life cycle. Lastly, the events of membrane dissociation of the final model, indicated as pathway D in Figure 1.5, occur in the reverse order of the third model and designated as the ‘Outside-in’ model, whereby the PV membrane surrounding the merozoites remains intact, forming a ‘merozoite-cluster’ within the erythrocyte. Once the erythrocyte membrane dissociates, the merozoite cluster is released, preceded by rupture of the PV membrane and release of individual merozoites. This model was supported and described by Salmon *et al.* (43) and Soni *et al.* (44).

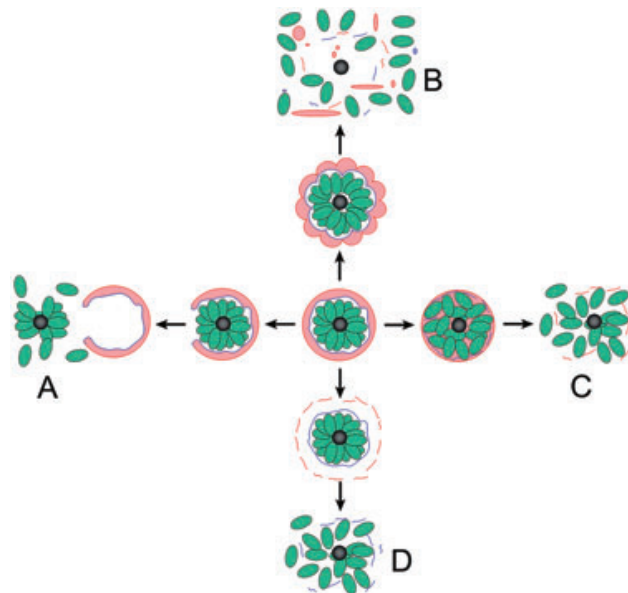


Figure 1.5 Merozoite egression models. Pathway A represents the ‘Membrane fusion’ model by Winograd *et al.* (1999) (39). Pathway B represents the ‘Explosive-rupture’ model by Glushakova *et al.* (2005) (41). Pathway C represents the ‘Inside-out’ model by Wickham *et al.* (2003) (42). Pathway D represents the ‘Outside-in’ model by Salmon *et al.* (2001) (43) and Soni *et al.* (2005) (44). This figure is from Blackman, 2008 (38) with permission.

1.2.2 Merozoite Invasion of the Erythrocyte

The *Plasmodium* merozoite, depicted in Figure 1.6, utilises a cascade of proteins during the erythrocyte invasion process, which is a swift action that takes place in approximately 30 seconds.

This process is clearly represented in Figure 1.7, together with the vital surface proteins involved. A number of these surface proteins are known as the merozoite surface proteins (MSP), which are expressed during merozoite development and are distributed over the merozoite's surface via glycosylphosphatidyl inositol (GPI) anchors (15,45). These MSP molecules are reputed to mediate the initial attachment of the merozoite to the erythrocyte membrane. Ten MSP proteins have been identified with MSP-1 being recognised as the most important protein required for attachment to the erythrocyte surface, it forms a 'co-ligand complex' with MSP-9 which then binds to the Band 3 receptor (18,31,46,47).

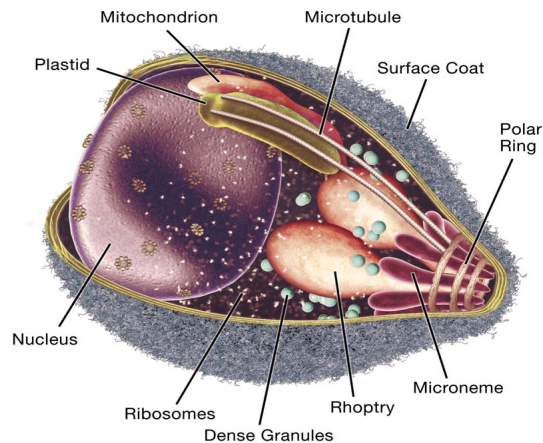


Figure 1.6 The characteristic structure of a *Plasmodium* merozoite. Image from Cowman *et al.* (2006) with permission.

Once the merozoite has attached to an erythrocyte it will re-orientate itself, this is so that the apical organelles can be brought into close contact with the membrane of the erythrocyte. The apical complex consists of secretory organelles of which the most important are the micronemes and rhoptries that store and secrete AMA-1 and rhoptry neck proteins (RON-2, 4), respectively. These proteins interact during the formation of the tight junction between the two cell membranes (48-50). Unlike the attachment phase, once the tight junction has been established, an irreversible bond is formed which

commits the merozoite to invading the host cell. As the parasite enters the host cell it will shed its surface proteins by means of a membrane bound ‘shedase’ protease, (51-53), which is a subtilisin-like serine protease called *PfSUB-2* (54).

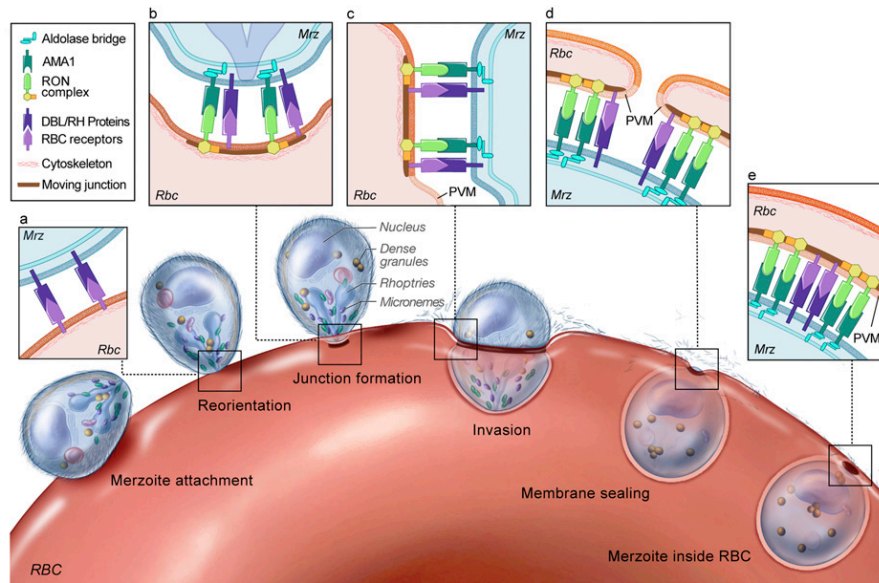


Figure 1.7 Merozoite invasion model. **A:** Attachment. **B:** Reorientation. **C:** Tight-junction formation. **D:** PV membrane formation. **E:** Completely invaded merozoite. From Srinivasan *et al.* (2011) (51) with permission.

1.2.3 The Apical Membrane Antigen-1 Protein

(a) Function, Importance and Future of *PfAMA-1*

PfAMA-1 plays a vital role during the invasion process, as it assists the RON proteins to form the specialised tight-junction through which the merozoite may infiltrate the erythrocyte. Publications on antibodies specific to *PfAMA-1* have shown that binding of *PfAMA-1* antibodies prevents merozoite invasion in *in vitro* studies (55) and research also suggests that gene manipulation of the *Ama1* gene may affect the viability of merozoites, though the results of the research were generally inconclusive (56).

However, *PfAMA-1* is an ideal candidate for a vaccine, as the PAN domains and hydrophobic trough of the ectoplasmic region of *PfAMA-1* have proven to be an ideal target as an antibody-binding site (57). This, together with *PfAMA-1*'s structural homology, within the *Plasmodium* family and its structural orthology in *Toxoplasma gondii* and *Babesia bovis*, which are also parasites of the Apicomplexa phylum (58), as

well as being found in the sporozoites, would make *PfAMA-1* a vital ‘broad-spectrum’ vaccine target as it would not be species or stage specific (57).

(b) *Type of Protein and Structure*

AMA-1 is a Type I integral membrane protein (59). This means, once it has been processed and secreted, it lies within the lipid bilayer of the merozoites membrane, where it consists of 3 regions: an N-terminal ectoplasmic region, a transmembrane region and a small cytoplasmic region. This is illustrated as protein 3 in Figure 1.8, which depicts the different types of protein-membrane associations (58, 60-61).

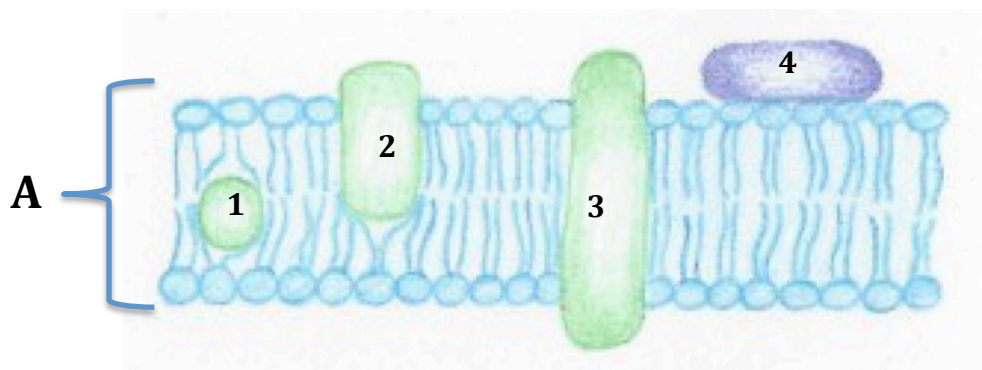


Figure 1.8 Types of protein-membrane associations. **A** indicates the lipid bilayer of the membrane. The types of proteins are represented from 1 to 4; with integral proteins represented as 1, 2 and 3. While 4 represents a peripheral protein. Protein 1: lies entirely within the membrane. Protein 2: projects into the membrane, Protein 3: transverses the membrane. Protein 4: associates with the membrane surface.

AMA-1 consists of 622 amino acids that are folded to form its tertiary structure (62). The crystal structure of AMA-1’s ectoplasmic region has been described in previous research as having 3 domains, where domain I and II follow the Plasminogen Apple Nematode (PAN) folding motif. This motif defines the protein folds of the domains as generally having carbohydrate- or protein-receptor binding functions. The PAN domains of AMA-1 have 16 cysteine (Cys) residues that form the disulphide bridges within the domains. These Cys residues are found in all characterised *Plasmodium* species AMA-1 (63) and form a hydrophobic trough, which was speculated, by early research, to be the ligand-binding pocket of AMA-1 (63,64).

(c) *Proteolytic Processing*

AMA-1 is sequenced as an 83 kDa (*PfAMA-1₈₃*) precursor protein that is expressed in the developing merozoites, which undergoes proteolytic processing; this is depicted in Figure 1.9. Once the schizonts rupture, the short N-terminal region of *PfAMA-1₈₃* is cleaved to produce a 66 kDa fragment (*PfAMA-1₆₆*) that translocates to and redistributes circumferentially on the surface membrane of the merozoite. Here *PfAMA-1₆₆* experiences two C-terminal cleavages to give rise to two soluble forms; a 48 kDa (*PfAMA-1₄₈*) and a 44 kDa (*PfAMA-1₄₄*) fragment (52).

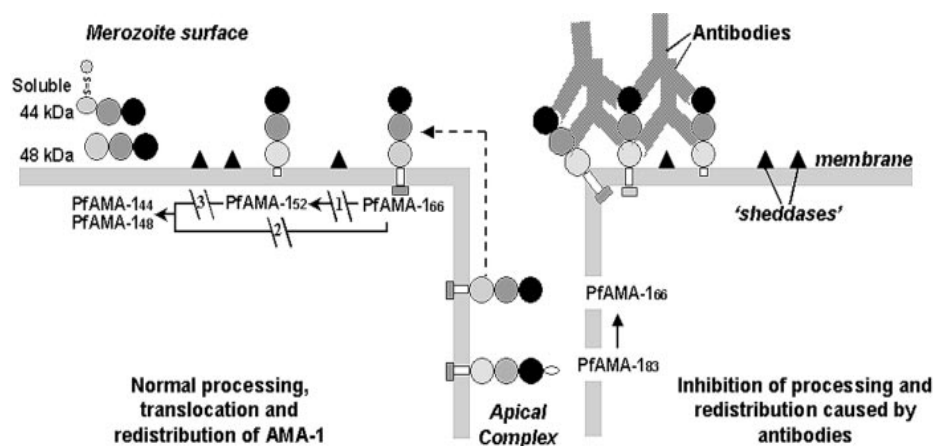


Figure 1.9 The proteolytic processing of *PfAMA-1*. The left side of the figure depicts the normal processing of *PfAMA-1* from the micronemes. The right side depicts the inhibition effect of *PfAMA-1* antibodies on the proteolytic processing. Image from Dutta *et al.* (2003)(53) with permission.

Studies done by S. Dutta, *et al.* (2003)(53), have shown that, with the use of polyclonal antibodies against *PfAMA-1*, the secondary proteolytic processing of *PfAMA-1₆₆* to *PfAMA-1_{48/44}* can be inhibited. Results also showed that, due to the binding of the antibody to the 66 kDa fragment that caused the inhibition of *PfAMA-1₆₆* processing, the antibodies gave rise to a 52 kDa fragment (*PfAMA-1₅₂*), as seen in Figure 1.9, which prevented the merozoite invasion of new erythrocytes.

Therefore, in order to examine the process of merozoite egression from the schizont and its invasion of the erythrocyte, as well as to analyse the novel merozoite protein targets, such as AMA-1, one needs to consider a number of visualisation and identification

approaches. Transmission electron, confocal microscopy and proteomics are the main techniques utilised for this investigation.

1.3 Methods Used for Visualisation of Merozoites and Identification and Isolation of PfAMA-1

1.3.1 Visualisation Methods

The field of microscopy has opened up the world of microorganisms to researchers, with the development of highly specialised microscopes, such as transmission electron microscopy (TEM) and confocal microscopy (CM). The different techniques made available through the development of specialised microscopes have allowed researchers to study the structural details and physiology of microorganisms.

TEM (Figure 1.10) requires the emission of electrons through an ultra-thin cross section of a sample to produce an image that displays the ultrastructure of a microorganism, with magnifications and resolutions in the nanometre range. From these images researchers are able to visualise the organisation of the cellular components of microscopic organisms and any structural changes that occur during life cycles or when organisms are placed under different environmental stresses, such as the changes that occur within the intraerythrocytic stage of the *Plasmodium* merozoite (65).

CM (Figure 1.11) involves the use of a fluorescent label to visualise complex inter- and intracellular processes. This requires labelling an antibody that binds to a specific protein, which is involved in a particular pathway that is under investigation. Each fluorescent label has a unique excitation and emission wavelength that fluoresces, with a particular colour when the fluorescent label is activated by a highly focussed laser, to produce a stacked three-dimensional image. These images assist researchers in understanding the fundamental cellular pathways that take place within microorganisms, like malaria, to determine how specific proteins function in order to identify new targets for the treatment of diseases (66).



Figure 1.10 Transmission Electron Microscope. The Joel JEM 2100F Field Emission Electron Microscope of the Laboratory of Microscopy and Microanalysis of the University of Pretoria. Photograph: Tanya Marie Downing.

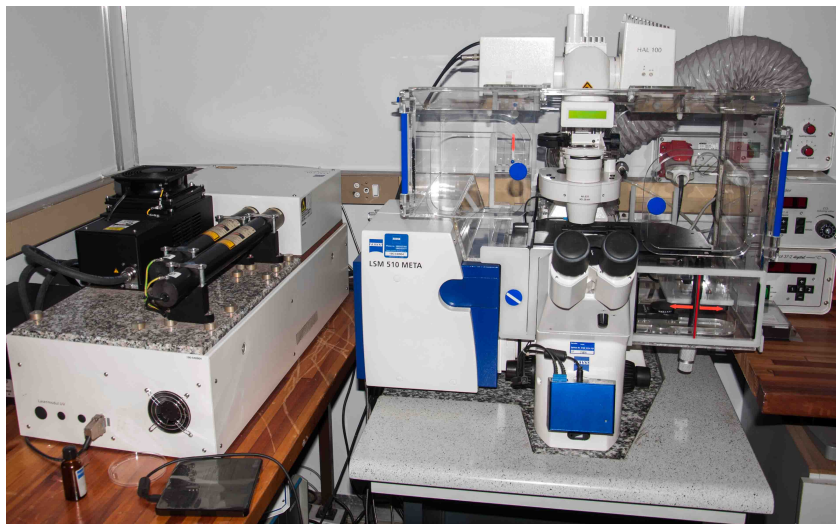


Figure 1.11 Confocal Microscope Zeiss 510 META model of the Laboratory of Microscopy and Microanalysis of the University of Pretoria. Photograph: Tanya Marie Downing.

1.3.2 Protein Identification and Isolation Methods

Proteomics is a multidisciplinary analysis of an organism's proteome that includes an array of techniques that are able to assist researchers in isolating and identifying target proteins.

Sodium dodecyl sulphate polyacrylamide gel electrophoresis (SDS-PAGE) and western blotting are the simplest and oldest techniques used in proteomics. A sample of mixed proteins from a dissected tissue or a microorganism can be separated by isoelectric focusing or according to molecular weight, these are known as 1-D electrophoresis, or by combining the separation by isoelectric focusing and molecular weight, which is known as 2-D electrophoresis, this is illustrated in Figure 1.12. Isoelectric focusing gels separate native proteins according to their net charge, using a fixed pH gradient. All proteins have different isoelectric points; this is the pH value where the protein no longer has a net charge, also known as the isoelectric pH (pI). When the proteins are run in an open gel they experience a changing pH environment, which causes their net charge to change. Proteins will migrate through the gel as their charges change, until they reach their pI value. At this point a protein has no net charge and will no longer migrate, therefore separating it from the remaining proteins. On the other hand, all proteins differ in their molecular weight and charge. The cross-linked polyacrylamide within the PAGE gel provides the sieving effect needed to separate the proteins. The proteins with the largest molecular weight experience the most resistance; therefore these molecules do not migrate as far down the gel as the smaller proteins (60).

Western blotting is the identification of a target protein with the use of polyclonal or monoclonal antibodies against particular proteins. Once the proteins, from a sample, have been separated on a gel they are then transferred to a polyvinylidene difluoride (PVDF) membrane. The membrane is incubated in a blocking buffer to block all the non-specific protein-binding sites. Then the membrane is incubated overnight with an antibody that has an affinity for the target protein. The antibody is labelled with a fluorescent label or enzyme that can be detected under UV light, which produces an immunoblot image for the researcher to determine at what MW the target protein's band occurs and the intensity for relative quantitation for further analysis, this is illustrated in Figure 1.13 (60).

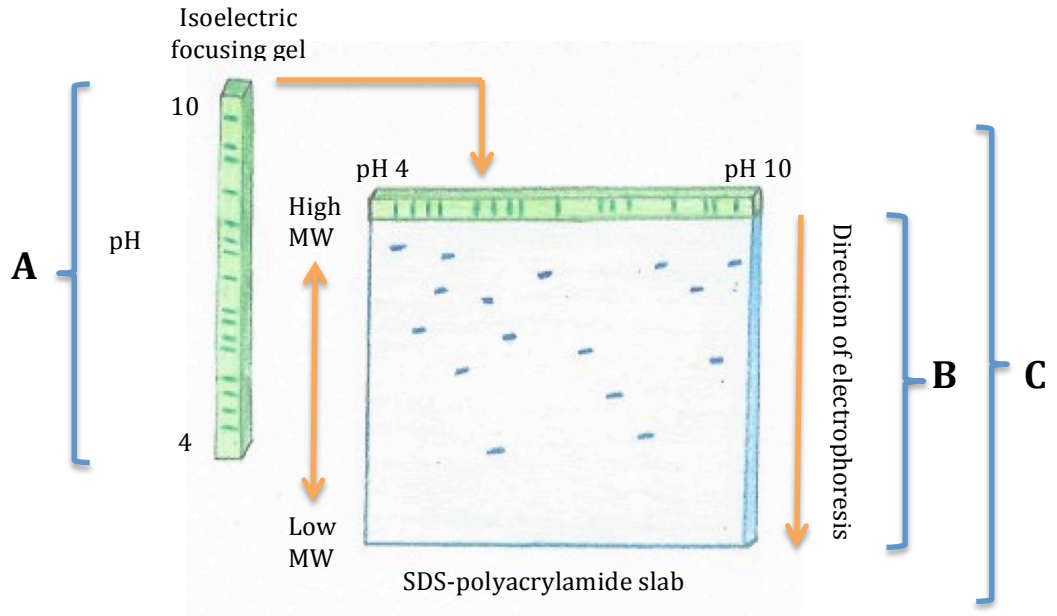


Figure 1.12 SDS-PAGE. **A** illustrates protein separation according to charge by using isoelectric focusing. **B** is separation according to MW. **C** is a 2-D gel with separation first by charge and then MW.

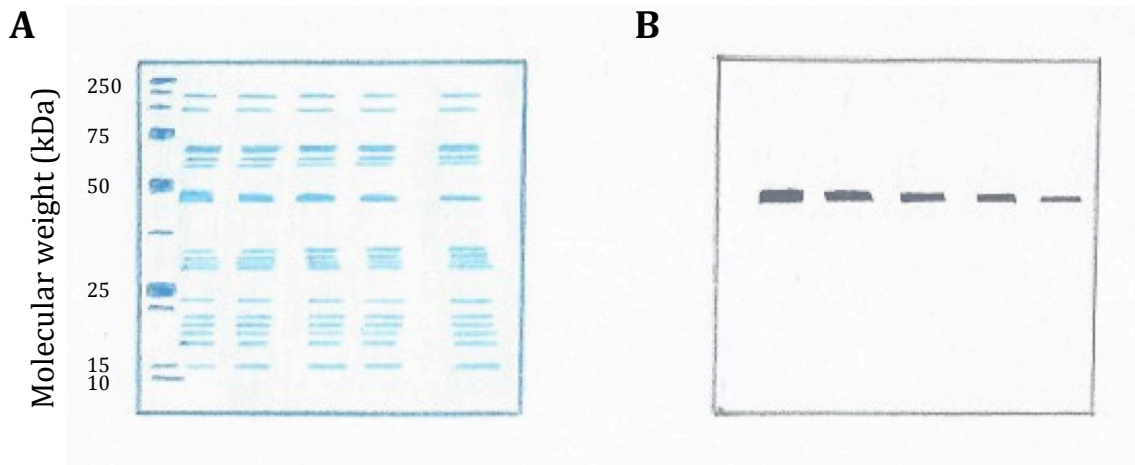


Figure 1.13 Western blotting **A** represents proteins separated on a gel. **B** represents a western blot membrane with target proteins visible.

Liquid chromatography tandem mass spectrometry (LC-MS/MS) is a technique used to identify and characterise proteins by means of their peptides. LC-MS/MS can provide a highly sensitive analysis of targeted proteins, from a mixture of proteins, in the femtomolar range. Isolated target proteins are digested using protease enzymes of which trypsin is the most common, to reduce them into their various unique peptides and the peptides are then analysed using mass spectrometry, this sequence of protein preparation and identification is illustrated in Figure 1.14 (67).

The peptide sample for LC-MS/MS analysis can be prepared in two ways: using in-gel digestion or an in-solution digestion with trypsin. An in-gel digestion involves separating the target protein from the mixed protein sample of the microorganism by SDS-PAGE, then cutting the bands of the target protein from the gel and preparing the gel pieces for the protease digestion. The in-solution digestion procedure only requires an aliquot of the mixed protein sample, to which the protease is then added to allow for digestion of all the proteins in the sample (67). Trypsin is the most commonly utilised enzyme for the LC-MS/MS protease digestion procedure as it provides ideal doubly charged peptides that are relatively easy to sequence as it cleaves proteins into peptides only at the C-terminal of the lysine (Lys or K) and arginine (Arg or R) residues (60).

The use of the microscopy and proteomic techniques, in this investigation, will be to visualise the development and function of the merozoite and for the analysis of the merozoite proteome, with *PfAMA-1* as a target protein to better understand how the merozoite utilises each of the *PfAMA-1* fragments.

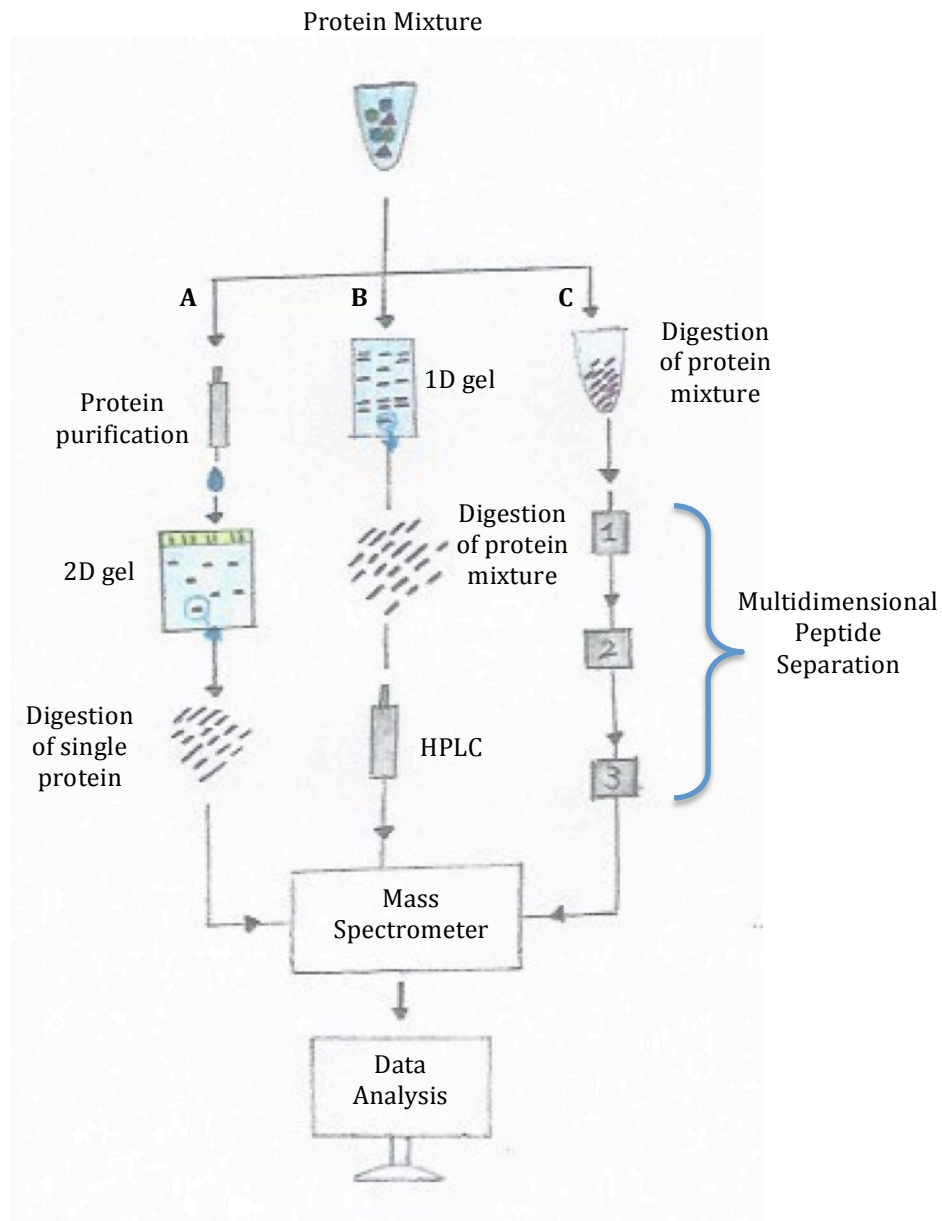


Figure 1.14 A Flow diagram of the different analytical methods of protein mixtures for MS. **A** and **B** represent the electrophoresis methods and **C** represents the non-electrophoresis method. **B** represents the procedure followed for protein analysis for this investigation of *PfAMA-1*.

1.4 Study Outline

1.4.1 Aim

To culture large volumes of synchronised parasite cultures in order to perform a proteomic analysis of *Plasmodium falciparum* merozoites.

1.4.2 Objectives

To culture large numbers of highly synchronised merozoites (less than 4 hours) from *Plasmodium falciparum* cultures to isolate PfAMA-1 protein.

To perform transmission electron microscopy to capture images of final stages of merozoite maturation and merozoite invasion sequence.

To use fluorescently labelled rabbit polyclonal PfAMA-1 antibodies and isolated merozoites, and confocal microscopy to perform localisation of PfAMA-1 after erythrocyte egression.

To isolate PfAMA-1 from 3D7 merozoites, post erythrocyte egression using electrophoretic and chromatographic techniques.

Chapter 2

2. Materials and Methods

All chemicals used were of the highest quality available from reputable chemical suppliers. The polyclonal rabbit anti-*Pf*AMA-1 IgG antibody used in this study was donated by Prof. Robin Anders of La Trobe University Australia. For all the reagent recipes please refer to Appendix III.

This study was approved by the University of Pretoria Health Sciences Faculty Research Ethics Committee (reference number 305/2013) who approved the use of the *Plasmodium falciparum* 3D7 laboratory strain of the parasite and the collection of blood for harvesting of erythrocytes, with informed consent from volunteers, for this study (Appendix I and Appendix II).

2.1 *Culturing of Plasmodium falciparum* parasites

2.1.1 *Erythrocytes and Strain of P. falciparum*

The *Plasmodium falciparum* 3D7, chloroquine sensitive, strain was cultured under strict sterile conditions at the Biochemistry Department of the University of Pretoria. Type O blood was donated by healthy volunteers at the National Blood Bank facilities where the blood was collected into CPDA-1 single use BPU 500 mL blood bags (Adcock Ingram Critical Care BP) and stored at 4°C.

2.1.2 *In vitro* Conditions

Cultures with starting parasitemia of 0.5-1% of an unsynchronised culture of parasites were cultured in 25 cm² culture flasks (Greiner Bio-one Cellstar), with erythrocytes at a 10% haematocrit (Hct) (68,69) in RPMI-1640 culture medium (Refer to Appendix III for the complete recipe) containing 20 mL of 1.25 M HEPES buffer at pH 7.2, 10 mL of 20% glucose, 0.48 µL of 50 mg/mL gentamycin, 2.5 mL of 80 mM hypoxanthine and enriched with 1% AlbuMax-II. All solutions were sterilised by filtration (0.2 µm filter). The entire culture medium was also filter sterilised using a 0.2 µm filter and vacuum system (Integra Vacusafe Labotec) into sterile bottles (70).

Parasite culture medium was changed every 24 hours (h). Cultures were transferred to a sterile 50 mL tube (Greiner Bio-one Cellstar Tubes) and centrifuged (C-28A Centrifuge Boeco Germany) at 2000 g for 2 minutes (min). The supernatant was discarded and 9 mL of AlbuMax-II culture medium (ACM), which was pre-heated in a warm bath (Mettler) at 37°C for 30 min, was added to the pellet; the pellet was re-suspended by gentle agitation. The culture was then transferred into a new 25 cm² culture flask, gassed for 15-30 seconds (s) with 5% O₂, 5% CO₂ and 90% N gas mixture (Afrox, Germiston, RSA), and incubated at 38°C in a shaking incubator (Ratek Orbital Mixer Incubator) at 60 rpm for 24 h (71), this was done to mimic the natural environmental conditions of the human blood stream. Once parasite cultures had reached parasitemia levels between 5-10%, an additional 4-5 mL of ACM was provided.

2.1.3 Parasitemia

To determine the parasitemia, a small aliquot (~50 µL) of the culture was pipetted onto a glass slide (the remaining culture was placed in a warm bath at 37°C), with a second slide the droplet of culture was smeared thinly over the first slide. The slide was gently blow-dried, with a hairdryer. Once dried, the slide was submerged in 100% methanol (MeOH) for 10 s to fix the cells onto the slide. Excess MeOH was removed by tapping the end of the slide on a paper towel and blow-dried. The slide was submerged in a solution of Giemsa stain, a 1:7 ratio of Giemsa to distilled water (dH₂O), for 5-6 min. The excess Giemsa solution was rinsed off with water and the slide blow-dried. A small drop of microscope oil was placed in the middle of the slide and viewed under a light microscope (Zeiss West Germany Light Microscope) with 40X and 100X magnification. Images of Giemsa stains were taken by an Olympus BX41 Light Microscope with an Olympus U-TVIX-2 camera using Life Sciences analySIS Olympus Software Image. The parasites stain dark blue within the erythrocytes and are clearly visible with the morphology also distinct for each stage.

The percentage parasitemia is an indication of the number of infected erythrocytes and was calculated, during culturing (or when indicated), using the following formula according to the SOP protocol of the Biochemistry Department:

$$\% \text{ Parasitaemia} = \frac{\# \text{ of } iRBCs}{\text{Total \# of RBCs counted}} \times 100$$

Where iRBC is the total number of infected erythrocytes and the total number of erythrocytes is the addition of the number of infected and uninfected erythrocytes counted. The parasitemia was calculated from a minimum count of 500 cells.

2.1.4 Washing of Erythrocytes

Whole blood was collected in CPDA-1 single BPU 500 mL blood bags and stored at 4°C overnight. The blood was aliquoted equally (~40 mL) into sterile 50 mL tubes and centrifuged for 10 min at 2500 g. The plasma and buffy coat were removed using a sterile plastic pasture pipette. The red blood cell pellet was washed with 10 mL of sterile PBS, centrifuged for 10 min at 2500 g and the supernatant and any remaining buffy coat were discarded; this process was repeated a number of times (5-6) until the erythrocytes were free of any remaining buffy coat. The remaining pellet of pure erythrocytes was re-suspended in AlbuMax-II-deficient (incomplete) culture medium (ICM) to obtain a 50% Hct. The washed erythrocytes were stored at 4°C and kept for use for a period of 3 to 4 weeks. The erythrocytes were pre-heated in a warm bath at 37°C for 30 min, when required for any procedure involving the parasite culture (72).

2.1.5 Working Sterile

It was of the utmost importance to carry out all procedures in strict sterile conditions to prevent any bacterial or fungal contamination of the parasite cultures. The culture medium solutions were made with autoclaved distilled double deionised water (dddH₂O). The PBS and sorbitol solutions were made with ddH₂O. The solutions used for culture medium were sterile filtered using sterile 0.2 µm filters and sterile syringes. PBS and sorbitol solutions were sterilised by autoclave.

All procedures involving the parasite culture were carried out in a sterile laminar flow cabinet within a sterile laboratory. Solutions of 1% SDS and 70% Ethanol (EtOH) were used to clean the working surfaces. A paper towel, soaked with 70% EtOH, was used to wipe the edges of the culture medium, PBS and sorbitol bottles after they were used; as well as for wiping clean the culture flasks. A new sterile pasture pipette was used for every measurement to prevent contamination of solutions.

2.1.6 *Sorbitol Synchronisation of a Non-Homogeneous 3D7 Culture*

A non-homogeneous culture of parasites, included all stages of the asexual life cycle, was grown, in a 10% Hct, until a parasitemia of 5-10% was reached, with majority (> 50%) of the parasites in the ring stage. This was confirmed with Giemsa staining before synchronisation. The 10 mL culture was then transferred to a sterile 50 mL tube and centrifuged at 2000 g for 2 min. The supernatant was discarded and 10 mL of 5% sorbitol, which was pre-heated in a warm bath at 37°C for 30 min, was added to the culture. The pellet was gently agitated to re-suspend the culture in the sorbitol and incubated in a warm bath at 37°C for 15 min; from time to time the culture was gently agitated by inversion to prevent sedimentation of the erythrocytes. The culture was centrifuged at 2000 g for 2 min and the sorbitol supernatant was discarded. The pellet was washed twice with 10 mL of ICM, which was pre-heated in a warm bath at 37°C for 30 min, and centrifuged at 2000 g for 2 min. A 1 mL of warm 50% Hct erythrocytes were added to each pellet to maintain a high hematocrit between 8-10% and re-suspended in 9 mL of warm ACM. Before the cultures were transferred back to the culture flasks, each of the flasks were rinsed twice with 10 mL of ICM to remove any of the remaining unsynchronised culture. Once the cultures were transferred to the flasks, they were gassed with 5% O₂, 5% CO₂ 90% N₂ for 15-30 s then incubated at 38°C in a shaking incubator at 60 rpm (73).

This procedure was performed 3-4 hours after schizont rupture (or hours post infection –hpi) and again when the parasites had reached 18-22 hpi of the same life cycle. These two synchronisation procedures were done to obtain a 3-4 hour merozoite egression window period to obtain the maximum concentration of merozoites.

2.1.7 *Isolation of Synchronised Cultures*

(a) *Preparation of the MAC Column*

The VarioMACS magnetic separator (Miltenyi Biotech), illustrated in Figure 2.1 (74), was sterilised with 70% EtOH and placed under the laminar flow cabinet. The MAC magnetic separation column (CS+ column, MAC, Miltenyi Biotech) was assembled under the laminar flow cabinet and placed in the VarioMACS magnet. The column was first washed with 50 mL of 100% EtOH and the air bubbles were removed. Sterile ddH₂O was used to rinse the 100% EtOH from the column and then equilibrated with

~50 mL of ICM prior to the parasite cultures being introduced and for elution of non-retained erythrocytes. After isolation and harvesting of the trophozoite stages of the parasites, the column was washed in the reverse order, ICM first, ddH₂O and then 100% EtOH. The column was stored with 100% EtOH and parafilm over the openings of the column and the 3-way stopcock, to prevent contamination, and could be reused for 3-4 isolations.

(b) Isolation of Late Stage Trophozoites

Once cultures reached a parasitemia of 6-10%, and were at late stage trophozoites (~34-38 hpi) the infected erythrocytes were isolated from uninfected erythrocytes. Cultures were transferred to 50 mL tubes, centrifuged at 2000 g for 2 min and fresh ACM added. A slide was prepared by Giemsa staining with an aliquot of the cultures to determine the parasitemia and stage of parasite development. The cultures were slowly eluted through the prepared CS⁺ columns while in the high strength magnet, using ~25 mL of pre-heated ICM to ensure the entire culture was eluted through the column and to keep the column 'wet' and culture in medium. The flow-through (FT) of erythrocytes was collected and Giemsa stains were made to determine if any infected erythrocytes were being passed through the column. If so, the flow-through fraction would be passed through the CS⁺ column a second time.

After the elution process, the column with the captured trophozoites was removed from the VarioMACS and placed in a burette stand. The trophozoite stage parasitized cells were then washed from the column with pre-heated ACM and placed in 100 mL of pre-heated ACM. At this point, a sample of the eluent was Giemsa stained to confirm the purity and % parasitemia of the isolated parasites; 1 mL of the culture was transferred to a sterile microcentrifuge tube and centrifuged (Combi-Spin FVL 2400N Boeco Germany) at 700 g for 5-6 min. The pellet was used to make a Giemsa stained slide.

The parasites were then transferred to a 175 cm² culture flask with 900 µL of 10 µM E64, a protease inhibitor that selectively inhibits the rupture of the parasite vacuole membrane, which prevents the release of the merozoites from the schizonts. The culture was gassed for 90-120 s and incubated at 38°C for 12-14 h in a shaking incubator at 60 rpm (32).

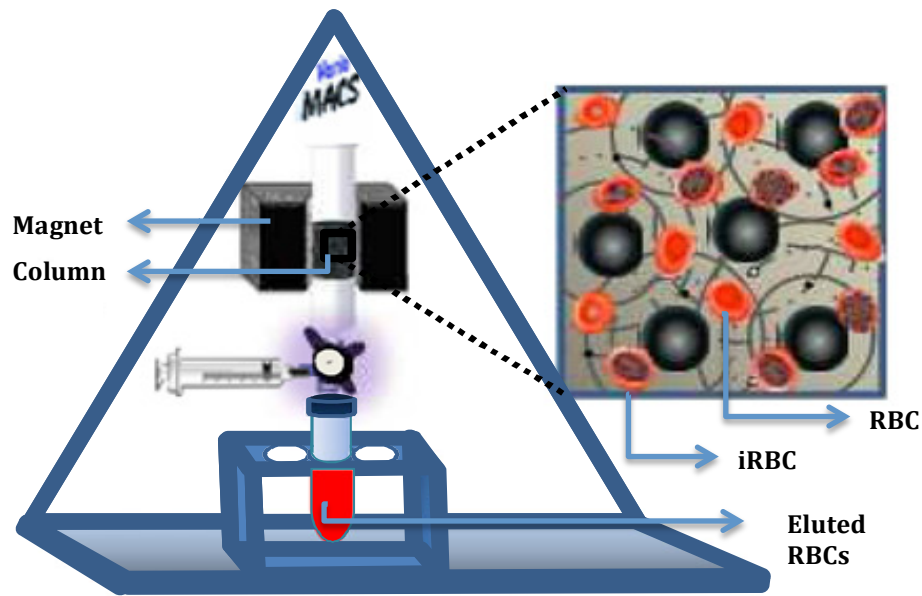


Figure 2.1 Set up of the VarioMACS magnetic separator. Late stage parasites (iRBC) become paramagnetic and can be captured by the column while in a strong magnetic field, while uninfected erythrocytes (RBCs) are eluted from the column. This image is an adaptation from Mata-Cantero *et al.* (2014) (74) with permission.

(c) *Isolation of Merozoites*

After approximately 12 h of incubation with E64, after isolation by magnetic capture, a Giemsa stain slide was made to determine if majority (~90%) of the parasites had developed into mature schizonts (~48 hpi). If not, parasites were gassed and incubated for an additional 1-2 h to allow younger schizonts to develop to maturity. Mature schizonts containing merozoites were transferred to 50 mL tubes, centrifuged at 2500 g for 5-6 min and the supernatant was discarded. Five millilitres of 0.15% saponin-PBS solution was added to the parasite pellet and gently vortex mixed (Wizard Advanced IR Vortex Mixer) for 30 s, to lyse the erythrocyte membrane, then incubated at 4°C for a further 10 min. The parasites were centrifuged at 2500 g for 5-6 min and the pellet was washed with 5 mL of PBS, centrifuged at 2500 g for 5-6 min. The pellet was washed with PBS twice and re-suspended in 5 mL of fresh PBS (75,76).

2.2 *Visualisation of Merozoite Maturation and Merozoite-Erythrocyte Invasion Sequence*

2.2.1 *Isolation of Schizonts and Merozoites*

Once the late trophozoites (~34-38 hpi) were isolated, as described in Section 2.1.7 (b), they were incubated at 38°C for ~12 h without E64. After the incubation a Giemsa stained slide was made to determine the development stage that the parasites had reached, late schizont (~44-48 hpi) or free merozoite stages. Once at the mature schizont or free merozoite stage, they were transferred to 50 mL tubes, centrifuged at 2500 g for 7 min and re-suspended in 3 mL of ACM with erythrocytes added to reach a 5% Hct, the use of a lower hematocrit was sufficient to induce and capture the invasion process. The culture was transferred to a 25 cm² culture flask, gassed for 15 s and incubated in the shaking incubator at 38°C for 5 min. A Giemsa stain slide was made to visualise if the merozoite-invasion sequence had taken place. This method was adapted from that described in Boyle *et al* (2010) (32).

The method of sample preparation for the transmission electron microscopy followed the in-house protocol for erythrocytes of the Laboratory of Microscopy and Microanalysis of the University of Pretoria.

2.2.2 *Fixation of Merozoites Invading Erythrocytes*

If Giemsa staining revealed initiation of merozoite invasion, then 1 mL of the culture was transferred to a sterile microcentrifuge tube, centrifuged at 700 g for 6 min and as much as possible of the supernatant aspirated and discarded. A 1 mL of a 2.5% glutaraldehyde/formaldehyde in 0.075 M phosphate buffer at pH 7.4 was added to the pellet. The pellet was re-suspended in the fixative solution and incubated at RT for 1 h. The sample was centrifuged at 700 g for 6 min, the supernatant discarded, the pellet re-suspended in 1 mL of 0.075 M phosphate buffer and incubated at RT for 15 min. This washing process was repeated three times. The sample was then fixed with 0.5% aqueous osmium tetroxide (SPI-Chem Suppliers) and incubated for 1 h. This step was done under a fume hood, as osmium tetroxide is volatile and toxic. The sample was then washed three times with 0.075 M phosphate buffer as described above (77).

2.2.3 *Dehydration*

Samples were dehydrated by sequentially treating for 15 min in each of the following concentrations of ethanol in dH₂O [30%, 50%, 70%, 90%, 100%, 100%, 100% - three 100% dehydration steps ensure optimal dehydration of samples] (78). After the last dehydration step the sample was centrifuged at 700 g for 5 min, the supernatant discarded and the pellet re-suspended in 1 mL of 100% EtOH overnight.

2.2.4 *Polymerisation*

A Quetol resin solution was prepared according to the recipe described in Appendix III Section A3.2.3. Quetol is an epoxy resin that aids the polymerisation process of the microorganism by completely permeating the sample.

The sample pellet was re-suspended in 1 mL of 50% (v/v) Quetol resin in 100% EtOH solution and incubated at RT for 1 h. This process was repeated with 100% Quetol resin solution and incubated at RT for 4 h. The sample was then centrifuged at 700 g for 5 min, the supernatant resin discarded and 1 mL of fresh resin added to the pellet, but not re-suspended, and then incubated at 60°C for 40 h.

2.2.5 *Preparation of the Copper Disc*

The polymerised samples were cut into 0.5 µm thin sections, at the Laboratory of Microscopy and Microanalysis at the University of Pretoria using an Ultracut E Ultramicrotome by Ms Antoinette Buys. The sections were placed on the shiny side of the copper discs, which were stained for 5 min in 4% aqueous uranyl acetate, rinsed in 3 small beakers of dH₂O by dunking the disc with a tweezers 20 times in each beaker and stained with Reynold's lead citrate solution (79) for 2 min, and rinsed again with dH₂O by dunking the disc with a tweezers 20 times in each beaker. These stains amplify the electron-scattering properties of the biological components of the sample.

2.2.6 *Visualisation*

The sections were then visualised in a Joel JEM 2100F Field Emission Electron Microscope with the use of the iTEM Olympus software. The microscope was operated at 200 kV and images captured were of the maturing schizont stage (~44-48 hpi) and of the invasion process of the free merozoites.

2.3. *Visualisation of Fluorescently Labelled PfAMA-1 of Merozoites*

2.3.1 *Fluorescent Labelling of PfAMA-1 Antibody*

Rabbit anti-PfAMA-1 (1F9) antibodies (Ab) were labelled with Cy3 (Abcam antibody labelling kit). A 100 μL aliquot of the 1 mg/ml PfAMA-1 Ab was pipetted into a sterile microcentrifuge tube and 10 μL of the modifier reagent (MR) was added, according to the following ratio [1 μL MR: 10 μL Ab] and mixed well. The Ab-MR solution was then added to the 30 μg of Cy3 powder, gently mixed and left over night at room temperature (RT) in the dark. The MR aids the binding of the antibody to the dye to form an antibody-dye conjugate. Then 10 μL of the quencher reagent (QR) was added, according to the following ratio [1 μL QR: 10 μL Ab], this inhibits the conjugation reaction to prevent any excess dye from binding to the antibodies. The labelled antibody was stored at 4°C.

2.3.2 *Fluorescent Labelling of Merozoites*

(a) *Isolation of Merozoites*

After the late trophozoites (~34-38 hpi) were isolated, as described in Section 2.1.7 (b), they were incubated for 12 h without E64. After the incubation, a Giemsa stained slide was made to determine the status of the schizonts and if the majority were showing merozoite egress. If not the culture was gassed again and incubated for an additional 1 h. The mature schizonts and free merozoites were transferred to 50 mL tubes, centrifuged at 4000 g for 5 min and re-suspended in 2-3 mL of ACM.

(b) *Preparation of Cover Slips for Confocal Microscopy*

(i) *Acid Wash*

Five to six coverslips were incubated at RT in 50 mL of 1 M HCl for 24 h to remove any impurities from the slides. The cover slips were washed with dH₂O three times for 10 minutes each, then washed three times with 95% EtOH.

(ii) *Lysine Coating*

With the use of a pair of tweezers, two of the six acid-washed cover slips (The remaining 4 cover slips were stored in a test tube) were placed in separate wells of a 6-well plate, (Greiner Bio-one Cellstar). The cover slips were incubated for 5 min with 1 mL of 0.1 mg/mL poly-L-lysine solution. The poly-L-lysine coated cover slips were

then washed three times with 2 mL of PBS and air-dried. Then 1 mL of isolated merozoite suspension was added to each of the coated cover slips and centrifuged (Heraeus Megafuge 40 Centrifuge Thermo Scientific) at 300 g for 3 min. From this step onwards, special care was taken to keep the cover slips from drying out to prevent cracks from forming in the adhered sample.

(iii) *Fixation*

The excess culture media was removed and 2 mL of 0.25% (v/v) formaldehyde (FA) solution added to each of the coated cover slips. They were then incubated at RT for 1 h to allow the parasites to fix to the cover slips. The excess fixative was removed and washed three times with 2 mL of a 0.1% (v/v) Tween-20 PBS (PBS-T) solution (80).

(iv) *Blocking and Ab Labelling*

The coated cover slips were blocked at RT for 1 h with 1 mL of 1% (w/v) bovine serum albumin (BSA) solution made up in PBS-T. The blocking buffer was removed and 1 mL of diluted Cy3 labelled Ab (Cy3-Ab) was added to each cover slip and incubated overnight at 4°C on a stable shelf or surface. The Cy3-Ab was diluted at a ratio 1: 400 in 0.1% (v/v) PBS-T solution (51).

(v) *DAPI Staining*

The excess Ab solution was removed and washed with 2 mL of PBS three times. DAPI (1 mM) was diluted in PBS at a ratio of 1:1000 and 1 mL of the diluted DAPI solution was added to each well with a cover slip and incubated in the dark at RT for 10 min. The DAPI solution was removed and washed with 2 mL of PBS three times. The cover slips were then mounted onto glass slides by placing a drop of Fluorshield (Sigma-Aldrich) on the glass slide and, with the use of a pair of tweezers, the coated side of the cover slip was carefully placed onto the drop of Fluorshield (81).

(vi) *Visualisation*

A Zeiss LSM 510 META confocal microscope with LSM 5 software was used to visualise and capture images of the labelled merozoites. The excitation wavelengths were set at 543 nm for Cy3 and 405 nm for DAPI by the assistance of Mr Alan Hall.

2.4 Proteomic Analysis of 3D7 Merozoites

2.4.1 SDS-PAGE

Merozoites were isolated, as described in Section 2.1.7 and washed three times with PBS to eliminate the excess AlbuMax II by centrifugation (Beckman Coulter Allegra X-22 Centrifuge) at 4000 *g* for 6 min. The parasites were then homogenised for 10 min with a power output of 40% and the pulser set between 20-30% for 5 minutes on a stepped micro-tip fitted Model 3000 Ultrasonic Homogeniser (BioLogics Inc. Manassas, USA).

A low volume BCA assay was performed in a sterile 96 well flat bottom plate (Greiner Bio-one Cellstar) to determine the protein concentration of the sample using the BioTek Synergy 2 or BioTek ELx 800 Plate Reader with the Gen5 2.03 software. The standards concentrations used in the assay can be found in Appendix II. A volume of 250 μ L of the BCA working solution was pipetted into each well, to which 5 μ L of each of the BSA standards was added, in triplicate. A volume of 5 μ L of PBS was used for the blank. Then a volume of 5 μ L of diluted (a half and quarter dilution) homogenised sample was added to the working solution (also in triplicate). The plate was covered and placed on a plate shaker for 5 min, to thoroughly mix the protein standards and sample with the working solution. After which, it was incubated at 60°C for 30 min. The plate was read at a wavelength of 570 nm. The final concentration of the sample was calculated using GraphPad Prism version 5.0a software.

An aliquot of the homogenised sample, with a final concentration of ~3 mg/ml (or ~75 μ g per well), was then used for the gel electrophoresis procedure. The samples were prepared in Laemmli sample buffer. Two sets of identical samples, including the isolated merozoite proteins (3 mg/mL), *Pf*AMA-1 antibody (3 mg/mL) as the positive control and BSA (2 mg/mL) as the negative control of the *Pf*AMA-1 antibody were used. To one set of samples, Laemmli sample buffer with 5% (v/v) β -mercaptoethanol was added to reduce the disulphide bonds. To the second set of samples, Laemmli sample buffer without any reducing agent was added, in order to keep the structural integrity of the disulphide bonds. The samples were incubated at ~98°C for 10 min in a water bath, to denature the tertiary and secondary structures of the protein. A 4-20% gradient SDS-PAGE 'Stain-free' Criterion midi size gel (Bio-Rad) was used to carry out

the electrophoretic separation of the sample proteins. A volume of 25-30 μL of the sample was pipetted into individual wells and 10 μL of the Bio-Rad Precision Plus Protein All Blue Standard for the molecular weight (MW) standards was added to at least one lane. A 1x Tris base running buffer was used and the samples were run under reduced (5% (v/v) β -mercaptoethanol Laemmli sample buffer) and non-reducing (Laemmli sample buffer without β -mercaptoethanol) conditions. Once the samples and standards were loaded, the gel was run for 15 min at 60 V and then for 60 – 90 min at 120 V using the Bio-Rad Mini-Protean System with a Hoefer PS 300-B power supply. Bands were visualised using Bio-Rad Gel Doc EZ Imager, then stained with Coomassie blue stain overnight followed by destaining. The gels were again visualised using the white plate in the Gel Doc EZ Imager. The gels that were not used for western blotting were then stored in 20 mL of fixing solution at RT for 30 days.

2.4.2 *Western Blotting*

(a) *Protein Transfer*

The ‘Stain free’ gels were then blotted onto midi size PVDF membranes (Bio-Rad) for 10 min using the semi-dry Bio-Rad Trans Blot Turbo Transfer System, using the mixed MW or high MW protocol set at 2.5 A and 25 V. The membranes were then stained with Ponceau S solution to confirm that the proteins had been transferred from the gels and then de-stained by washing with dH_2O .

(b) *Blocking of Membrane*

The membranes were transferred to 50 mL tubes, with the use of a tweezers. One set of membranes were blocked with 5 mL of 2% (w/v) milk solution and one set with 5 mL of 2% (w/v) BSA solution, both solutions made in Tris base solution with 0.2% (v/v) Tween-20 (TBS-T), at RT for 1 hr on a test tube roller. Each membrane was then washed with 5 mL of TBS-T for 5 min; this wash step was repeated three times.

(c) *Binding of Ab*

The primary PfAMA-1 Ab was diluted in a 2% (w/v) BSA-PBS-T-sodium azide solution in a 1:2000 ratio. The membranes were incubated at 4°C in 5 mL of the primary Ab solution overnight. The primary Ab solution was removed and the membranes washed with 5 mL of TBS-T for 5 min, this wash step was repeated three

times. The secondary Ab was a goat anti-rabbit IgG conjugated with horseradish peroxidase (Santa Cruz Biotechnology), which was diluted in a 2% (v/v) BSA-TBS-T solution in a 1:5000. A volume of 5 mL of the diluted antibody solution was added to each membrane and incubated with agitation at RT for 1 hr, then washed four times with 5 mL of TBS-T for 5 min each.

(d) Visualisation

Each membrane was incubated for 5 min in Clarity Western ECL substrate solution (Bio-Rad) and visualised, by means of chemiluminescence, using Bio-Rad ChemiDoc XRS+ System with the auto exposure setting or 10 sec data collection time.

2.4.3 In-gel Digestion

This method followed the standard protocol for in-gel digestion as modified by the Bioscience Department at the CSIR (82). This was done to digest the merozoite proteins and extract the peptides from the gel, for LC-MS/MS analysis of the merozoite proteome in order to identify *PfAMA-1*.

(a) De-staining of Bands

Bands were selected from the MW regions according to the MW of the *PfAMA-1* fragments (*PfAMA-1*₈₃, *PfAMA-1*₆₆ and *PfAMA-1*_{48/44}). The selected bands were excised from the Coomassie stained SDS-PAGE gels run as described in Section 2.4.1, were diced into small cubes using a new ethanol wiped scalpel blade ~1 mm x 1 mm and placed into 0.5 mL Lo-Bind (Merck) Eppendorf tubes (each marked clearly according to lane number and MW of bands). These Lo-Bind eppendorf tubes are ideal for protein digestion experiments as they minimise the binding of proteins/peptides to the surface of the tubes and therefore, maximise peptide recovery. Then 200 µL of 50 mM NH₄HCO₃/50% MeOH solution was added to each tube and incubated at 24°C for 20 min in a Thermomixer (Thermomixer Comfort) at 1500 rpm, after which the supernatant was discarded. This step was repeated three times. Then 100 µL of 75% acetonitrile (ACN) was added and incubated at 24°C for 20 min in a Thermomixer at 1500 rpm, after which the supernatant was discarded. This step was repeated 2-3 times until the gel pieces were completely colourless. The samples were then vacuum dried using a Speedvac (CentriVap Concentrator and CentriVap Cold Trap, LABCONCO).

(b) *Reduction and Alkylation*

The gel residue was then resuspended in 25 μL of 10 mM dithiothreitol (DTT) solution and the samples vortex mixed (Spinmix Gallenkamp) for 3 min and incubated in the Thermomixer at 60°C for 1 h. The samples were allowed to cool to RT. Then 500 μL of 100% ACN was added and samples incubated at RT for 10 min. The supernatant was discarded and 25 μL of 50 mM iodoacetamide (IAA) was added, vortex mixed for 3 min and incubated at RT in the dark for 20 min. The supernatant was discarded. Then samples were washed with 100 μL of 50 mM NH_4HCO_3 – H_2O solution and vortex mixed for 10 min. The supernatant was discarded and 100 μL of 25 mM NH_4HCO_3 – 50% ACN solution was added and centrifuged in a mini-centrifuge (Hermle 2100M) for 5 min. The supernatant was removed and the gel pieces were vacuum dried using the Speedvac as described above.

(c) *Trypsin Digestion*

Once the gel pieces were completely dry, 25 μL of 10 ng/ μL of sequence-grade trypsin was added and the samples were incubated on ice for 30 min. The samples were checked to see if the trypsin was still covering the gel pieces, if not more trypsin solution was added and incubated on ice for 1 h. The samples were then centrifuged, using a mini centrifuge, for 1 min and ~50 μL of 25 mM NH_4HCO_3 – 50% ACN solution was added to cover the gel pieces, centrifuged for 1 min and then incubated in a water bath (Mettmert) at 37°C overnight (\pm 16 h.).

(d) *Extraction of Peptides*

The digestion solution was transferred to a new 0.5 mL Lo-Bind tube and placed on wet ice. Then 300 μL of 50% ACN/ 5% formic acid solution was added to the gel pieces, vortex mixed in the Thermomixer for 30 min, centrifuged for 5 min, sonicated (Ultrasonic UMC 2 Integral Systems) for 5 min and the solution added to the initial digestion solution. This process was repeated twice more. The gel pieces were then discarded and the combined digestion solution and gel extracts vacuum dried using the Speedvac as described above. Samples were stored at -20°C until LC-MS/MS analysis.

2.4.4 *In-solution Digestion*

Merozoite samples were obtained as described in Section 2.1.7; two samples were isolated on separate occasions, to one sample a cocktail of protease inhibitors of 10 μ M E64 (Sigma-Aldrich), 1 mM EDTA (Sigma-Aldrich) and 1 mM PMSF (Sigma-Aldrich), was added. EDTA is a metal chelator that inhibits metalloproteases and PMSF is a serine protease inhibitor. The second sample was free of EDTA and PMSF. The in-solution digestion method and LC-MS/MS analysis followed the in-house protocols of the Bioscience Department at the CSIR.

(a) *Acetone Precipitation*

A volume of 80 μ L of the 12 mg/mL merozoite protein sample was centrifuged (Biofuge 13 Heraeus Instruments) at 4°C for 10 min at 14 000 g and 40 μ L of the supernatant was transferred to a 0.5 mL Lo-Bind tube. Then 160 μ L of cold (-20°C) acetone (Sigma Life Sciences) was added to the samples, vortex mixed and incubated at -20°C for 60 min. The samples were then centrifuged at 4°C for 10 min at 14000 g and the supernatant removed. To allow the remaining acetone to evaporate, the samples were left to dry at RT for 5 min. To the pellet, 40 μ L of 5 M urea in 50 mM $\text{NH}_4\text{HCO}_3 - \text{H}_2\text{O}$ solution was added. The pellet was re-suspended by vortex mixing for 30 s and sonicated for 5 min; this resuspension step was repeated twice. The sample was centrifuged for 5 min at 14 000 g and the supernatant was transferred to a new 0.5 mL Lo-Bind tube. A standard Bio-Rad Bradford assay was carried out on the sample to determine the protein concentration. The assay was conducted in duplicate with BSA used as the standard (with concentrations of 2, 1.5, 0.75, 0.5, 0.25 and 0.125 mg/ml) and the urea buffer as the blank. A volume of 5 μ L of the standard, the urea buffer or sample were added to 250 μ L of Bradford solution in a 96-well plate, which was incubated for 5 min at RT in the dark and read at a wavelength of 595 nm. The sample protein concentration was calculated using Microsoft Excel 2011 version 14.6.9.

(b) *Reduction and Alkylation*

In order to reduce the sample a 100 μ g of the total protein sample was transferred to a new 0.5 mL Lo-Bind tube (~50 μ L) and 40 μ L of 5 M urea in 50 mM $\text{NH}_4\text{HCO}_3 - \text{H}_2\text{O}$ solution was added. A volume of 45 μ L of 0.2 M DTT in 50 mM $\text{NH}_4\text{HCO}_3 - \text{H}_2\text{O}$

solution was added to the samples to achieve a final concentration of 10 mM DTT and incubated at RT for 30 min.

Following the reduction process, the proteins were then alkylated by adding a volume of 5.7 μL of 0.5 mM IAA in 50 mM $\text{NH}_4\text{HCO}_3 - \text{H}_2\text{O}$ solution to the samples, as a final concentration of 30 mM IAA, and incubated at RT for 45 min. The samples were then diluted with 50 mM $\text{NH}_4\text{HCO}_3 - \text{H}_2\text{O}$ solution so that the Urea concentration was less than 1 M. Any excess IAA would be removed during C-18 clean-up (Section 2.4.4 d) or quenched with additional DTT to prevent N-alkylation of the peptides.

(c) Trypsin Digestion

Then 10 μL of 10 ng/ μL Trypsin was added to each of the samples. A ratio of 1:50 [Trypsin : Protein] was used to determine the volume of Trypsin needed for the digestion. The samples were incubated in a warm bath at 37°C overnight. A 20 μL aliquot of the sample was run on a SDS-PAGE gel to confirm that the samples had been completely digested. The samples were then split into two equal volumes, vacuum dried and stored at -20°C until LC-MS/MS analysis.

(d) C18 Digest Sample Clean-up

A protease inhibitor sample clean-up using an in-house protocol was performed by Mr Ireshyn Govender. SOLA μC18 columns were pre-equilibrated using 200 μL of 70% ACN and a pressure of 700 mbar, then the C18 columns were conditioned using 200 μL of 0.1% TFA and a pressure of 700 mbar. The sample was acidified by adding an equal volume of 0.1% TFA. The sample was then loaded at a pressure of 750-800 mbar and was washed using 2 x 200 μL of 0.1% TFA at a pressure of 700 mbar and then using 100 μL of 0.1% formic acid at a pressure of 700 mbar. The peptide sample was eluted using 2 x 25 μL of 70% ACN at a pressure of 750-800 mbar. The eluted sample was then split into two equal volumes and vacuum dried using the Speedvac as described above. The dried digests were stored at -20°C or re-suspended for LC-MS/MS analysis.

2.4.5 LC-MS/MS

All digests prepared in Sections 2.4.3 and 2.4.4 were re-suspended in 20 μL of a 2% acetonitrile and 0.2% formic acid solution and analysed using a Dionex Ultimate 3000 RSLC UHPLC system coupled to an AB Sciex 6600 TripleTOF mass spectrometer. Peptides were first de-salted on an Acclaim PepMap C18 trap column (20 mmx 100 μm) for 2 min at 15 $\mu\text{L}/\text{min}$ using 2% acetonitrile in 0.2% formic acid solution, then separated on Acclaim PepMap C18 RSLC column (150 mm x 300 μm , 2 μm particle size). Peptide elution was achieved using a flow-rate of 8 $\mu\text{L}/\text{min}$ with a gradient: 4-60% of solution B in 15 min (Mobile phases: A: 0.1% formic acid; B: 80% acetonitrile/0.1% formic acid). An electrospray voltage of 5.5 kV was applied to the emitter; this voltage was optimum for microflow, which was checked during instrument optimisation using the standard peptide GluFib. The 6600 TripleTOF mass spectrometer was operated in Data Dependant Acquisition mode. The Precursor MS scans were acquired from m/z 400-1500 using an accumulation time of 250 ms followed by 30 MS/MS scans, acquired from m/z 100-1800 at 100 ms each, for a total scan time of 3.3 sec. Multiple charge ions (2^+ - 5^+ , with 400 -1500 m/z) were automatically fragmented in the Q2 collision cells using nitrogen as the collision gas. Collision energies were chosen automatically as a function of m/z and charge. Dynamic exclusion was set as: charge states of 2^+ to 5^+ , mass range of 360 to 1500 m/z , minimum of 200 cps, exclusion window of 30 s. Acquired MS and MS/MS scans were collected and processed to provide peak lists that were imported into ProteinPilot software for further analysis. This section was assisted and completed by Mr I Govender and Dr. Stoyan Stoychev at the CSIR.

ProteinPilot software Version5 using a Paragon search engine (AB Sciex) was used for comparison of the obtained MS/MS spectra with a custom database containing all known protein sequences of *Plasmodium falciparum* and *Homo sapiens* (UniProt/SwissProt), as well as a list of sequences from common contaminating proteins. Only proteins with a confidence threshold above $\geq 99.9\%$ were then reported (83).

The raw data (wiff.) files obtained from the MS/MS analysis were converted to mgf. files using MSConvertGUI to be processed through SearchGUI 3.1.0 and Peptideshaker

1.13.1 (84) to compare and confirm the identification of the proteins, specifically *PfAMA-1*, from the ProteinPilot results. Three search engines, X!Tandem, Comet and MS-GF+, were used to compare the MS/MS spectra with the target database of sequences from UniProt/SwissProt used in the ProteinPilot search. Peptideshaker was set to the following modifications; a fixed modification of the carbamidomethylation of cysteine and the variable modifications were oxidation of the methionine, sodium adduct to aspartic and glutamic acid, acetylation of the N-terminal and pyrrolidone formation of N terminal glutamine and glutamic acid residues.

The *PfAMA-1* peptides identified from the two datasets (ProteinPilot and Peptideshaker) were processed through BLAST (<http://blast.ncbi.nlm.nih.gov/Blast.cgi>) using a protein-protein blast (pblast). The peptides were compared against the UniProt/SwissProt database using the *Plasmodium* and *Homo sapiens* proteins to confirm that the peptides were unique to *PfAMA-1* and not peptides of a human protein that was incorrectly identified.

Chapter 3

3. Results and Discussion

3.1 Isolation of Highly Synchronised Parasite Cultures

3.1.1 Culturing Parameters for Synchronised Cultures of 3D7s

In order to achieve a highly synchronised parasite culture, the 3D7 parasites were cultured from a starting parasitemia of 0.5-1% of unsynchronised parasites in a 25 cm² culture flask with fresh erythrocytes in albumin enriched culture medium.

It was observed that culturing the parasites at a higher hematocrit of 10%, compared to previously described culturing methods, where cultures were grown at a haematocrit of between 3-5% by Boyle *et al.* (2010) (32) and 1-1.5% by Radfar *et al.* (2009) (72), lead to more invasions by the merozoites, which increased the parasitemia at a faster rate. As merozoites are not motile organisms (85), they depend on the circulation of the blood system to move them into close contact with the erythrocytes in order for them to invade the host cell. Therefore, increasing the hematocrit of the culture, which increases the number of erythrocytes in culture, increases the chances of each merozoite coming into contact with an erythrocyte, resulting in a higher parasitemia.

Culturing 3 to 4 flasks of 10 to 15 mL parasite cultures simultaneously allowed for higher numbers of merozoites to be harvested from 10% parasitemia cultures, which yielded a combined protein concentration of ~12 mg/mL. These results are comparable with those obtained by Li *et al.* (2003) (86), where parasites were cultured at a high hematocrit of 45 to 100% Hct in 17.5 mL of culture medium, using hollow-fibre capillary bioreactors which yielded high numbers of parasitised erythrocytes (5.5×10^9 – 1.2×10^{10}) from cultures grown at 7 to 8% parasitemia. The method described by Radfar *et al.* (2009) (72), achieved only 1.17×10^{10} parasites from a 60% parasitemia culture in the lower hematocrit levels (1-1.5%) from volumes of ~300 mL of culture medium, obtaining a parasite protein concentration of ~1.2 mg/mL.

Multiple cultures were split from an unsynchronised culture, containing the diverse stages of the asexual intraerythrocytic life cycle as indicated in Figure 3.1, once the cultures had reached a parasitemia of 3 to 5%. Cultures were monitored for two cycles

of their life cycle to determine when cultures contained a higher percentage of ring stage parasites, between 2 to 4%, for synchronising.

The cultures were synchronised twice (See Section 2.1.6), once at 3-4 hpi of the life cycle and a second time at 18-22 hpi of the same life cycle, to decrease the period of time between schizont ruptures. Theoretically, this method of synchronisation should achieve a merozoite egression window of 3 to 4 hours as any parasites older than 22 hours would be eliminated during the sorbitol treatment. However, this method resulted in a merozoite egression window of approximately 6 hours, which was determined by the observation of the presence of trophozoites between the 32-38 hpi stage of the life cycle. Taking into consideration that the parasite growth rate could differ between individual parasites, would account for the observed increased egression window, and compared to previous studies that obtained an 18 hour window from a single sorbitol synchronisation step (73), a double sorbitol treatment in a single life cycle proved to be a better method to achieve a narrower egression window period. It was also observed that synchronising mixed cultures of 10% parasitemia, with ring stages accounting for more than 5% parasitemia, proved to be difficult as not all the trophozoite and schizont stage infected erythrocytes would lyse during the sorbitol treatment, which increased the merozoite egression window to over 10 hours between schizonts releasing their merozoites. This was determined during the pilot study of this investigation.

The first phase of synchronisation was performed at 3 to 4 hours after the majority of the schizonts had burst or 3-4 hpi, allowing invading merozoites to develop into early rings, as indicated in Figures 3.2A and B. The second phase of synchronisation was achieved when the parasites had matured to between 18-22 hpi of the ring stage, which is indicated in Figure 3.2C. As the sorbitol treatment lysed erythrocytes infected with parasites between 22-48 hpi of the life cycle (that is the trophozoite and schizont stages), the parasitemia of the cultures decreased to ~2%, so the parasites were allowed to multiply through 3 or 4 life cycles and monitored every 24 hours until the desired parasitemia of 10% was reached prior to isolation.

In some cases a small percentage of the parasites developed outside of the 6 hour window period, therefore the cultures were synchronised for a third time at 3-4 hpi and allowed to mature through a complete life cycle before being isolated in the next life cycle.

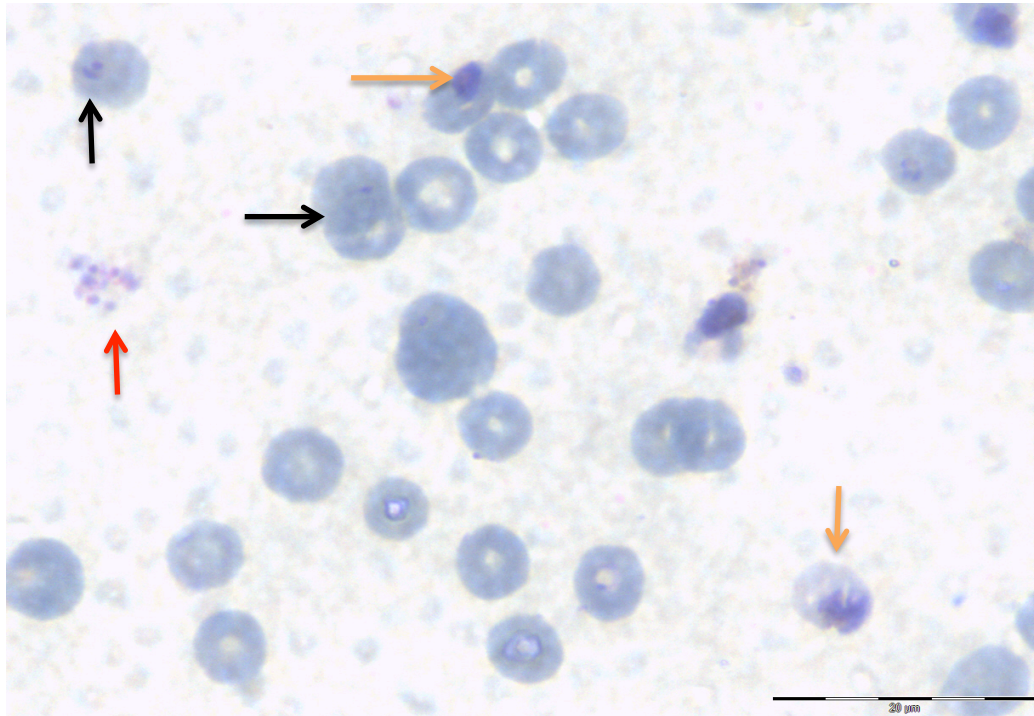


Figure 3.1 Giemsa stain of unsynchronised culture. The heterogeneous stages of *Plasmodium falciparum* asexual intraerythrocytic life cycle. The black arrows indicate ring stages. The orange arrows indicate trophozoite stages. The red arrow indicates merozoites bursting from a schizont. Image was taken at 100X magnification with 20 µm scale bar.

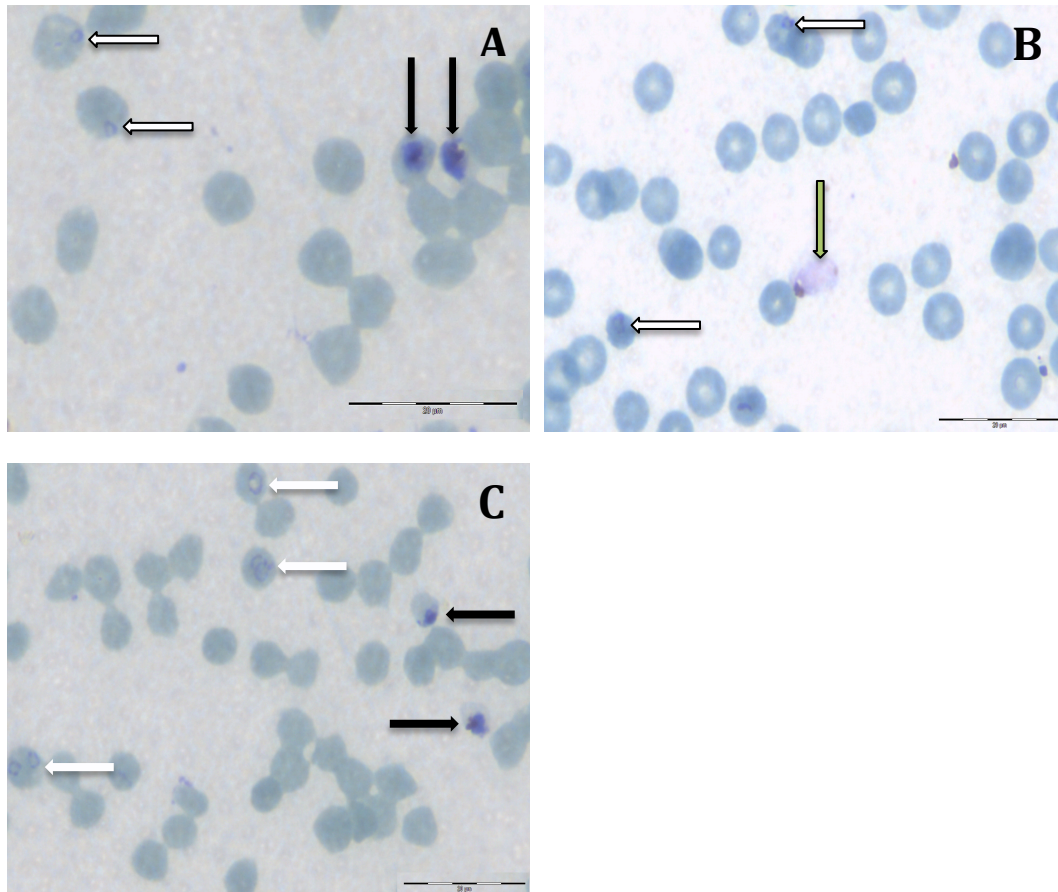


Figure 3.2 Synchronisation. **A** represents the unsynchronised culture before the first synchronisation: the white arrows indicate young rings ~3-4 hpi. The black arrows indicate late stage trophozoites ~30-34 hpi. **B** shows the culture after sorbitol lysis, where the green arrow indicates a lysed trophozoite containing erythrocyte. **C** represents the culture before the second synchronisation, where the white arrows indicate late rings ~18-22 hpi. The black arrows indicate early stage trophozoites ~26-30 hpi. Images were taken at 100X magnification with 20 µm scale bar.

The use of sorbitol as a method of synchronisation for malaria parasites depends of the mechanism of osmotic lysis, where sorbitol molecules move through a selectively permeable membrane causing the cell to burst (87). As the parasites develop from their late ring stage onwards, the membrane of the infected erythrocytes begins to alter and its permeability becomes less selective toward various solutes (68), making it susceptible to osmotic forces (73). Sorbitol acts as a hyperosmotic solution, this allows the sugar molecules, followed by water molecules, to move across the altered membrane of the later parasite stage infected erythrocytes causing them to swell and burst, thus eliminating the more advanced stages of the parasites from the culture, a basic illustration of this is seen in Figure 3.3 C. For sorbitol solutions to induce the selective

lysis of infected erythrocytes, their osmolality must range between 141 to 855 mOs/kg; a 5% sorbitol solution has an approximate osmolality of 287 mOs/kg (73).

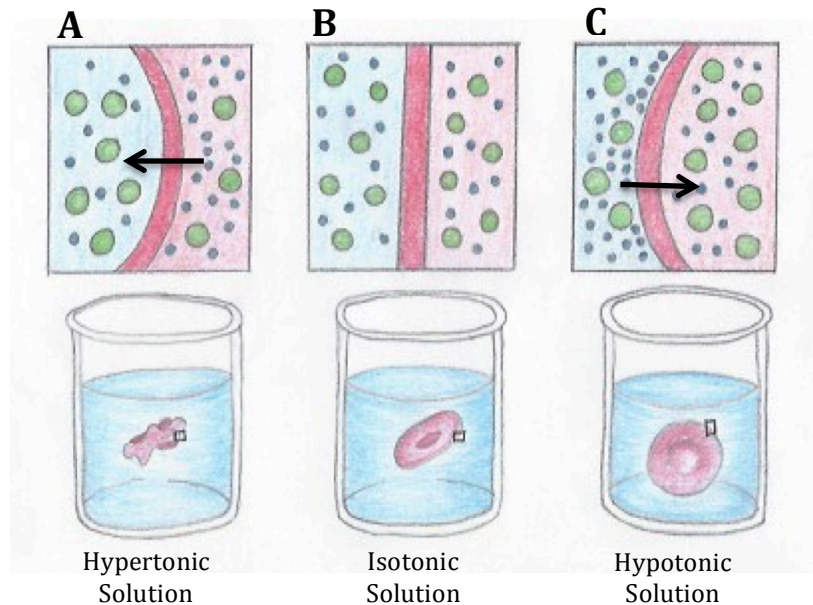


Figure 3.3 Response of erythrocytes to different osmotic pressures. **A** illustrates when an erythrocyte is placed in a hypertonic solution, water molecules move out of the cell and it shrinks. **B** illustrates the effects an isotonic solution has on an erythrocyte, no net movement of water molecules. **C** illustrates when an erythrocyte is placed in a hypotonic solution, water molecules move into the cell; it swells and bursts. **C** illustrates the effect of sorbitol on infected erythrocytes.

As suggested by Radfar *et al.* (2009) (72), the cultures were not synchronised more than three times as the sorbitol treatment impairs the membranes of the uninfected erythrocytes as well, consequently reducing merozoite invasion. Therefore, after each synchronisation phase it was important to add the additional volume of uninfected erythrocytes to not only introduce fresh, unaffected erythrocytes, but to maintain the high hematocrit, as it was observed that both played an important role in increasing the invasion rate of free merozoites.

As cultures multiplied to parasitemia levels between 6 to 10%, after synchronisation, an additional volume of 3-5 mL of AlbuMax-II complete medium was supplied to the parasites and the hematocrit was decreased to 6-8%. This was important as cultures at a higher parasitemia produce higher concentrations of their by-products, which are toxic to the parasites and impair their development. Therefore, the additional medium diluted

the concentration of metabolic waste products and their detrimental effect, but also maintained the high hematocrit levels for merozoite invasions, and supplied sufficient fresh nutrients to the developing parasites (88).

3.1.2 *Isolation of Merozoites*

Synchronised parasites were isolated at their late trophozoite stage, ~34 to 38 hpi by magnetic separation. This has been proven to be an effective method of isolating the infected erythrocytes from uninfected erythrocytes (74,89), as is visible in Figure 3.4, where the population of late trophozoites is more concentrated after isolation, with an extremely low number of uninfected erythrocytes that become trapped in the column.

This technique takes advantage of the paramagnetic hemozoin crystals found in the food vacuole of the parasitised erythrocyte (90). The hemozoin is a by-product of the digested haemoglobin that the parasite uses as a source of protein during its development. The formation of the hemozoin climaxes during the development of the trophozoites (91), and the presence of this paramagnetic crystal by-product of haemoglobin was used to optimise the isolation of the parasites.

The cultures were passed through a column twice while placed in a strong magnetic field, and after each elution a Giemsa stain was performed to determine whether any infected erythrocytes had been eluted through the column. For conformation of improved isolation, Figure 3.5 displays the flow through of the remaining culture, in which the uninfected erythrocyte population are of the highest concentration.

With higher percentage parasitemia cultures, between 6 to 10%, approximately 0,5% of parasites were eluted after FT₁ and approximately 0,1% after FT₂, which is indicated in Figure 3.5. With cultures at a parasitemia of 3 to 5% only one capture step was required. Determining the FT- parasitemia also provided a means of testing the capturing ability of the column, if FT-parasitemia was above 2% a new column was then used for isolation.

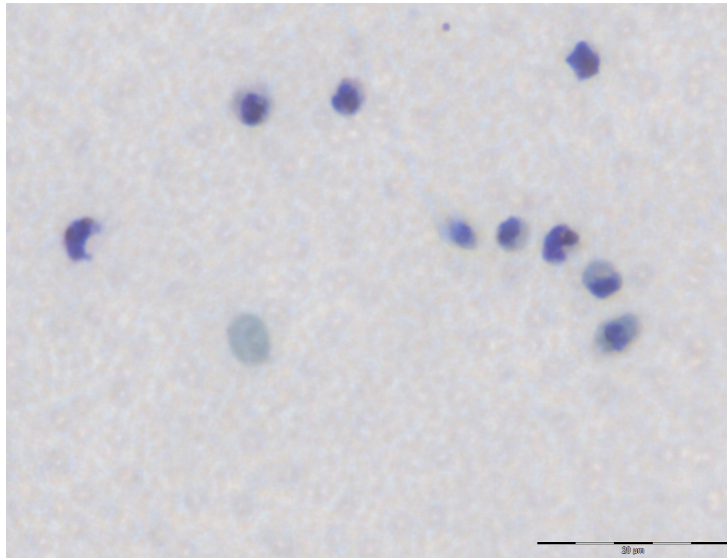


Figure 3.4 After magnetic isolation. Late trophozoites (~34-38 hpi) were isolated from uninfected erythrocytes. Images were taken at 100X magnification with 20 μm scale bar.

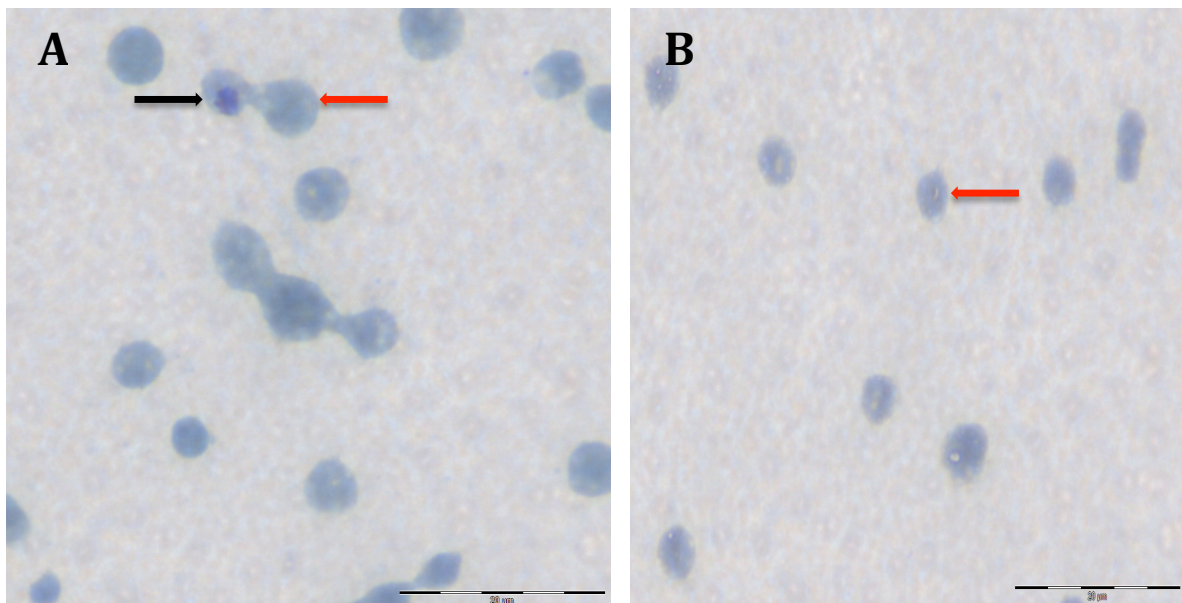


Figure 3.5 The eluted sample fractions showing the low numbers of parasitised erythrocytes that were not retained by the column. **A** represents the FT_1 of the eluted culture where a small percentage of the parasites (black arrow) escape the column. **B** represents FT_2 once the culture has been passed through the column a second time, with uninfected erythrocytes (red arrow) remaining and $\sim 0,1\%$ of infected erythrocytes. Images were taken at 100X magnification. Scale bar = 20 μm .

The late stage trophozoites were incubated for 12 to 14 hours to allow for maturation to schizonts, containing fully developed merozoites, which is clearly indicated in Figure 3.6. The isolated parasites were incubated with 10 μM of E64 in order to prevent the egression of the merozoites from older schizonts, allowing the slower maturing schizonts to develop further into mature merozoites. However, the results of the E64-treated parasites obtained from Giemsa stains did show numerous free merozoites, indicating that the E64 was not completely effective at inhibiting the merozoite egress. Due to this premature rupturing of schizonts only 70 to 80% of the parasites were allowed to mature before being treated with saponin. This was done to prevent the loss of viable merozoites and therefore reducing the ability to isolate *PfAMA-1*. On a separate occasion, a synchronised culture of isolated parasites was incubated with 20 μM of E64 to determine if a higher concentration of E64 would prevent the premature rupturing of schizonts. This high concentration of E64 proved to be fatal to the development of the late trophozoites into schizonts, as indicated in Figure 3.7.

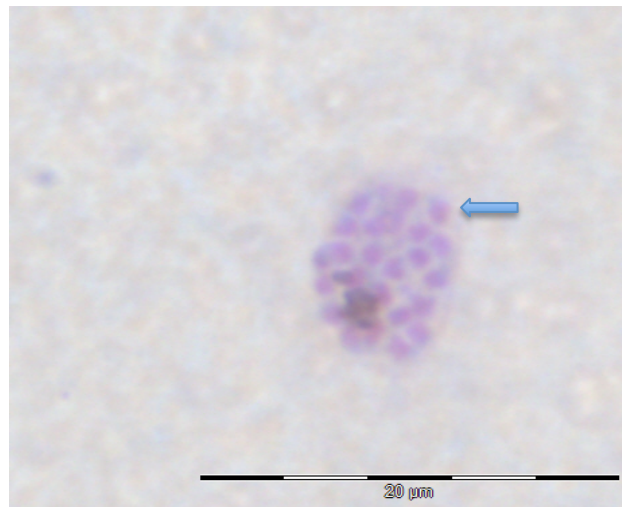


Figure 3.6 After incubation with 10 μM E64. A mature schizont where merozoites are clearly visible as indicated by the blue arrow. Image was taken at 100X magnification. Scale bar = 20 μm .

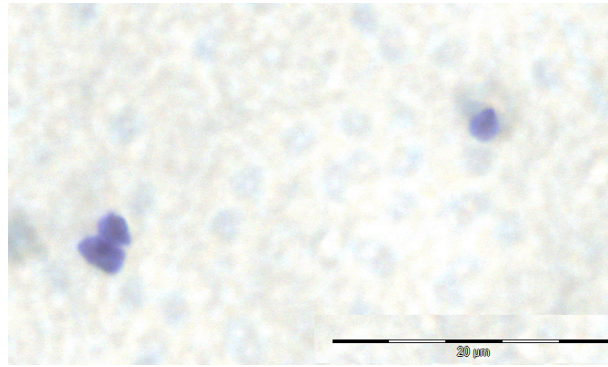


Figure 3.7 Incubation with 20 μM of E64. Parasites die within the erythrocyte and cellular contents condenses. Image was taken at 100X magnification. Scale bar = 20 μm .

E64 is an epoxide-based cysteine protease inhibitor that is reported to selectively inhibit the rupture of the parasite vacuole (PV) membrane, prohibiting the egression of the merozoites. Although the membrane of the infected erythrocyte degrades once the schizont develops functional merozoites, the E64-treated PV membrane remains intact allowing for a higher concentration of merozoite-schizont clusters for harvesting large numbers of merozoites (43). However, the results of the incubation procedure, with 10 μM E64, of this study did not correlate with previous studies by Boyle *et al.* (2010) (32), and Salmon *et al.* (2001) (43), where large clusters of unruptured merozoite containing schizonts were observed.

A possible reason, that could account for the difference in the results acquired in this study to those described in the above-mentioned research, would be the incubation period. There was a 4 to 6 hour difference between the incubation period of this study to Boyle *et al.* (2010) (32) and Salmon *et al.* (2001) (43), where parasites were incubated for 6 to 8 hours and \sim 8 hours with 10 μM E64, respectively, compared to the 12 to 14 hour incubation period of this study which could have caused a decrease in the inhibiting activity of E64.

In order to harvest the merozoites from the schizonts, a saponin lysis method, modified from Sanderson *et al.* (1981) (75) and Delplace *et al.* (1987) (76), was preferred to the filtration method described by Boyle *et al.* (2010) (32). Filtration of schizonts from such high parasitemias proved ineffective, as the filter became clogged from membrane debris and trapped the free merozoites, resulting in a decreased concentration of isolated

merozoites. In comparison, saponin lysis allowed for harvesting of all merozoites released from schizonts. However, a limitation associated with saponin lysis was that it affected the subsequent invasion ability of the merozoites and therefore was not used for harvesting merozoites for the confocal microscopy and TEM experiments of this study.

During all procedures involving the parasite cultures, it was important to maintain the temperature of the cultures at $\sim 37^{\circ}\text{C}$, as a decrease in temperatures to below 22°C reduces the development of the ring stage parasites (92), and therefore increases the merozoite egression window. As a result of this effect, all solutions involved in parasite experiments were pre-heated before coming into contact with the cultures and when cultures were removed from the shaking incubator, they were incubated in a warm bath at 37°C during all procedures.

3.2 *Visualisation of Plasmodium falciparum Merozoites*

3.2.1 *TEM of Merozoite Maturation and Merozoite-Erythrocyte Invasion Sequence*

The parasites were isolated from synchronised cultures of approximately 5% parasitemia with a merozoite egression window of about 6 hours but without E64 incubation, allowing the merozoites to develop, mature and egress from the schizonts naturally.

Once the incubated parasites had been pelleted and re-suspended in fresh AlbuMax-II complete medium, a small aliquot was added to a small culture flask with 3 mL of AlbuMax-II complete medium with a 5% Hct, gassed for 15 seconds and incubated in a shaking incubator for 5 minutes. This allowed the free merozoites to invade fresh erythrocytes under normal culturing conditions. A Giemsa stained slide from an aliquot of the sample was made to determine if the merozoite invasion sequence process had occurred.

Figure 3.8 clearly indicates the success of capturing the invasion sequence, with free merozoites observed in Figure 3.8A, and a merozoite attached to an erythrocyte in Figure 3.8B. A merozoite can be seen in the process of invading an erythrocyte with indentations clearly visible in the erythrocyte membrane in Figure 3.8C and lastly an invading merozoite completely within an erythrocyte in Figure 3.8D.

This method was modified and optimised from the research on viable merozoites by Boyle *et al.* 2010 (32), where the invasion ability of merozoites were tested under a number of different culturing parameters. During the optimisation process of this study, the merozoites were isolated from a 3% parasitemia culture and added to 1 mL of incomplete culture medium with a 1% Hct in an Eppendorf tube and initially incubated at 37°C in a warm bath for 2 to 3 minutes. However, after producing a Giemsa stain of the experiment, no invasion was observed, therefore the incubation period was increased to 5 minutes. From a 5 minute incubation period, invasion was observed, however the entire sequence as illustrated in the images of Figure 3.8A-D were not detected, as the invading step indicated in Figure 3.8C could not be captured. Therefore, after careful consideration, it was decided that the merozoites should be isolated from a culture with at least a 5% parasitemia, incubated under normal culture conditions with a 5% Hct and without the use of E-64 protease inhibitor. These conditions increased the number of merozoites undergoing the invasion process considerably and as a result the entire invasion sequence could be captured within the collected samples.

When invasion was observed in the isolated cultures, the culture was fixed with glutaraldehyde-formaldehyde fixing solution and prepared for TEM analysis. The results obtained from TEM captured the merozoite maturation process from ~44 hour schizonts, illustrated in Figure 3.9, to free merozoites, illustrated in Figure 3.13. The merozoite-erythrocyte invasion sequence is illustrated in Figures 3.14 to 3.17, however, the invading process seen in Figure 3.8C was not captured clearly in any of the TEM sections made.

Transmission electron microscopy provides researchers with an effective method of determining finer details of structural components of microscopic organisms (93). Figure 3.9A represents the asexual intraerythrocytic life cycle at approximately 44 to 45 hpi, clearly showing that the parasite has undergone a number of mitotic divisions to form 10 to 11 individual, but still under-developed merozoites.

In Figure 3.9B it was observed that the merozoites had started developing their various organelles, such as the nucleus, rhoptries and dense granules. By the 48th hour of the

parasite's life cycle, the schizont was completely occupied with 10 to 11 mature merozoites, as illustrated in Figure 3.10. Up to 25 individual merozoites were identified from the Giemsa stained samples, as indicated by the blue arrow in Figure 3.6. These observations were consistent with previously reported research (39), where as many as 32 individual merozoites have been identified originating from a mature schizont.

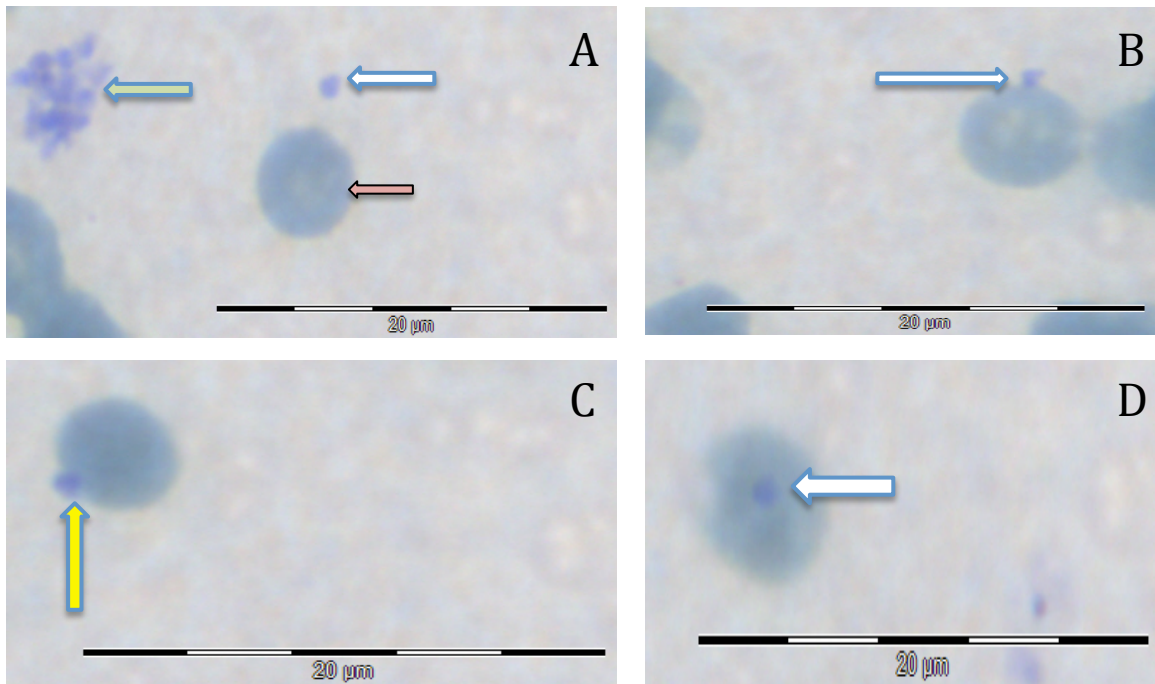


Figure 3.8 Merozoite-erythrocyte invasion sequence as seen under light microscopy after Giemsa staining. **A:** Free merozoite (mz); where the green arrow indicates a mz cluster from a burst schizont and the white arrow indicates a single free mz opposite an erythrocyte, indicated by the red arrow. **B:** The white arrow indicates the attached mz on the surface of the erythrocyte membrane. **C:** A mz clearly invading an erythrocyte, as indentations in the erythrocyte membrane are indicated with a yellow arrow. **D:** A completely invaded mz indicated by a white arrow. Images were taken at 100X magnification with 20 µm scale bar.

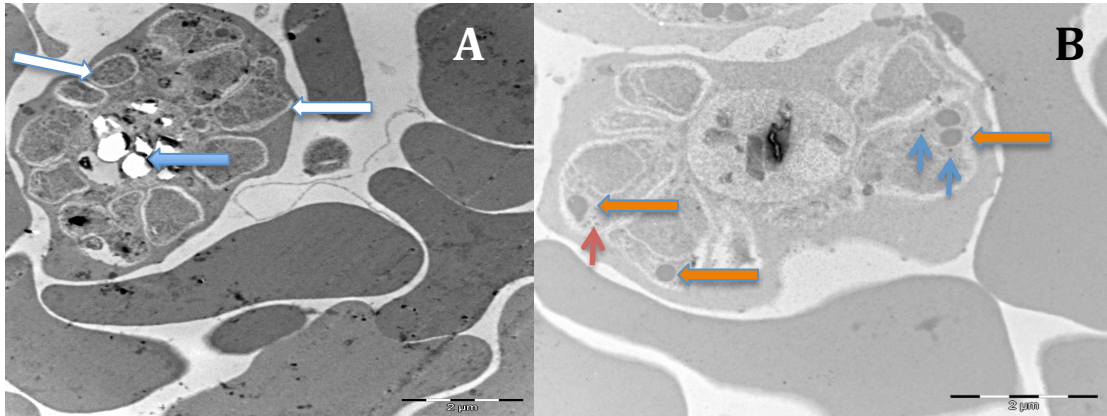


Figure 3.9 TEM images of developing merozoites in schizonts. **A:** A schizont between ~44 to 45 hpi. Separate merozoites can be seen developing as indicated by the white arrows. The blue arrow indicates the hemozoin crystals. **B:** ~46 hpi schizont with a number of the merozoites developing organelles, the orange arrows indicates the rhoptries, the red arrow indicates the micronemes and the blue arrows indicate the dense granules. Scale bar = 2 µm.

Dissociation of both the erythrocyte and PV membranes were observed when fully developed merozoites egressed from mature schizonts, as indicated in Figure 3.11. With the liberation of the merozoites, the remaining erythrocyte cell contents was released which resulted in a distinct loss of cell density, seen in Figure 3.11, where the burst schizont appeared lighter, in comparison to the uninfected erythrocytes surrounding it, as well as to the mature schizonts seen in Figure 3.10.

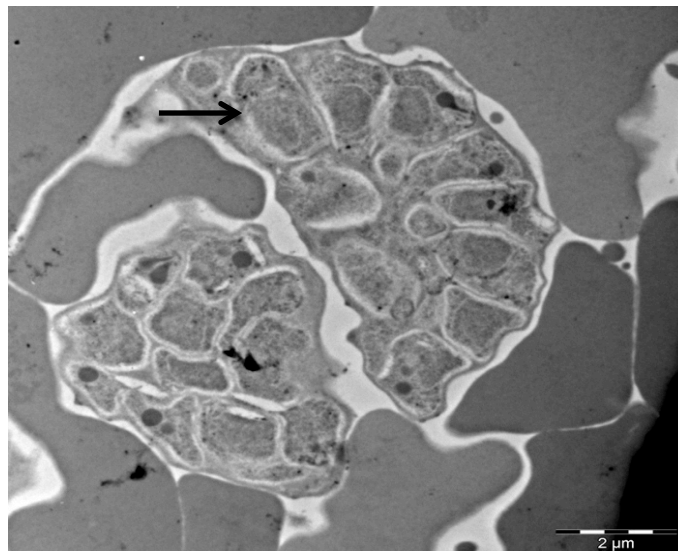


Figure 3.10 Mature schizonts. At the 48th hour of the life cycle with matured merozoites completely filling the erythrocyte. The black arrow indicates a mature mz. Scale bar = 2 µm.

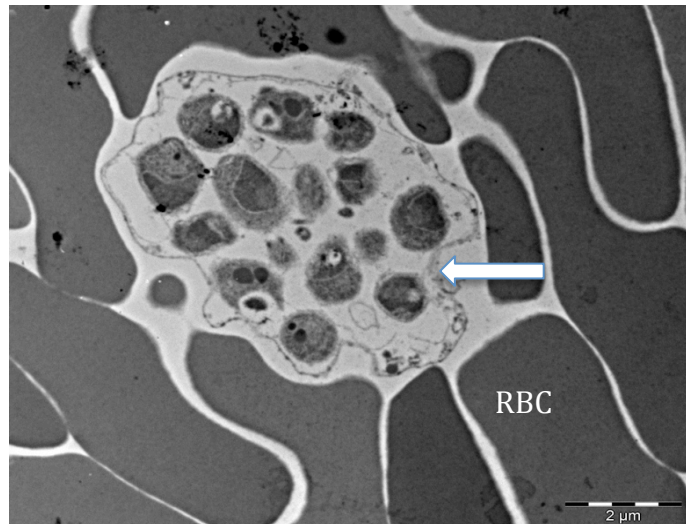


Figure 3.11 Egression of merozoites. The erythrocyte membrane has dissociated, releasing its cytoplasmic contents and the mature merozoites. The white arrow indicates the dissociated PV membrane. (RBC indicates uninfected erythrocytes). Scale bar = 2 μm .

Although this study only sought to visualise the events prior to and after merozoite invasion, and did not investigate the details of the membrane dissociation phenomenon, it can be argued from the effects observed in Figure 3.11 that merozoite egression of *P. falciparum* 3D7 cultures follow the membrane dissociation patterns of either the ‘Inside-out’ or ‘Outside-in’ model that were referred to in Figure 1.5.

From Figure 3.12A, a cluster of merozoites was observed to be devoid of both membranes. The merozoites in this image measured roughly 1 μm in diameter. A magnified image of a cross-section of a single free merozoite is shown in Figure 3.12B with a clear view of the structural components. It contains a fairly large round nucleus, measuring 300 nm in diameter. The two rhoptry organelles were between 100 to 120 nm in diameter and the microneme organelles had a diameter of ~ 20 nm and a length of ~ 80 nm.

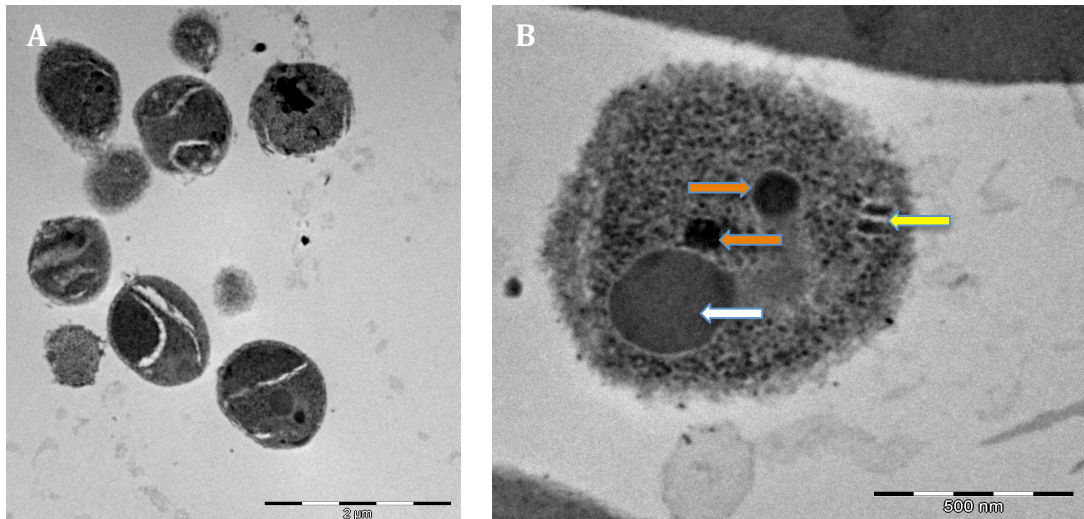


Figure 3.12 Merozoites. **A:** A number of free merozoites. With a 2 µm scale bar. **B:** Merozoite structure. 4X magnification of a single merozoite along side an erythrocyte. The white arrow indicates the nucleus, the orange arrows indicate the rhoptry organelles and the yellow arrow indicates the microneme organelles. Scale bar = 500 nm.

The length and diameter measurements of merozoites can vary slightly, depending on the position in which they were fixed and in which stage of schizont maturation the merozoite is. Bannister *et al.* (2003) (50) reported the length of merozoites to be between 1.2 to 1.8 µm with a height of 0.7 µm, as they had captured images of mature merozoites within a late schizont, where the position of the merozoite within the schizont was longitudinal and ellipsoid in shape. This is similar to the measurements of the merozoites within this study, where the largest merozoite within the mature schizont indicated by the black arrow in Figure 3.10, had a length of ~2 µm and a width of ~1 µm. There were also similar findings in the measurements of the merozoites organelles of this study to that of Bannister *et al.* (2003). However, due to the cross sectioning of the samples and positioning of the merozoites, the true club-shape of the rhoptry organelles were not visible in the images of the merozoites.

Nevertheless, the image of the free merozoite in Figure 3.12B clearly exhibits the surface coating of merozoite membrane proteins, which give the merozoite its ‘fuzzy’ appearance. These surface proteins, as mentioned before, are of vital importance to the merozoite for the successful invasion of an erythrocyte. The evidence of which can be seen in Figure 3.13, where the merozoite has detected an erythrocyte and has attached

itself to the human host cell, by means of a weak bond between its surface proteins and erythrocyte membrane receptors (51).

The second step in the invasion process is the ‘merozoite orientation and tight-junction formation’. This can be seen in Figure 3.14, where a merozoite has apically positioned itself toward the erythrocyte to form the tight-junction, through which the parasite will invade the host cell. Apical orientation occurs once the merozoite has formed a firm attachment to the erythrocyte membrane by means of its surface proteins, erythrocyte binding antigen (EBA) (94) and reticulocyte homology (RH) (95) family ligands, where this attachment in the 3D7 line is an irreversible one (96). The merozoite has positioned itself so that its apical organelles are in proximity to the erythrocyte membrane. At this stage the rhoptry organelles secrete the rhoptry neck proteins (RON) that then interact with the *Pf*AMA-1 proteins, which are secreted from the micronemes during merozoite egression, and together interact with the erythrocyte membrane to form the tight-junction, a channel through which the merozoite will infiltrate the host cell, see Figure 3.8C (97).

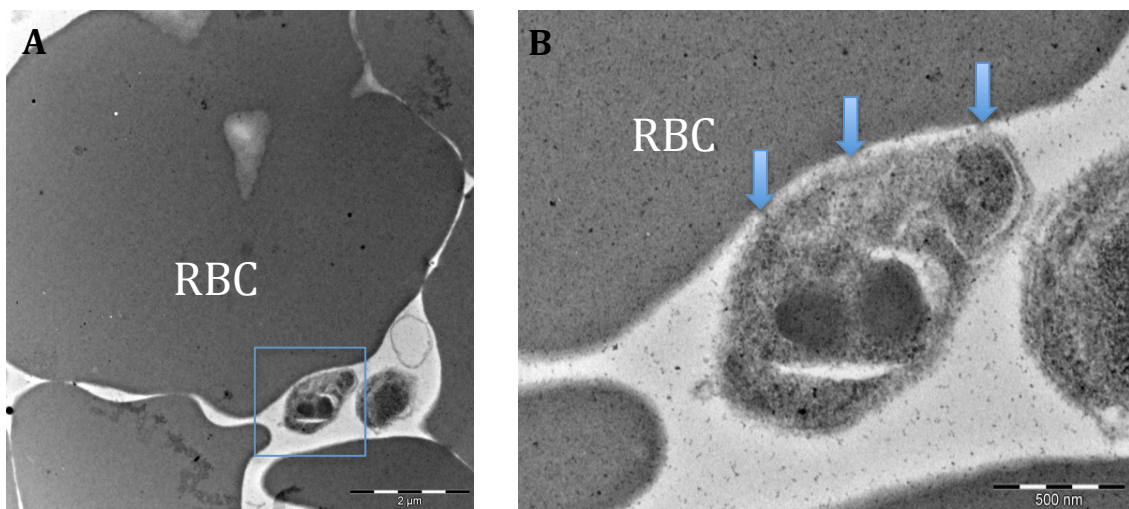


Figure 3.13 Merozoite attachment. **A** indicates the attachment phase of the merozoite invasion process; the square indicates the merozoite attaching to the erythrocyte (indicated as RBC). **B** is a 4X increased magnification of **A**, where RBC indicates the erythrocyte and the blue arrows indicate to the surface protein attachments of the merozoite. **A** has a 2 μ m scale bar and **B** a 500 nm scale bar.

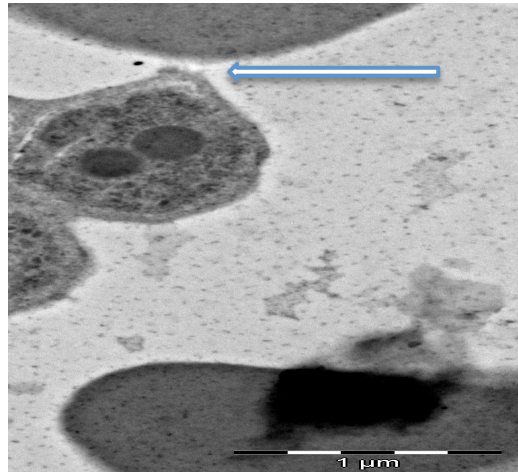


Figure 3.14 Merozoite orientation and tight-junction formation. The mz has orientated itself for invasion and beginning to form the tight-junction, as indicated with a white arrow. Scale bar represents 1 μm .

As the merozoite invades, the tight-junction produces an orifice within the erythrocyte which creates the PV membrane that will completely surround the invaded parasite (98), as is indicated in Figure 3.15. This concludes the entire merozoite invasion process that was referred to in Figure 1.7.

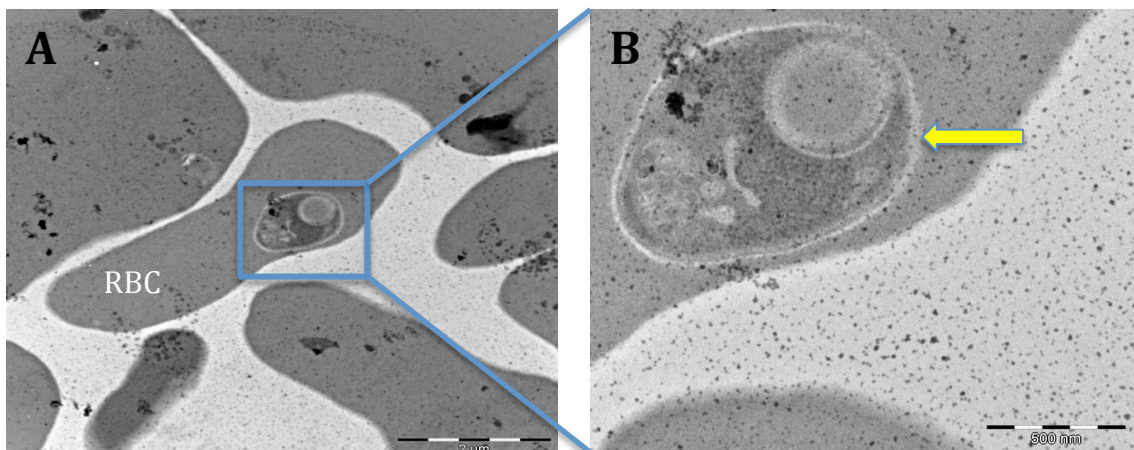


Figure 3.15 Merozoite invaded erythrocyte. **A** represents an invaded erythrocyte (RBC) by a merozoite as indicated within the blue box. Scale bar = 2 μm . **B** is a 4X magnification of **A** with a scale bar of 500 nm. The PV membrane, a distinct white lining around the merozoite, which is indicated by the yellow arrow, surrounds the completely invaded merozoite.

3.2.2 Confocal Microscopy of Fluorescently Labelled *PfAMA-1* of Merozoites

Schizonts (~47-48 hpi) and free merozoites were isolated from a 3-5% parasitemia culture and incubated without E64. A number of fixative and blocking methods were tested to determine the optimal method for fixing malaria parasites to cover slips; this is described in more detail in Table A1 of Appendix IV. The optimal results were obtained from fixing the parasites with 0,25% formaldehyde, blocking the parasites with 1% BSA-PBS-T solution and labelling with a 1:400 concentration of the *PfAMA-1* antibody. This method was adapted from the combined research published by Michael Blackman in *Methods for Malaria Research* (80) and Srinivasan *et al.* (2011) (51).

The 1F9 antibody recognises domain 1 of *PfAMA-1* and therefore binds to the 83 kDa and 66 kDa fragments of the *PfAMA-1* protein (99), where the 83 kDa precursor protein is found in the micronemes and then processed into the 66 kDa fragment, which is secreted circumferentially onto the surface of the merozoite. Therefore, labelled *PfAMA-1* should be found apically in the micronemes of merozoites in mature schizonts and circumferentially on free merozoites. From the results obtained in this study, there appeared to be apical localisation of *PfAMA-1* detected on merozoites within the mature schizonts, as shown in Figure 3.16, which is congruent with the theory of the literature. Unfortunately, the labelled *PfAMA-1* of the free merozoites was not observed as being circumferentially distributed and was only detected apically, as seen in Figure 3.17. According to the results of previously published research (49,100), labelled *PfAMA-1* was seen to be distributed circumferentially, not only on free merozoites, but also those encapsulated in mature schizonts.

Two reasonable explanations could account for no observed circumferentially distributed *PfAMA-1*₆₆ on the free merozoites. Firstly, due to the rapid processing of *PfAMA-1* during merozoite egression, the 66-kDa fragment could have already been digested into its smaller fragments during the isolation and slide preparation procedures. And secondly, due to the low binding affinity of the 1F9 antibody to *PfAMA-1*, which was observed during this study, could have been caused by minor changes to the antibody that affected its binding affinity. This may have been caused during the lyophilisation process (101) of the antibody or during the conjugation to the Cy3 dye, which affected the antigen binding F_{ab} regions.

Therefore, localisation of *Pf*AMA-1 was observed prior to merozoite release with the identification of *Pf*AMA-1₈₃, however localisation of the *Pf*AMA-1₆₆ fragment on the merozoite was not observed.

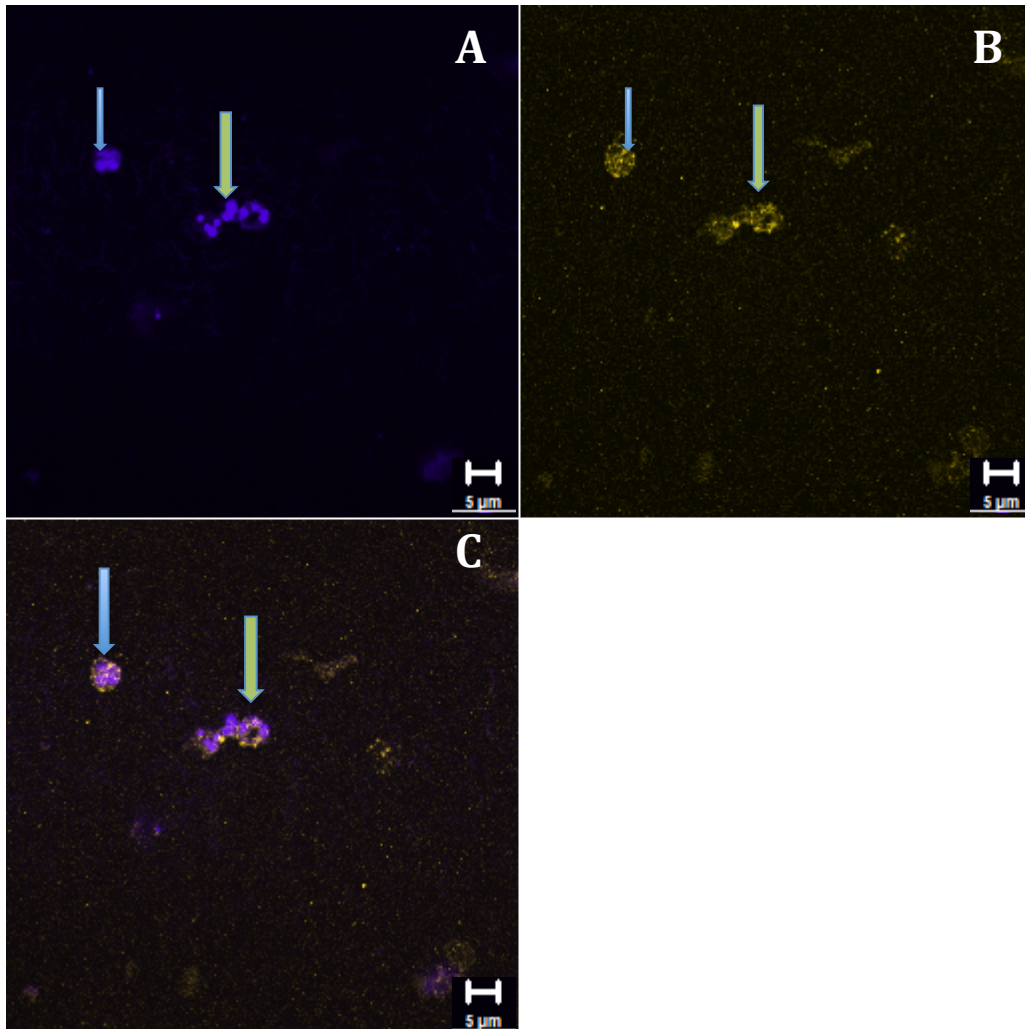


Figure 3.16 Localisation of *Pf*AMA-1 in mature schizonts (~48 hpi). **A** is the DAPI (blue) stain only. **B** is the Cy3-*Pf*AMA-1 (yellow) stain only. **C** is the overlay of **A** and **B**. The blue arrows indicate an intact mature schizont with merozoites. The green arrows indicate an erupted schizont with merozoites egressing. Scale bar = 5 µm.

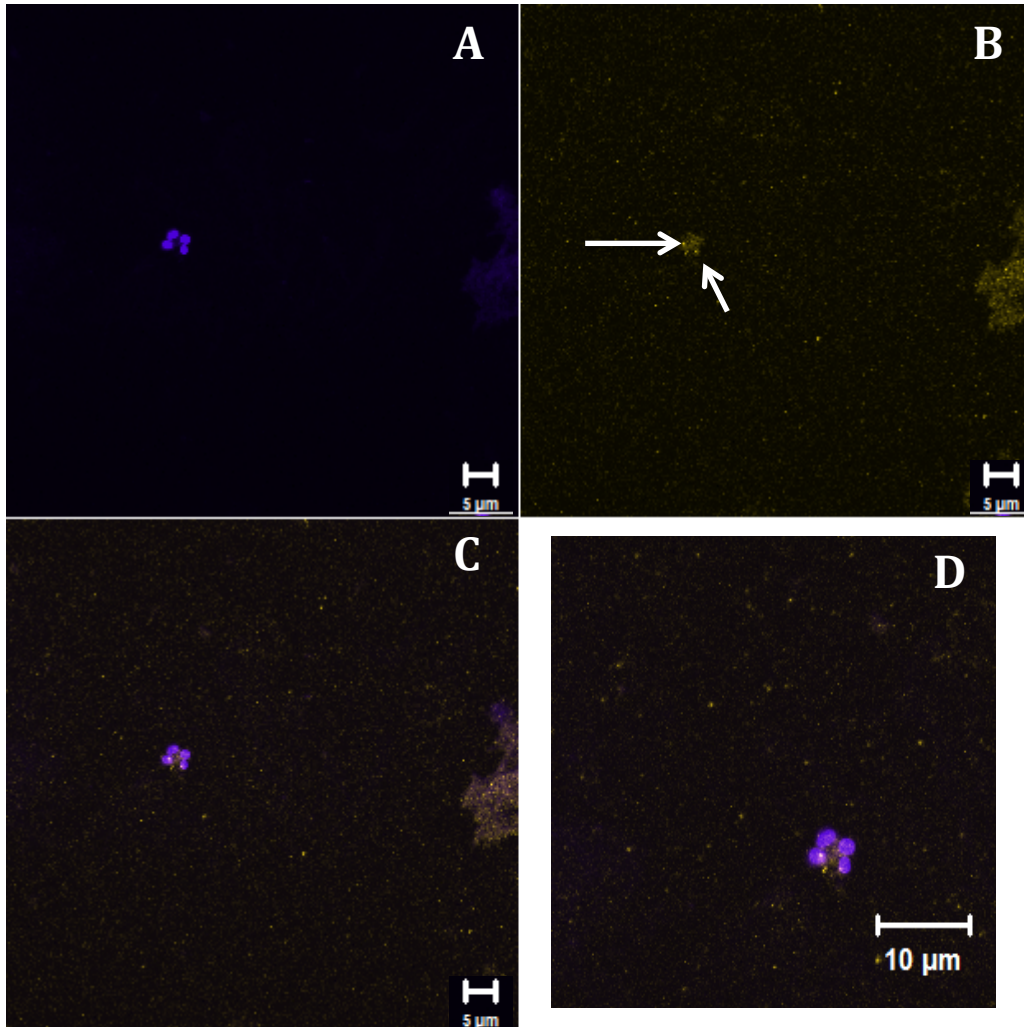


Figure 3.17 Localisation of *PfAMA-1* in free merozoites. **A** is the DAPI (blue) stain only. **B** is the Cy3-*PfAMA-1* (yellow) stain only. **C** is the overlay of **A** and **B**. The white arrows indicate the apical localisation of labelled *PfAMA-1*. Scale bar = 5 µm. **D** is an enhanced overlay image of **C** that shows the apical localisation of *PfAMA-1*. Scale bar = 10 µm.

3.3 Proteomic Analysis of 3D7 Merozoites

During the method optimisation phase of isolating high concentrations of merozoite proteins from synchronised cultures, merozoites were, firstly, harvested from 30 mL synchronised cultures of 3 to 5% parasitemia with a 3 to 5% Hct (Boyle *et al.* 2010) (32) that were VarioMACS isolated and incubated in the presence of E64 (Section 2.1.7), then homogenised through ultrasonic disruption (Section 2.4.1) for 3-5 minutes. Through a standard BCA assay, the total protein concentration of merozoites isolated from a single 30 mL culture was found to be ~0.8 mg/mL. From this sample, a volume of 25 μ L was prepared with Laemmli sample buffer for separation by PAGE electrophoresis, under non-reduced conditions, as indicated in Figure 3.18A. Due to the low protein concentration only a number of thin faint bands were observed.

From this point, a pooled sample that was comprised of 7 to 8 synchronised cultures of 3-5% parasitemia with a 3-5% Hct, from a volume of 30 mL each, were harvested for merozoites, on separate days. This collective sample yielded a protein concentration of approximately 6 mg/mL. Approximately 3 mg/mL of the sample, or ~ 75 μ g/ well, was separated by PAGE electrophoresis in the same manner as the first sample, with the results indicated in Figure 3.20B. Although the protein concentration of the second sample was higher, only two distinct bands were observed in the 60 kDa range (which was not observed in the first sample, A of Figure 3.20) and 10 kDa, as well as a number of thin faint bands.

The SDS-PAGE separated proteins of the collective sample were transferred electrophoretically, using the semi-dry technique, onto a PVDF membrane. The membrane was blocked with a 2% BSA-Tris solution and incubated with the primary (1F9 anti-*Pf*AMA-1) and secondary (goat anti-rabbit IgG horseradish peroxidase) antibody at a ratio of 1:1000 and 1:2500, respectfully. The results of this blot are shown in Figure 3.20C. The probe revealed a single white or ghost band in the region of 60 kDa. The proteins from this region were excised from an equivalent gel for an in-gel digestion (Section 2.4.3) and LC-MS/MS analysis (Section 2.4.5), to determine whether the *Pf*AMA-1 was perhaps present but not detected by the antibody due to degradation. Unfortunately, the analysis revealed that this band was largely comprised of albumin, a contamination from the AlbuMax-II within the medium.

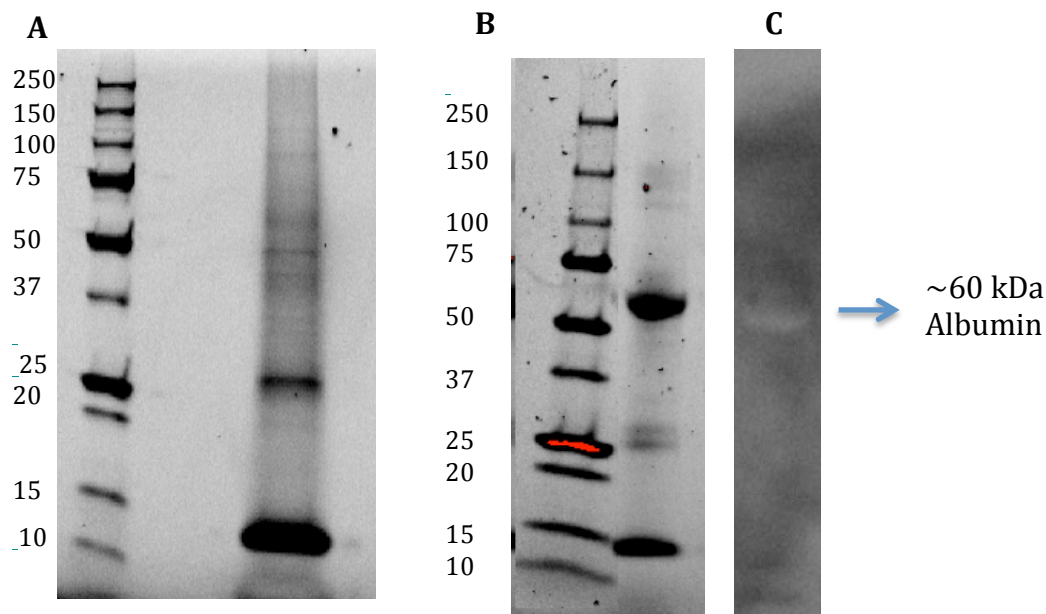


Figure 3.18 A SDS-PAGE of isolated *Pfmerozoite* proteins from **A** single 30 mL synchronised culture of 3-5% parasitemia with 3-5% Hct and **B** a collective sample of 7-8 synchronised cultures of similar culture parameters as **A**. **C** is the western blot of **B** where the white band at ~60 kDa indicates non-specific binding of the 1F9 antibody and was identified as Albumin by gel digestion and LC-MS analysis.

Therefore, several changes were made to the culturing parameters and the protein sample preparation method, to achieve a higher concentration of parasite proteins and to decrease the concentration of the albumin and erythrocyte protein contaminants. The culturing parameters were changed to increase the merozoite protein concentration by increasing the haematocrit to 8-10% and increasing the parasitemia to ~10%, as discussed in Section 3.1.1. Samples of merozoites were harvested from 3 to 4 flasks of 10-15 mL synchronised cultures with a parasitemia of 9 to 10% (Section 2.1.6) that were VarioMACS isolated and incubated with E64 (Section 2.1.7), then homogenised for 10 minutes (Section 2.4.1). The protein concentration of the homogenised sample was determined using a standard BCA assay and calculated as ~12 mg/mL, which was double the average concentrations of the previous isolation of the collective samples from 7-8 flasks of 30 mL cultures with 3-5% Hct and 3-5% parasitemia.

An aliquot of the sample was diluted with dH₂O to ~3 mg/mL (or ~75 µg per well) for protein separation by PAGE electrophoresis. The results obtained from the gel electrophoresis procedure are shown in Figure 3.19. A comparison of the merozoite

proteins under non-reduced and reduced conditions was done to determine if the proteins would separate best under reduced conditions, as previous runs under non-reduced conditions did not produce many distinct bands, as was seen in Figure 3.18. As illustrated in Figure 3.19 the merozoite proteins, indicated as Lane B, separated into a number of distinct bands at approximately 80 kDa, 60 kDa, 40 kDa, 25 kDa and 10 kDa. It was also observed that a fraction of the sample still remained in the wells. This was more prominent in the well of Lane A of the non-reduced samples, as a darker band in the well was generally observed compared to that of Lane B, which indicated that the parasite proteins migrated better, from the well into the gel, under reduced conditions.

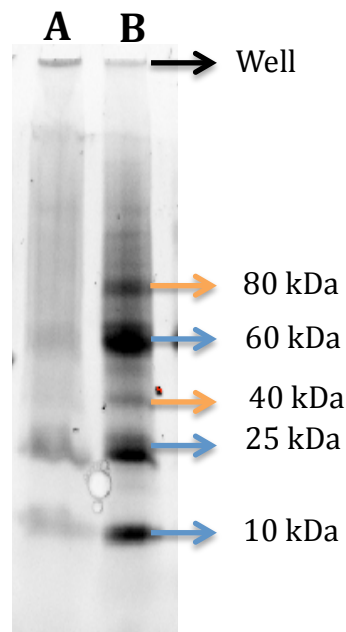


Figure 3.19 SDS-PAGE of *Pf*merozoite proteins. Samples were prepared from the same protein extract and prepared under **A**: Non-reducing conditions **B**: Reducing conditions. There were clear differences in band intensities between the two conditions of sample preparation. The blue arrows indicate protein bands with the same mass that were found in both lanes while the orange arrows indicate the difference of band intensity between both conditions.

Two identical gels of the merozoite proteins, under reduced and non-reduced conditions, were run and electrophoretically transferred using the semi-dry technique onto two membranes. The membranes were stained with Ponceau S solution to verify the proteins had been transferred onto the membranes. Once the membranes were washed to remove the Ponceau S solution, they were then blocked with either 2% BSA (Figure 3.20) or 2% milk (Figure 3.21) to determine which blocking procedure would prevent the non-specific binding of the primary antibody that had been previously observed on

membranes (Figure 3.18C) blocked with 2% BSA. The 1F9 antibody (3 mg/mL) was used as a positive control and BSA (2 mg/mL) was used as a negative control. Both membranes were probed for *Pf*AMA-1 with a diluted solution of each of the antibodies; the 1F9 antibody as the primary antibody, was incubated over night, at a ratio of 1:2000 and the goat anti-rabbit IgG horseradish peroxidase as the secondary, was incubated for an hour, at a ratio of 1:5000 to minimise the appearance of ghost bands on the membrane; this effect is due to the antibody quenching the substrate, which reduces the signal.

Although the 1F9 antibody has an affinity for the non-reduced *Pf*AMA-1₈₃ and *Pf*AMA-1₆₆ fragments (99,102–104), previous western blot results did not show evidence of the antibody binding to *Pf*AMA-1 fragments under non-reduced conditions, hence the comparison of separation of the merozoite proteins under both non-reduced and reduced conditions.

The results obtained from the western blot blocked with milk produced less non-specific binding of the antibody than that of the BSA blocking buffer and far less quenching of the substrate as less white bands appeared on the membrane. However, no dark bands appeared in either the 83 kDa or 66 kDa regions where the two largest processed forms of *Pf*AMA-1 have been observed in previous publications (99,102–104). This result could not have been from a defective antibody as the size of rabbit antibodies are approximately 150 kDa (105), which is evident from Figure 3.20 B2, when the antibody was run under non-reduced conditions. The antibody migrated between 150 and 100 kDa, this indicated that it was intact with no major structural deformities and therefore would still have an affinity, however low, to bind to the non-reduced *Pf*AMA-1 fragments at the 83 kDa and 66 kDa bands.

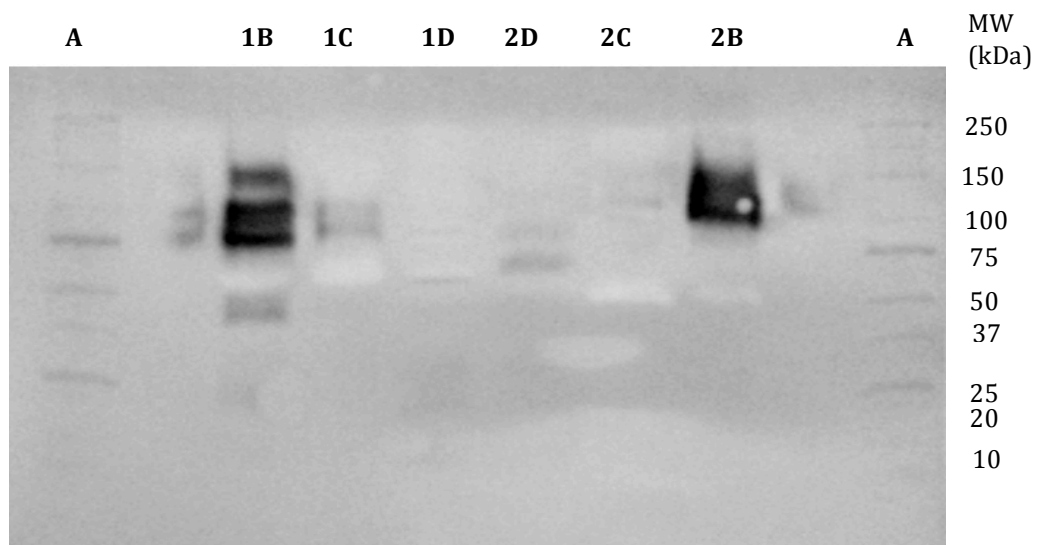


Figure 3.20 Western blot membrane blocked with 2% BSA. **A** represents the molecular weight standards. Samples **1B-D** were run under reduced conditions and **2B-D** under non-reduced conditions. **B**: *Pf*AMA-1 antibody (1F9), **C**: BSA standard, **D**: Isolated *Pf*merozoite sample. The dark bands indicate binding of the 1F9 antibody and the white bands indicate quenching of the substrate.

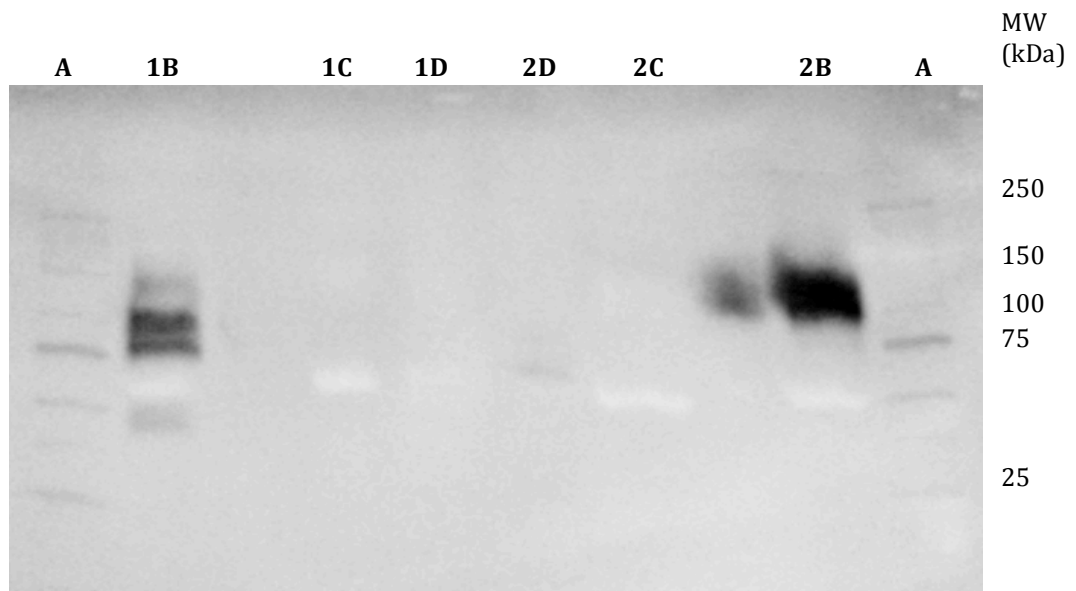


Figure 3.21 Western blot membrane blocked with 2% milk. **A** represents MW standards. Samples **1B-D** were run under reduced conditions and **2B-D** under non-reduced conditions. **B**: *Pf*AMA-1 antibody (1F9), **C**: BSA standard, **D**: Isolated *Pf*merozoite sample. The dark bands indicate binding of the 1F9 antibody and the white bands indicate quenching of the substrate.

Although, *PfAMA-1* is a membrane protein and membrane proteins are said to be insoluble, this could be ruled out as a possible explanation as to why *PfAMA-1* was not identified, as the SDS within the sample buffer would solubilise the membrane proteins. Two possible reasons were considered as the cause of the observed results of the western blots; firstly, that the *PfAMA-1* protein had degraded and become unrecognisable to the antibody, or that the *PfAMA-1* isolation was not successful, leading to the in-gel trypsin digestion of the bands in the range of all the known *PfAMA-1* processed fragments (83 kDa, 66 kDa, 48 kDa and 44 kDa), as well as an in-solution trypsin digestion to clarify whether *PfAMA-1* was present in the isolated merozoite samples.

As the merozoite proteins were separated on a 'Stain-free' gel, the gels were initially visualised using the UV exposure prior to overnight staining with Coomassie, to visualise the bands in order to excise them. Bands representing the mass of ~80 kDa, ~60 kDa and ~40 kDa were excised and in-gel digested with trypsin as described in Section 2.4.3 and analysed by LC-MS/MS (Section 2.4.5) to identify the gel separated proteins. The peptides from the digested proteins were run within the following LC-MS/MS parameters: a 1% false discovery rate (FDR), an initial mass error tolerance (IMET) of 0.05 Da for MS1 and an IMET of 0.5 Da for MS2, with a cysteine alkylation due to the treatment with iodoacetamide and optional methionine oxidation as protein modifications.

From the three major bands (~80 kDa, ~60 kDa and ~40 kDa) a total of 540 proteins were identified using ProteinPilot software and the UniProt/SwissProt database. As a number of the proteins were identified within two or all of the bands the total number of individual proteins identified were 358. Of the 358, only 284 proteins were taken into consideration, as the remaining 74 proteins were identified with one peptide only; which reduces the confidence level with which a protein could be identified. Therefore, only proteins identified with 2 or more unique peptides, with a high confidence level, were considered as valid proteins (106). Of the 284 proteins, 66.5% [189 proteins] were *Plasmodium* proteins and 33.5% [95 proteins] were human proteins.

Many of the *Plasmodium* proteins were identified as DNA and RNA associated proteins, structural and transport proteins, signalling proteins, cytoskeleton proteins as well as a number of enzymes, together with a small number of parasite food vacuole membrane proteins and erythrocyte adhesion proteins (Appendix IV Table A2). The actin and myosin proteins, which are required for the movement of the merozoite through the tight-junction into the erythrocyte, were also identified (107). Many of the major merozoite surface proteins involved in the invasion process were identified within the bands; of these, three were unique to the 40 kDa band and a single unique protein identified in both the 60 kDa and the 80 kDa band (Table 3.1), with another 7 invasion proteins that were common in two or all of the bands (Table 3.2).

Table 3.1 Proteomic Profile of Gel Digestion

	Digested Bands		
	~40 kDa	~60 kDa	~80 kDa
Total # of proteins	185	110	106
Unique (U) proteins	95	56	41
# H proteins	63	52	39
# P proteins	122	58	67
# UP proteins	76	32	31
Unique surface proteins	RAP-3	RH-2a/2b	SUB-1
	GPI -AMA		
	RhopH-3		
# : Number; H : Human; P : Parasite; UP : unique parasite			

Table 3.2 A list of common merozoite surface proteins found in the different bands excised from the SDS PAGE gel

Surface proteins	Digested Bands		
	~40 kDa	~60 kDa	~80 kDa
MSP 1	+	+	+
RAP 1	+	+	+
RhopH 2	+	+	+
SERA 7	+	-	+
RAP 2	+	-	+
ABRA	+	+	+
RON 3	+	+	+
MSP-P92	+	+	+
+ : Yes , - : No			

The GPI anchored micronemal antigen (GAMA), rhoptry associated protein 3 (RAP-3) and high molecular weight rhoptry protein 3 (RhopH-3) were the unique surface proteins located within the 40 kDa band. These assist the merozoite in various ways to invade the erythrocyte. GAMA is a microneme protein that is secreted to the surface of

the merozoite and, as the name suggests, becomes anchored to the merozoite surface by the glycolipid, glycosylphosphatidyl inositol (GPI). In previous studies GAMA has been shown to have a binding affinity for erythrocyte membrane receptors and therefore assists with merozoite attachment during invasion (108). The RAP-3 and RhopH-3 proteins are two of the seven rhoptry proteins that form the Rhop protein complex. This complex consists of three low molecular weight rhoptry proteins (RAP-1, RAP-2 and RAP-3), three high molecular weight rhoptry proteins (RhopH-1, RhopH-2 and RhopH-3) and a GPI-anchored rhoptry protein, the rhoptry associated membrane antigen (RAMA). Once the merozoite has attached itself to the erythrocyte, it secretes this complex onto the erythrocyte membrane to assist with invasion (109,110).

The only unique merozoite surface proteins identified within the 60 kDa band were the reticulocyte binding protein 2 homologue *a* and *b* (RH-2a/2b). The RH-2a/2b proteins form part of the reticulocyte binding protein family that have been identified as adhesive proteins for erythrocyte invasion. There are six of these proteins in total: RH-1, RH-2a, RH-2b, RH-3, RH-4 and RH-5. This family of proteins are expressed according to the invasion phenotype of the parasite line. A sialic acid dependent parasite line, such as Dd2, would express RH-1 at higher levels, whereas a sialic acid independent line, such as the 3D7 line, as used in this study, express the RH2a/2b proteins at higher levels (111).

From the 80 kDa band, the unique merozoite related protein identified was subtilisin-like protease 1 (SUB-1), which is a serine protease that processes the merozoite surface proteins, such as MSP family proteins and SERA proteins into their active forms for invasion and for PV membrane degradation, respectfully (112).

It is not uncommon to find a number of similar merozoite proteins within different bands, as many merozoite surface proteins undergo proteolytic processing before secretion, during relocation onto the merozoite surface and after invasion. Hence, the distribution of MSP-1 (113) and MSP-*Pf*92 (114), the rhoptry proteins (115) and SERA-7 (116) proteins, within each of the excised bands from the gel. The MSP-P92 protein belongs to the MSP family and is coded by the gene P92 (114). The serine repeat-antigen 7 (SERA-7) is another major malaria protease family, which was identified

within band 40 kDa and 80 kDa. This is classified as a cysteine protease, which is found in the mature schizont and assists with merozoite release by degrading the PV membrane (116).

The in-solution trypsin digestion of the same merozoite isolate sample identified peptides from a total of 483 proteins of which only 329 proteins were identified with two or more peptides and, therefore, were considered as valid proteins. From the 329 proteins, 78.4% [258 proteins] were identified as *Plasmodium* proteins and 21.6% [71 proteins] were identified as Human proteins.

Table 3.3 and Table 3.4 indicate the similarities and differences between the results of the in-gel and in-solution trypsin digestion methods. An additional 162 *Plasmodium* proteins were identified from the in-solution digestion, which were not identified from the in-gel digestion. While only 73 *Plasmodium* proteins were unique to the in-gel digestion and not identified in the in-solution digestion.

Table 3.3 Protein Comparisons of Gel Digestion^a and In-solution Digestion^a

	Method	
	Gel Digestion	In-solution Digestion
Total number of proteins	284	329
Proteins identified in both methods	137	
Number of addition parasite proteins identified	73*	162
a : The same sample of isolated merozoites was used for each of these methods * : Of the 120 unique parasite proteins found from the gel digestion only 73 were found solely in the gel digestion. The remaining 47 parasite proteins were also identified in the in-solution digestion.		

The greater advantage of using an in-solution digestion method, for this investigation, was that an aliquot of the entire sample was probed for the target protein (*PfAMA-1*), whereas with gel separation of the sample, specific bands were probed for the various fragments of the target protein. As can be seen from the results (Table 3.3) the in-solution digestion method identified more proteins, as would be expected.

A number of the *Plasmodium* proteins identified from the gel digestion were marked as unidentified/invalid in the in-solution results, including merozoite surface proteins (Table 3.4), as many of these proteins were discarded from the data due to a low confidence level from being identified from a single peptide. The in-solution digestion

also identified similar merozoite surface protein families, apart from a number of individual surface proteins, such as the MSP family, the rhoptry complex, rhoptry neck proteins and the reticular binding homologue protein families, as well as from the SERA protease family. Interestingly, another type of merozoite surface protein was identified, the merozoite cap protein 1 (MCP-1). It was discovered in the late 1980's and may play a role in the formation of the tight-junction during the merozoite invasion of the erythrocyte (117).

Table 3.4 Comparison of merozoite surface proteins identified from an in-gel and in-solution trypsin digestion^a

Merozoite surface proteins	Trypsin Digestion Method	
	In-gel	In-solution
MSP 1	+	+
RAP 1	+	+
RhopH 2	+	+
SERA 7	+	-
RAP 2	+	+
ABRA	+	+
RON 3	+	+
MSP-P92	+	-
RAP 3	+	+
GAMA	+	+
RhopH 3	+	-
RH 2a/2b	+	-
SUB 1	+	-
MCP 1	-	+
RH-4	-	+
SERA-5	-	+

a : The same sample of isolated merozoites was used for each of these methods
+ : Yes , - : No

Another two important functional merozoite proteins identified were the cytoadherence-linked asexual protein 9 (CLAG-9) and the ring-infected erythrocyte surface antigen (RESA), which are involved in the structural changes that occur on the erythrocyte membrane as the parasite develops. CLAG-9 is a rhoptry protein that may be associated with erythrocyte adherence in the mature stages of the parasites life cycle (118). While RESA is a dense granular protein, that is secreted, once the merozoite is within the erythrocyte, and transported to the erythrocyte membrane (119).

The advantage of using an in-solution digestion, to confirm the presence or absence of *Pf*AMA-1, is that it is a simple, effective and timesaving method of identifying proteins from a complex mixture of proteins from an organism (120). As merozoite proteins are

known to be insoluble (82), there was a possibility that *PfAMA-1* did not migrate into the gel. As was seen from the results of the SDS-PAGE (Figure 3.19) some proteins did remain in the well.

The in-solution digestion proved to be effective in identifying almost twice as many *Plasmodium* proteins than the gel digestion, although, the absence of any of the peptides of the *PfAMA-1* protein from the LC-MS/MS data, confirmed the results of the gel digestion; that no *PfAMA-1* was present in the sample of the isolated merozoites.

The lack of *PfAMA-1* peptides being identified was thought to be a result of the rapid proteolysis of the protein by the merozoite's surface sheddase enzymes. Therefore a new batch of schizonts was isolated and once the merozoites were harvested from saponin lysis (Section 2.1.7), a cocktail of protease inhibitors was added to the sample (Section 2.4.4) to prevent any proteolytic processes from occurring (53). The sample was stored as such and once it was required for the in-solution digestion, the sample was washed in PBS to remove the proteases so that their activity would not inhibit the digestion ability of trypsin.

The results of an in-solution digestion of this sample verified the hypothesis that *PfAMA-1* was being proteolytically cleaved and the addition of the protease inhibitors to the isolated merozoites allowed for the successful identification of this microneme protein. Table 3.5 and Table 3.6 indicate some of the similarities and differences in the *Plasmodium* proteins identified from the in-solution digestions performed on the samples with and without the addition of protease inhibitors. There was little difference between the numbers of proteins identified. In the treated sample 331 proteins were observed and 329 proteins observed in the untreated sample. Of the 331 proteins identified, in the treated sample, 63.4% [208 proteins] originated from the *Plasmodium* parasite and 36.6% [123 proteins] from the human host. Many of the major apical organelle protein families' identified in the untreated sample were also identified in the treated sample, such as the MSP, RON, RAP, Rhop, ABRA and CLAG proteins. The only difference was the identification of the apical protein *PfAMA-1*, which was the primary aim of this experiment.

Although the majority of the proteins identified from the in-gel and in-solution digestions were of the *Plasmodium* merozoite proteome, the presence of the Human proteins still in the sample highlights the importance of isolating the merozoite proteins, via saponin lysis, from the erythrocytes. If merozoites were not freed from the erythrocytes and the sample contained both proteomes, the presence of the high abundant erythrocyte proteins would ‘swamp’ the LC-MS analysis and the lower abundant merozoite proteins would be lost.

Table 3.5 In-solution digestion method: a proteomic comparison of a protease inhibitor cocktail (PIC) treated sample^a versus a non protease inhibitor (NPI) treated sample

	Merozoite Sample	
	PIC	NPI
Total # of proteins	331	329
Similar parasite proteins identified	158	
Human proteins	123 (36.6%)	71 (21.6%)
Parasite proteins	208 (63.4%)	258 (78.4%)
Additional parasite proteins identified	50	100
Uncharacterised proteins*	18	20

a = Protease inhibitors used: E64, PMSF & EDTA
* Uncharacterised proteins are proteins that have not yet been fully annotated in the UniProt/SwissProt database.

Table 3.6 Comparison of Merozoite Surface Proteins Identified from the Protease Inhibitor Cocktail (PIC) Treated Sample^a versus a Non Protease Inhibitor (NPI) Treated Sample

Merozoite proteins	In-solution Samples	
	PIC	NPI
MSP 1	+	+
RAP 1	+	+
RhopH 2	+	+
RAP 2	+	+
ABRA	+	+
RON 3	+	+
RAP 3	+	+
GAMA	-	+
RhopH 3	+	-
MCP 1	-	+
RH-4	-	+
SERA-5	-	+
CLAG-9	+	+
AMA-1	+	-

a = Protease inhibitors used: E64, PMSF & EDTA
+ : Yes , - : No

To confirm the presence and valid identification of *Pf*AMA-1 from the ProteinPilot data, the raw data of the LC-MS/MS analysis (of both the in-solution samples) was processed through SearchGUI and Peptideshaker. The software confirmed the identification of *Pf*AMA-1 from the protease inhibitor treated sample of merozoites by matching peptide spectra to three *Pf*AMA-1 peptides. Figure 3.22 represents the amino acid sequence of *Pf*AMA-1 with the cleavage sites of trypsin and the possible unique peptides produced from an *in-silico* (computer simulated) digestion, which was generated from UniProt/SwissProt. From the ProteinPilot software analysis, 4 of the 72 possible peptides of *Pf*AMA-1 were identified and 3 peptides were identified from the Peptideshaker analysis, these are listed in Table 3.7. ProteinPilot identified three of the peptides with a 95 to 99% confidence, however the fourth was identified with less than a 50% confidence, as a possible miscleavage may have occurred between the lysine (K) and aspartic acid (D). PeptideShaker software identified three peptides with a 100% confidence.

10	20	30	40	50	60
MRKLYCVLLL	SAFEETYMIN	FGRGQNYWEH	PYQKSDVYHP	INEHREHPKE	YQYPLHQEHT
70	80	90	100	110	120
YQQEDSGEDE	NTLQHAYPID	HEGAEPAPQE	QNLFSSEIEIV	ERSNYMGNPW	TEYMAKYDIE
130	140	150	160	170	180
EVHGSGIRVD	LGEDAEVAGT	QYRLPSGKCP	VFGKGIIEIN	SNTTFLTPVA	TGNQYLKDGG
190	200	210	220	230	240
FAFPPTPEPLM	SPMTLDEMRH	FYKDNKYVKN	LDELTLCSRH	AGNMIPDNDK	NSNYKYPAVY
250	260	270	280	290	300
DDKDKKCHIL	YIAAQENNGP	RYCNKDESQR	NSMFCFRPAK	DISFQNYTYL	SKNVVDNWEK
310	320	330	340	350	360
VCPRKNLQNA	KFGLWVDGNC	EDIPHVNEFS	AIDLFECKL	VFELSASDQP	KQYEQHLTDY
370	380	390	400	410	420
EKIKEGFKNK	NASMIKSAFL	PTGAFKADRY	KSHGKGYNWG	NYNTETQKCE	IFNVKPTCLI
430	440	450	460	470	480
NNSSYIATTA	LSHPIEVEHN	FPCSLYKNEI	MKEIERESKR	IKLNDNDDEG	NKKIIPRIF
490	500	510	520	530	540
ISDDKDSLKC	PCDPEIVSNS	TCNFFVCKCV	ERRAEVTSNN	EVVVKKEEYKD	EYADIPEHKP
550	560	570	580	590	600
TYDKMKIIIA	SSAAVAVLAT	ILMVYLYKRR	GNAEKYDKMD	EPQHYGKSNS	RNDEMLEDPEA
610	620				
SFWGEEKRAS	HTTPVLMKPK	YY			

Figure 3.22 The amino acid sequence of *Pf*AMA-1. The yellow highlight represents the trypsin cleavage sites. The green highlight represents the peptides positively identified by LC-MS/MS.

Table 3.7 The LC-MS/MS results of identified *PfAMA-1* peptides

AA position	Sequence	ProteinPilot Confidence %	Peptideshaker Confidence %
340	LVFELSASDQPK	99	100
377	SAFLPTGAFK	99	100
117	YDIEEVHGSGIR	95	100
479	IFISDDKDSLK	50	Not identified

Although the merozoite is a simple single cellular organism, its proteome is diverse and requires an efficient means of analysing and identifying key proteins. This was attained through the highly sensitive technology of mass spectrometry, which identifies proteins rapidly and accurately from a complex mixture of peptides, produced from the trypsin digested proteome (121,122). In order to identify the hundreds of proteins from thousands of peptides a high-throughput system is required. ProteinPilot and Peptideshaker are two such software systems used in proteomics to analyse whole proteomes. The ProteinPilot software is coupled to the MS instrument to give a comprehensive report of the proteome analysis and Peptideshaker allows researchers to re-analyse the raw data for a specific purpose. One such purpose would be for the confirmation of the presence of a target protein, as was executed in this investigation for *PfAMA-1*.

To accomplish this, the raw LC-MS/MS data was processed through SearchGUI and Peptideshaker. The raw data consisted of MS/MS peptide spectra, which were generated from the peptides (of the digested protein) when they were eluted (by liquid chromatography) and fragmented by the mass spectrometer. These spectra were then compared to the theoretical peptide spectra of the *Plasmodium* and *Homo sapiens* UniProt/Swissprot sequence database, this is known as peptide spectrum matching or PSM. SearchGUI transfers the PSM files to Peptideshaker, which identifies the proteins from the validated peptides and displays the data as seen in Figure 3.23.

The highlighted protein, PF3D7_1133400, is the UniProt/SwissProt accession number of *PfAMA-1*. As can be seen from Box A, *PfAMA-1* was identified with a 100% confidence from 3 peptides. The three peptides were sequenced with a 100% confidence and identified from 3 peptide spectra with a 100% confidence, which is indicated in Box B and C, respectively. A 5.47% coverage of the total *PfAMA-1* amino acid sequence was confidently sequenced as is displayed in Box E.

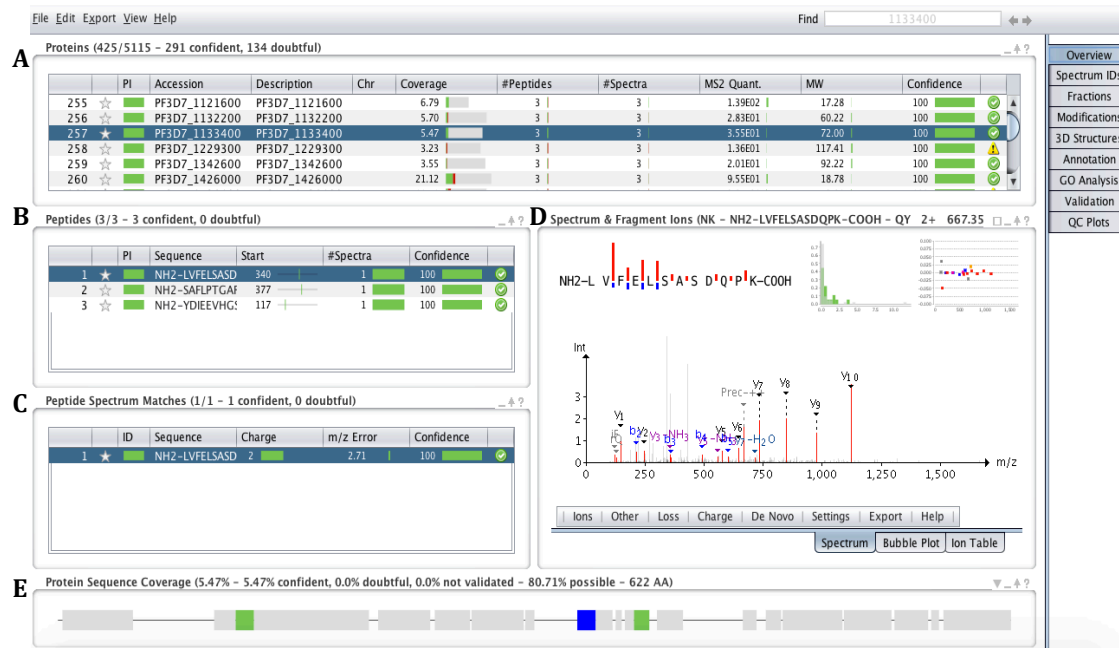


Figure 3.23 The overview display of the Peptideshaker data of the protease inhibitor treated merozoite sample. The highlighted protein, PF3D7_1133400, is *PfAMA-1*. Box A displays the identified proteins. Box B displays the selected protein's identified peptides with their respective PSM in Box C. Box D displays the spectrum of the selected peptide and Box E displays the coverage percentage of the protein from the identified peptides.

The advantage of using Peptideshaker, as a means of confirming the identification of *PfAMA-1* from the ProteinPilot data, was its use of multiple search engines (75). Processing data through multiple search engines increases the overall confidence of identifying a protein from a peptide(s), unlike the single search engine programme (Paragon) of ProteinPilot (123), because the combined algorithms of the search engines increase the sensitivity of the PSM hits for each peptide, which increases the software's ability to confidently identify peptides and their inferred proteins (124). In order for

peptides to be identified confidently from their respective peptide spectrum match and to eliminate false identifications, a decoy database was required. This decoy database was generated from the reverse sequence of the target (original) database to determine the false discovery rates or FDR (false positives or p-values) of the dataset (125); with the threshold FDR set at 1%, which is generally accepted by researchers, as this gives confidence that a protein has been identified correctly. From the Peptideshaker data of the treated in-solution sample (Figure 3.23) 5115 proteins were identified of which 425 were within the 1% FDR threshold, but 134 of those proteins were doubtful as one or two of the peptides were not identified with 100% confidence from the PSMs and therefore fall within the 1% FDR. With regards to *PfAMA-1*, it was identified and validated as a true protein as it falls within the 291 proteins that were identified above the 1% FDR threshold. Interestingly, *PfAMA-1* was identified from the Peptideshaker data of the untreated in-solution sample, indicated in Figure 3.24. Unfortunately the protein was not validated, as the peptides were not identified with any confident PSMs, so did not fall within the 1% FDR threshold and was therefore considered a false positive.



Figure 3.24 The overview display of the Peptideshaker data of the untreated merozoite sample. *PfAMA-1* is the highlighted protein with the accession number of PF3D7_1133400. Box **A** displays the identified proteins. Box **B** displays the selected protein's identified peptides with their respective PSM in Box **C**. Box **D** displays the spectrum of the selected peptide and Box **E** displays the coverage percentage of the protein from the identified peptides.

Of the four *Pf*AMA-1 peptides identified, the three peptides with the highest confidence were subjected to a protein-protein blast (pblast) analysis to determine if any of the peptides belonged to a human protein and were incorrectly identified as a *Plasmodium* protein. The National Centre for Biotechnology Information of the U.S.A provides an online open access programme called Basic Local Alignment Search Tool or BLAST. This tool was used to determine the homology or similarities between protein (or nucleotide) sequences by comparing a query sequence to a database of sequences (126). For the interest of this study the BLAST tool was used to deduce if there was a probability that one or more of the identified peptides of *Pf*AMA-1 were a false positive hit. This was determined by comparing the peptides to the *Plasmodium* and *Homo sapiens* database from UniProt/SwissProt, this was to ensure uniformity of the databases used in all computing programmes.

From each of the pblasts AMA-1 produced the highest alignment score. Each query peptide was matched with 100% coverage to a subject sequence of AMA-1 from the database. This is indicated in Figure 3.25 and Figure 3.26, where the graphical summary, protein descriptions and sequence alignments of the peptide YDIEEVHGSGIR are shown. From the graphical summary (Figure 3.25), YDIEEVHGSGIR was identified by BLAST as a conserved domain of AMA-1 and each coloured line represents a different sequence that aligned with the query sequence. The blue lines indicate the sequences with the highest alignment scores, where the scores can be seen in the protein description box of Figure 3.26 A. AMA-1 attained the highest score of 42.2, whereas the first human protein that was matched to the YDIEEVHGSGIR peptide, only obtained an alignment score of 25.2. The sequence alignment results can be observed in Figure 3.26 B, where the query peptide was aligned to the corresponding AMA-1 sequence with 100% coverage. None of the human proteins were an exact match to the peptide in question, many of the sequences contained gaps or different amino acids, one such protein was the Methylcrotonoyl-CoA carboxylase human protein (Figure 3.26 C), and although it had a 91% coverage there were three miss-matched amino acids that did not allow for a complete alignment with the query peptide.

Similar results were observed from the pblast of the peptides SAFLPTGAFK and LVFELSASDQPK, with AMA-1, consistently, obtaining the higher alignment scores of 33.3 and 40.1 for the respective peptides. An additional pblast was performed on the peptides, where each peptide was compared to the entire UniProt/SwissProt database to determine if AMA-1 would still attain the highest alignment score, and this remained true for each peptide.

Therefore, from the results obtained from the BLAST search of each peptide, it could be said with complete confidence, that ProteinPilot and Peptideshaker correctly ascertained *PfAMA-1* as the protein of the three peptides identified.

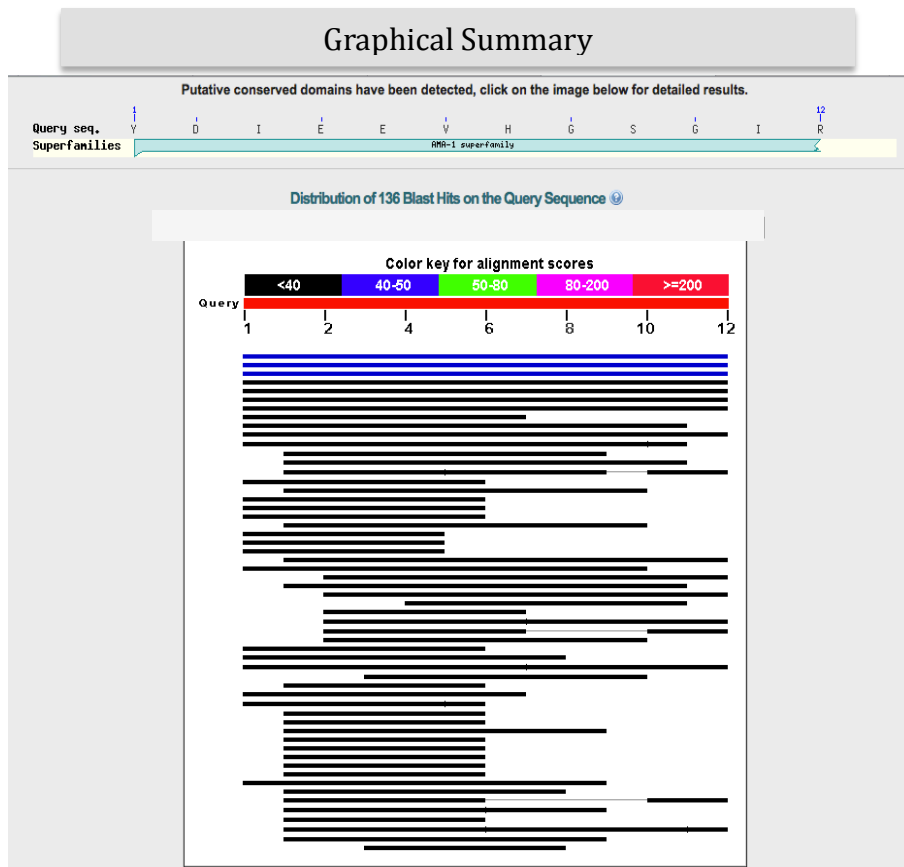


Figure 3.25 The protein BLAST results of YDIEEVHGSIGIR: The graphical summary.



Protein Description

A

Description	Max score	Total score	Query cover	E value	Ident	Accession
RecName: Full=Apical membrane antigen 1; AltName: Full=Merozoite surface antigen; Flags: Precursor	42.2	42.2	100%	3e-07	100%	P22621.1
RecName: Full=Apical membrane antigen 1; AltName: Full=Merozoite surface antigen; Flags: Precursor	42.2	42.2	100%	3e-07	100%	P50489.1
RecName: Full=Apical membrane antigen 1; AltName: Full=Merozoite surface antigen; Flags: Precursor	42.2	42.2	100%	3e-07	100%	P50490.1
RecName: Full=Apical membrane antigen 1; AltName: Full=Merozoite surface antigen; Flags: Precursor	37.1	37.1	100%	2e-05	92%	P50492.1
RecName: Full=Apical membrane antigen 1; AltName: Full=Merozoite surface antigen; Flags: Precursor	37.1	37.1	100%	2e-05	92%	P50491.1
RecName: Full=Apical membrane antigen 1; AltName: Full=Merozoite surface antigen; Flags: Precursor	37.1	47.1	100%	2e-05	92%	P16445.1
RecName: Full=Probable cation-transporting ATPase 1	25.2	25.2	58%	0.32	86%	Q04956.1
RecName: Full=Methylcrotonyl-CoA carboxylase beta chain, mitochondrial; Short=MCCase subunit beta; AltName: Full=3-methylcrotonyl-CoA carboxylase 2;	24.4	24.4	91%	0.65	73%	Q9HCC0.1

Alignment Sequences

B

RecName: Full=Apical membrane antigen 1; AltName: Full=Merozoite surface antigen; Flags: Precursor
Sequence ID: [P22621.1](#) Length: 622 Number of Matches: 1

Score	Expect	Identities	Positives	Gaps
42.2 bits(92)	3e-07	12/12(100%)	12/12(100%)	0/12(0%)

Query 1 YDIEEVHGSGIR 12
 YDIEEVHGSGIR
Sbjct 117 YDIEEVHGSGIR 128

C

RecName: Full=Methylcrotonyl-CoA carboxylase beta chain, mitochondrial; Short=MCCa; Full=3-methylcrotonyl-CoA carboxylase non-biotin-containing subunit; AltName: Full=3-me
Sequence ID: [Q9HCC0.1](#) Length: 563 Number of Matches: 1

Score	Expect	Identities	Positives	Gaps
24.4 bits(50)	0.65	8/11(73%)	8/11(72%)	0/11(0%)

Query 1 YDIEEVHGSGI 11
 YD EEV G GI
Sbjct 109 YDNEEVPGGGI 119

Figure 3.26 The protein BLAST results of YDIEEVHGSGIR. **A** indicates to the protein descriptions. **B** indicates the alignment sequence of AMA-1 and **C** indicates the sequence of the human protein.

The addition of the protease inhibitors assisted in the successful identification of *Pf*AMA-1 from a sample of isolated merozoites through proteomic methods. Although *Pf*AMA-1 protein was to be characterised in terms of the mass fragments derived from the protein, the investigation was unable to perform a complete *de novo* sequence of the protein due to its relatively low abundance within the sample. This was evident from each of the peptides spectrum, observed in Figure 3.27 A-C. The ion intensity (y-axis) and spectral count (i.e. the number of PSM per protein) correlate with the relative abundance of a protein within a sample (127). The ion intensity of the *Pf*AMA peptides was between 2-12% (Figure 3.27) and the spectral count for *Pf*AMA was only 3 (Figure 3.23), as each peptide had a single PSM, this confirmed that it was a low abundant merozoite protein.

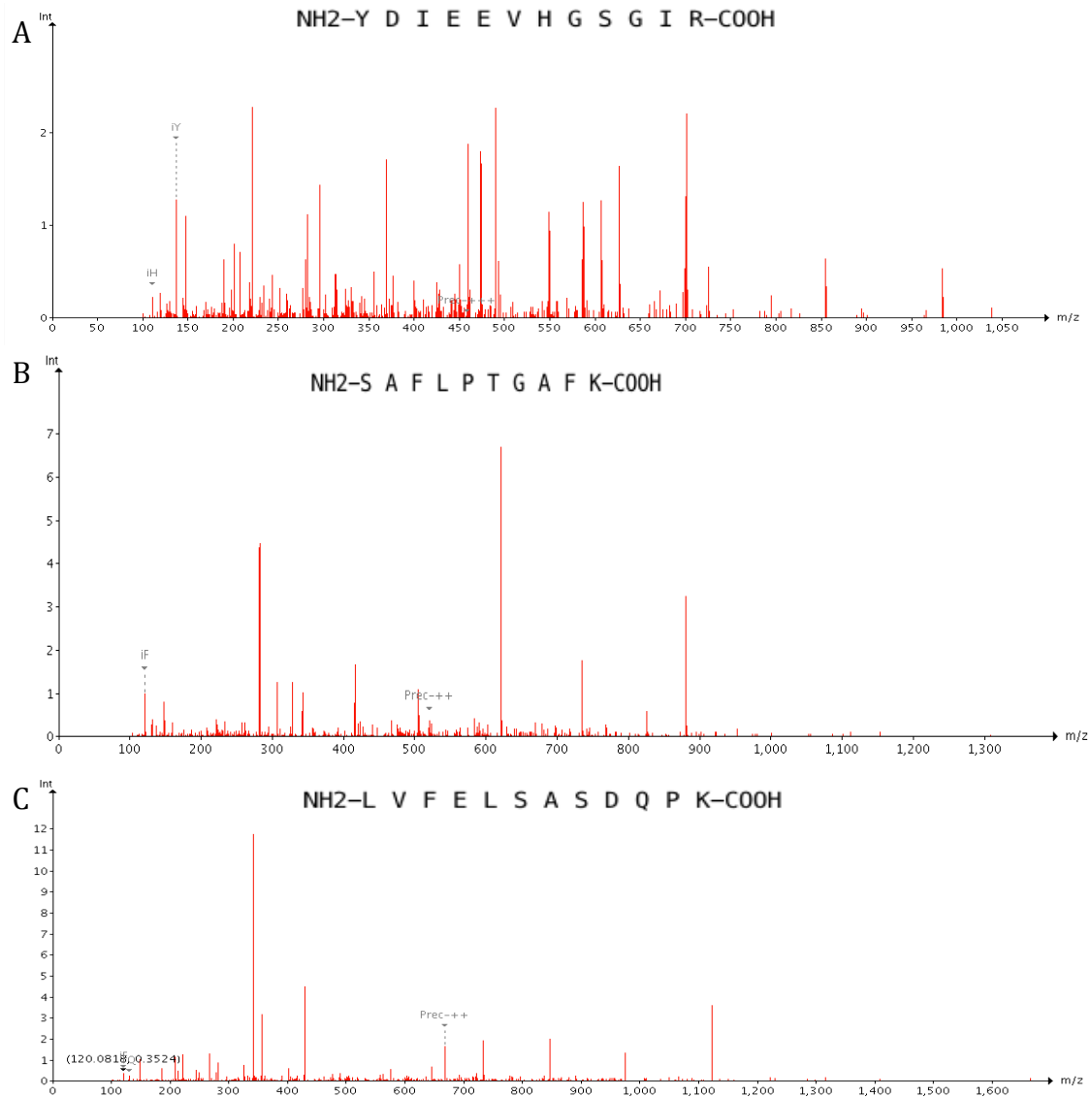


Figure 3.27 *Pf*AMA-1 peptide spectra. The y-axis represents the ion intensity (cps) and the x-axis represents the mass to charge ratio (m/z) of each peak. **A** is the MS spectrum of YDIEEVHGSIGIR with an ion intensity of less than 3 cps. **B** is the spectrum of SAFLPTGAFK with an intensity of 7 cps. **C** is the spectrum of LVFELSASDQPK with the highest intensity (and relative abundance) of 12 cps.

With the generation of LC-MS/MS spectra and the use of software, such as Peptideshaker, a partial *de novo* sequence of *Pf*AMA-1 was produced from the spectra of each peptide, displayed in Figure 3.28, where the amino acids were identified according to their mass, which was calculated from the mass difference between each y-ion peak. In mass spectrometry peptides are sequenced from the b- and y-ions that are formed when the trypsin digestion peptides are fragmented. Peptides fragment into two sets of ions, as seen in Figure 3.29. The ‘abc’-ions, which allow the peptide to be

sequenced from left to right, and the ‘xyz’-ions, which sequence the peptide in reverse (from right to left). The b- and y-ions are the most commonly produced, as the peptide bonds have the lowest energy and therefore break easiest during fragmentation (128). As can be seen from the spectra in Figure 3.30, the y-ions are more abundant than the b-ions, this is due to the y-ions being more stable within the TOF-MS instrument (129).

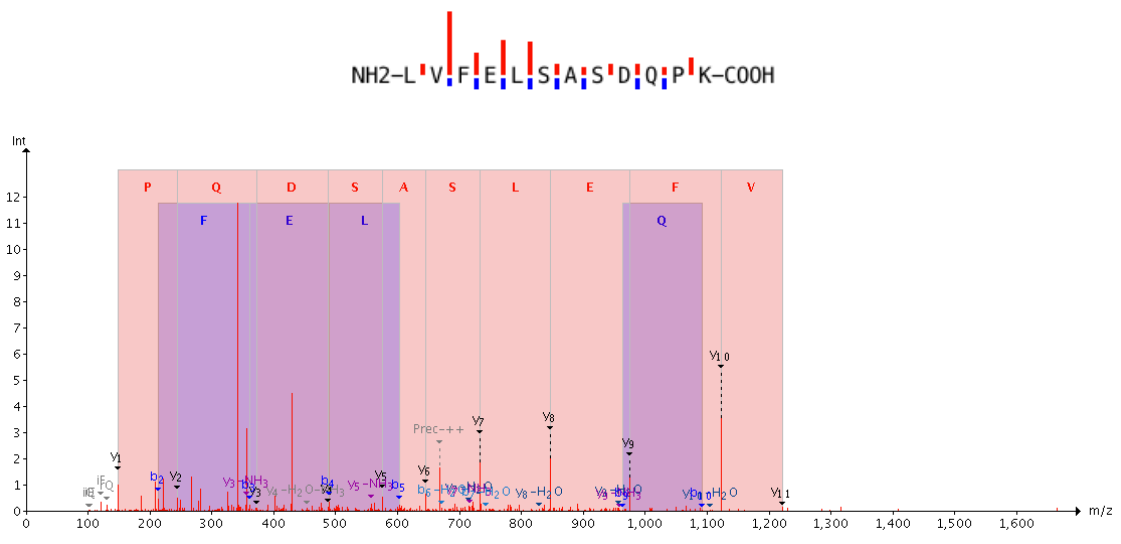


Figure 3.28 The *de novo* sequence of peptide LVFELSASDQPK. The red columns indicate the amino acids identified from the y-ions and the blue columns indicate the amino acids identified from the b-ions. The y-ions sequence the peptide in reverse order (right to left).

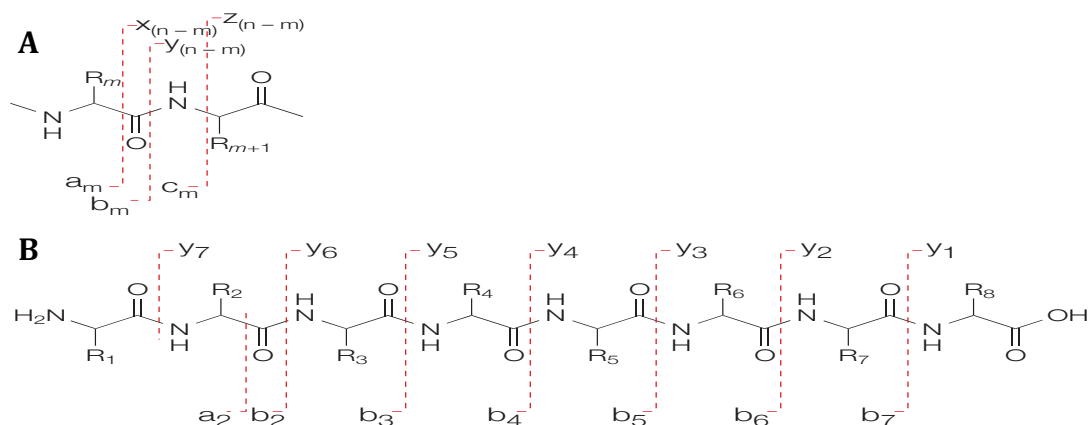


Figure 3.29 Peptide fragment ions. A illustrates all the possible ions that form from peptide fragmentation during ESI along the peptide bonds: a- and x-ions, b- and y-ions and c- and z-ions. B illustrates a peptide that can be fragmented into its different b-ions (left to right) and y-ions (from right to left). The b- and y-ion set of ions are the most commonly formed from peptide fragmentation. Image was from Steen H *et al.* (128) with permission.

A number of factors could have played a role in reducing the concentration of *PfAMA-1* from the sample of isolated merozoites. A biological factor that could still affect the concentration of *PfAMA-1*, is that it is a low abundance merozoite protein that is expressed within a small window period of time (130), as was confirmed from the observed peptide spectra (Figure 3.23 and Figure 3.27). A number of experimental factors, such as the ineffectiveness of the protease inhibitor, E64, and the addition of the washing steps after merozoite isolation. The inability of the E64 to effectively inhibit the degradation of the PV membrane caused the more mature schizonts to release their merozoites before the younger schizonts had fully developed merozoites. As release of merozoites results in the immediate secretion and proteolytic processing of *PfAMA-1*, premature release of merozoites would cause a decrease of the precursor *PfAMA-1* protein. The second factor that could have also contributed to the decrease of the protein's concentration was the addition of the wash steps immediately after the schizonts were lysed with saponin. These wash steps were added to reduce the amount of albumin and human contaminants. However, this could have discarded the two soluble fragments of *PfAMA-1* (*PfAMA-1*_{44/48kDa}) from the sample, as these two fragments are released into the surrounding medium as *PfAMA-1* is processed.

Although the focus of this investigation was to isolate and characterise each of the *PfAMA-1* fragments, the use of electrophoretic and chromatographic techniques to generate a proteomic profile of the merozoite proteome, as a whole, was successful. All the major invasive family proteins and other major apical organelle proteins that were identified in other proteomic studies conducted on the merozoite stage of the parasite's life cycle were also identified in this investigation (82,131).

Chapter 4

4. Conclusion

The aim of this investigation was to culture large synchronised parasite cultures in order to perform a proteomic analysis of *Plasmodium falciparum* merozoites. This was achieved by means of culturing the 3D7 laboratory strain of *Plasmodium falciparum*, synchronising the cultures and isolating the merozoites to construct a proteomic profile through electrophoretic and chromatographic analysis.

Culturing the parasites at a higher hematocrit of 10%, rather than in the lower range of 3-5%, yielded a larger concentration of merozoite proteins. This required synchronising the cultures twice, during the ring stage, using the sorbitol treatment to produce an approximate 6-hour window period between the early and mature schizonts. To enrich for the parasite protein, high enrichment of parasite-infected erythrocytes was achieved by specifically retaining the infected erythrocytes using magnetic assisted retention on MACS columns. After optimisation, parasite infected erythrocytes could be enriched to above 95% of the total erythrocytes in the sample using this technique. Of the parasitized erythrocytes, a 70-80% of merozoite-bearing schizonts isolation was achieved.

This combination of parasite synchronisation technique, together with transmission electron microscopy, was ideal for the purpose of visualising the development of the merozoite, its release from the mature schizont and its invasion into a new erythrocyte. Transmission electron microscopy used in malaria research assists scientists in obtaining knowledge of the parasite's physiology to have a better understanding of how the parasite interacts with its human host, to identify critical target areas for further research to advance the development of treatments against this devastating disease.

With the use of the successful culturing and synchronising parameters, mature schizonts and free merozoites were isolated to visualise the localisation of *PfAMA-1* with confocal microscopy techniques. The apical localisation of *PfAMA-1* was observed on free merozoites. However, due to the low binding affinity of the 1F9 antibody, the circumferential distribution *PfAMA-1* was not observed on either free merozoites or

merozoites within mature schizonts. This investigation did not consistently achieve visualisation of localised *PfAMA-1* on merozoites and it is thought that there may have been a degradation of the antibody used, possibly during the fluorescent labelling of the antibody. However, confocal microscopy techniques can be part of the fundamental methods used to distinguish the vital merozoite surface proteins and erythrocyte receptors that are required for merozoite invasion but would require validated antibody binding to the target haptens.

Lastly, isolated merozoites underwent tryptic digestion to generate a peptide mixture that was successfully used for proteomic profiling of the *Plasmodium falciparum* merozoites. This was achieved; firstly, through the separation of the proteins by SDS gel electrophoresis, desired bands were excised, digested with trypsin and the extracted peptides were analysed by LC-MS/MS to identify the merozoite proteins. Majority of the major invasion protein families were identified through this technique, however the target protein of this investigation, *PfAMA-1*, was not identified. After the addition of protease inhibitors to a newly isolated merozoite sample, *PfAMA-1* was identified through an in-solution tryptic digestion and LC-MS/MS analysis of the peptides. However, due to the low concentration of *PfAMA-1*, this investigation was unable to sequence the precursor protein and its processed fragments in order to fully characterise *PfAMA-1*. Nevertheless, with the assistance of advanced and user-friendly MS-analysis software, such as Peptideshaker, this investigation was able to validate that *PfAMA-1* can be characterised as a minor contributor to the total merozoite proteome from the observed peptide spectra, as well as generate a partial *de novo* sequence of *PfAMA-1* from the identified peptides.

To conclude, this investigation achieved a proteomic profile of the *Plasmodium falciparum* specifically in the merozoite stage.

Limitations and recommendations

In light of the deficient levels of *PfAMA-1* within the isolated merozoite proteome of this investigation, a number of adjustments could be applied to the methods in order to achieve a higher concentration of the low abundant protein.

With regards to the synchronisation and isolation methods. The limiting factor in the synchronisation method could be the length of the window period between schizonts. To decrease the length from 6 hours to possibly 2-3 hours sorbitol treatment could be used in conjunction with the Percoll separation method (132) or with heparin, as described by Boyle *et al* (2010) (45). The limiting factor in the isolation method was the incubation of the isolated parasites with E64. The ineffectiveness of this protease inhibitor resulted in premature release of the merozoites. To possibly counteract this effect the addition of an erythrocyte membrane inhibitor (133) could be used in conjunction with E64 to prevent the degradation of both membranes. Applying the recommendations in these two methods could increase the isolation of pure merozoites from 70-80% to 90-95% and prevent the premature release of merozoites to increase the concentration of *PfAMA-1*.

With respect to the observations of this investigation, this research lays a foundation for future studies focused on proteomic analysis of merozoites, in that a better understanding of how to isolate large volumes of merozoites can be achieved by avoiding the limitations discovered in this study and considering the advice of the recommendations given above, ensuring the isolation of high concentrations of the low abundant merozoite proteins for proteomic analysis.

Chapter 5

5. References

1. Morrison DA. Evolution of the Apicomplexa: Where are We Now? Trends in Parasitology. 2009;25(8):375–82.
2. Lang-Unnasch N, Reith ME, Munholland J, Barta JR. Plastids are Widespread and Ancient in Parasites of the Phylum Apicomplexa. International Journal of Parasitology. 1998;28(11):1743–54.
3. Kaya G. An Overview of Classification of the Phylum Apicomplexa. Kafkas Universitesi Veteriner Fakultesi Dergisi. 2001. Vol. 7, p. 223–228.
4. Blackman MJ, Bannister LH. Apical Organelles of Apicomplexa: Biology and Isolation by Subcellular Fractionation. Molecular Biochemical Parasitology. 2001;117(1):11–25.
5. Prugnolle F, Durand P, Ollomo B, Duval L, Ariey F, Arnathau C, *et al.* A Fresh Look at the Origin of *Plasmodium falciparum*, The Most Malignant Malaria Agent. PLoS Pathology. 2011;7(2):e1001283.
6. Krief S, Escalante AA, Pacheco MA, Mugisha L, André C, Halbwax M, *et al.* On the Diversity of Malaria Parasites in African Apes and the Origin of *Plasmodium falciparum* from Bonobos. PLoS Pathology. 2010;6(2):e1000765.
7. WHO. World Malaria Report 2015. 2015;1–157.
8. WHO. World Malaria Report 2014. 2014;1–142.
9. Rich SM, Leendertz FH, Xu G, LeBreton M, Djoko CF, Aminake MN, *et al.* The Origin of Malignant Malaria. Proceeding of the National Academy of Science USA. 2009 Sep 1;106(35):14902–7.
10. Snow, RW ; Guerra, CA ; Noor, AM ; Myint, HY ; Hay S. The Global Distribution of Clinical Episodes of *Plasmodium falciparum* Malaria. Nature. 2005;434(7030):214–7.
11. Rang HP, Dale MM, Ritter JM, Flower R. Rang and Dale's Pharmacology. 6th ed. Churchill Livingstone Elsevier Ltd; 2008.
12. Howland RD, Mycek M. Pharmacology. 3rd ed. Harvey, RA ; Champe P, editor. Lippincott Williams & Wilkins; 2006.
13. South East Asian Quinine Artesunate Malaria Trial Group. Artesunate Versus Quinine for Treatment of Severe *falciparum* Malaria: A Randomised Trial. Lancet. 2005;366(9487):1–9.
14. WHO. Guidelines for the Treatment of Malaria. 1st ed. Switzerland WHO Press; 2006. 256 p.
15. MacKintosh CL, Beeson JG, Marsh K. Clinical Features and Pathogenesis of Severe Malaria. Trends in Parasitology. 2004;20(12):597–603.
16. Blackman MJ. Proteases in Host Cell Invasion by the Malaria Parasite. Cellular Microbiology. 2004 Oct;6(10):893–903.
17. Bousema T, Drakeley C. Epidemiology and Infectivity of *Plasmodium falciparum* and *Plasmodium vivax* Gametocytes in Relation to Malaria Control and Elimination. Clinical Microbiology Reviews. 2011;24(2):377–410.
18. Iyer J, Grüner AC, Rénia L, Snounou G, Preiser PR. Invasion of Host Cells by Malaria Parasites: A Tale of Two Protein Families. Molecular Microbiology. 2007;65(2):231–49.

19. Matteelli A, Castelli F. Life Cycle of Malaria Parasites. In: Cariso G, Castelli F, editor. Handbook of Malaria Infection in the Tropics [Internet]. 1st ed. Bologna: Italian Association Amici di Raoul Follereau (AIFO); 2002. p. 17–23.
20. Fujioka H, Aikawa M. Malaria Immunology. 2nd ed. Perlmann, P; Troye-Blomberg M, editor. Basel: Krager; 2002. 1-26 p.
21. Angrisano F, Tan YH, Sturm A, McFadden GI, Baum J. Malaria Parasite Colonisation of the Mosquito Midgut--Placing the *Plasmodium* Ookinete Centre Stage. International Journal of Parasitology. 2012;42(6):519–27.
22. Talma AM, Domarle O, McKenzie FE, Ariey F, Robert V. Gametocytogenesis: the Puberty of *Plasmodium falciparum*. Malaria Journal. 2004; 3:24.
23. Delves MJ, Rueker A, Straschil U, Lelievre J, Marques S, Jose Lopez-Barragan M, et al. Male and Female *Plasmodium falciparum* Mature Gametocytes Show Different Responses to Antimalarial Drugs. Antimicrobial Agents and Chemotherapy. 2013; 57 (7): 3268-3274.
24. Greenwood BM, Fidock DA, Kyle DE, Kappe SHI, Alonso PL, Collins FH, et al. Malaria: Progress, Perils and Prospects for Eradication. Journal of Clinical Investigation. 2008;118(4):1266–76.
25. Sturm A, Amino R, van de Sand C, Regen T, Retzlaff S, Rennenberg A, et al. Manipulation of Host Hepatocytes by the Malaria Parasite for Delivery into Liver Sinusoids. Science. 2006;313(5791):1287–90.
26. Dyer M, Day KP. Regulation of the Rate of Asexual Growth and Commitment to Sexual Development by Diffusible Factors from In vitro Cultures of *Plasmodium falciparum*. The American Journal of Tropical Medicine and Hygiene. 2003;68(4):403–9.
27. Hanssen E, McMillan PJ, Tilley L. Cellular Architecture of *Plasmodium falciparum*-Infected Erythrocytes. International Journal of Parasitology. 2010;40(10):1127–35.
28. Lalloo DG, Shingadia D, Bell DJ, Beeching NJ, Whitty CJM, Chiodini PL. UK Malaria Treatment Guidelines 2016. Journal of Infection. Elsevier Ltd; 2016;72(6):635–49.
29. Blumberg, LH.. Recommendations for the Treatment and Prevention of Malaria : Update for the 2015 Season in South Africa. South African Journal of Medicine. 2015;105(3):175–8.
30. Cowman AF, Crabb BS. Invasion of Red Blood Cells by Malaria Parasites. Cell. 2006;124(4):755–66.
31. Gaur D, Mayer DCG, Miller LH. Parasite Ligand-Host Receptor Interactions During Invasion of Erythrocytes by *Plasmodium* Merozoites. International Journal of Parasitology. 2004;34(13–14):1413–29.
32. Boyle MJ, Wilson DW, Richards JS, Riglar DT, Tetteh KKA. Isolation of Viable *Plasmodium falciparum* Merozoites to Define Erythrocyte Invasion Events and Advance Vaccine and Drug Development. Proceedings of the National Academy of Science. 2010;107(32):14378–83.
33. Lalitha P V, Biswas S, Pillai CR, Saxena RK. Immunogenicity of a Recombinant Malaria Vaccine Candidate, Domain I+II of AMA-1 Ectodomain, from Indian *P. falciparum* Alleles. Vaccine. 2008;26(35):4526–35.
34. Mardani A, Keshavarz H, Heidari A, Hajjaran H, Raeisi A, Khorramizadeh MR. Genetic Diversity and Natural Selection at the Domain I of Apical Membrane Antigen-1 (AMA-1) of *Plasmodium falciparum* in Isolates from Iran. Experimental Parasitology. 2012;130(4):456–62.

35. Butler NS, Vaughan AM, Harty JT, Kappe SHI. Whole Parasite Vaccination Approaches for Prevention of Malaria Infection. *Trends in Immunology*. 2012;33(5):247–54.
36. Guinovart C, Aponte JJ, Sacarlal J, Aide P, Leach A, Doban C, *et al*. Insights into Long-Lasting Protection Induced by RTS,S / AS02A Malaria Vaccine : Further Results from a Phase IIb Trial in Mozambican Children. 2009;4(4):e5165: 1-8.
37. RTSS Clinical Trials Partnership. Efficacy and Safety of RTS,S:AS01 Malaria Vaccine With or Without a Booster Dose in Infants and Children in Africa - Final Results of a Phase 3, Individually Randomised, Controlled Trial. *Lancet*. 2015;6736(15):31–45.
38. Blackman MJ. Malarial Proteases and Host Cell Egress: An “Emerging” Cascade. *Cellular Microbiology*. 2008;10(10):1925–34.
39. Winograd E, Clavijo CA, Bustamante LY, Jaramillo M. Release of Merozoites From *Plasmodium falciparum*-Infected Erythrocytes Could Be Mediated By a Non-Explosive Event. *Parasitology Research*. 1999;85:621–4.
40. Clavijo CA, Mora CA, Winograd E. Identification of Novel Membrane Structures in *Plasmodium falciparum* Infected Erythrocytes. *Mem Inst Oswaldo Cruz*. 1998;93(1):115–20.
41. Glushakova S, Yin D, Li T, Zimmerberg J. Membrane Transformation During Malaria Parasite Release From Human Red Blood Cells. *Current Biology*. 2005;15(18):1645–50.
42. Wickham ME, Culvenor JG, Cowman AF. Selective Inhibition of a Two-Step Egress of Malaria Parasites from the Host Erythrocyte. *Journal of Biological Chemistry*. 2003;278(39):37658–63.
43. Salmon BL, Oksman A, Goldberg DE. Malaria Parasite Exit From the Host Erythrocyte: A Two-Step Process Requiring Extraerythrocytic Proteolysis. *Proceedings of the National Academy of Science U S A*. 2001;98(1):271–6.
44. Soni S, Dhawan S, Rosen KM, Chafel M, Chishti AH, Hanspal M. Characterization of Events Preceding the Release of Malaria Parasite from the Host Red Blood Cell. *Blood Cells, Molecules and Diseases*. 2005;35(2):201–11.
45. Boyle MJ, Richards JS, Gilson PR, Chai W, Beeson JG. Interactions with Heparin-Like Molecules During Erythrocyte Invasion by *Plasmodium falciparum* Merozoites. *Blood*. 2010;115(22):4559–68.
46. Kadekoppala M, Holder A. Merozoite Surface Proteins of the Malaria Parasite: The MSP1 Complex and the MSP7 Family. *International Journal of Parasitology. Australian Society for Parasitology Inc.*; 2010;40(10):1155–61.
47. Goel VK, Li X, Chen H, Liu SC, Chishti AH, Oh SS. Band 3 is a Host Receptor Binding Merozoite Surface Protein 1 During the *Plasmodium falciparum* Invasion of Erythrocytes. *Proceedings of the National Academy of Science USA*. 2003;100(9):5164–9.
48. Counihan NA, Kalanon M, Coppel RL, Koning-ward TF De. *Plasmodium* Rhoptry Proteins : Why Order is Important. *Trends in Parasitology. Elsevier Ltd*; 2013;29(5):228–36.
49. Riglar DT, Richard D, Wilson DW, Boyle MJ, Dekiwadia C, Turnbull L, *et al*. Super-Resolution Dissection of Coordinated Events During Malaria Parasite Invasion of the Human Erythrocyte. *Cell Host & Microbe. Elsevier Inc.*; 2011;9(1):9–20.

50. Bannister LH, Hopkins JM, Dluzewski AR, Margos G, Williams IT, Blackman MJ, *et al.* *Plasmodium falciparum* Apical Membrane Antigen 1 (PfAMA-1) is Translocated Within Micronemes Along Subpellicular Microtubules During Merozoite Development. *Journal of Cell Science*. 2003;116(Pt 18):3825–34.
51. Srinivasan P, Beatty WL, Diouf A, Herrera R, Ambroggio X, Moch JK, *et al.* Binding of *Plasmodium* Merozoite Proteins RON2 and AMA1 Triggers Commitment to Invasion. *Proceedings of the National Academy of Science USA*. 2011;108(32):13275–80.
52. Dutta S, Haynes JD, Barbosa A, Lisa A, Snaveley JD, Moch JK, *et al.* Mode of Action of Invasion-Inhibitory Antibodies Directed Against Apical Membrane Antigen 1 of *Plasmodium falciparum*. *Society*. 2005;73(4):2116–22.
53. Dutta S, Haynes JD, Moch JK, Barbosa A, Lanar DE. Invasion-Inhibitory Antibodies Inhibit Proteolytic Processing of Apical Membrane Antigen 1 of *Plasmodium falciparum* Merozoites. *Proceedings of the National Academy of Science U S A*. 2003 Oct 14;100(21):12295–300.
54. Harris PK, Yeoh S, Dluzewski AR, O'Donnell RA, Withers-Martinez C, Hackett F, *et al.* Molecular Identification of a Malaria Merozoite Surface Sheddase. *PLoS Pathology*. 2005;1(3):0241–51.
55. Kato K, Mayer DCG, Singh S, Reid M, Miller LH. Domain III of *Plasmodium falciparum* Apical Membrane Antigen 1 Binds to the Erythrocyte Membrane Protein Kx. *Proceedings of the National Academy of Science USA*. 2005;
56. Triglia T, Healer J, Caruana SR, Hodder AN, Anders RF, Crabb BS, *et al.* Apical Membrane Antigen 1 Plays a Central Role in Erythrocyte Invasion by *Plasmodium* Species. *Mol Microbiol*. 2000;38(4):706–18.
57. Lim, SS, Yang, W, Krishnarjuna, B *et al.* Structure and Dynamics of Apical Membrane Antigen 1 From *Plasmodium falciparum* FVO. *Biochemistry*. 2014;53(46):7310–20.
58. Chesne-Seck ML, Pizarro JC, Vulliez-Le Normand B, Collins CR, Blackman MJ, Faber BW, *et al.* Structural Comparison of Apical Membrane Antigen 1 Orthologues and Paralogues in Apicomplexan Parasites. *Molecular and Biochemical Parasitology*. 2005;144(1):55–67.
59. Peterson MG, Marshall VM, Smythe JA, Crewther PE, Lew A, Silva A, *et al.* Integral Membrane Protein Located in the Apical Complex of *Plasmodium falciparum*. *Molecular and Cellular Biology*. 1989;9(7):3151–4.
60. Campbell, MK ; Farrel S. *Biochemistry*. 4th ed. Thomson Learning Inc; 2003.
61. Ott CM, Lingappa VR. Integral Membrane Protein Biosynthesis: Why Topology is Hard to Predict. *Journal of Cell Science*. 2002;115(Pt 10):2003–9.
62. Mamatha D, Nagalakshamma K, Dev Rajesh VA, Sheerin VS. Protein Modeling of Apical Membrane Antigen-1 (AMA-1) of *Plasmodium cynomolgi*. *Journal of Biotechnology*. 2007;6(22):2628–32.
63. Bai T, Becker M, Gupta A, Strike P, Murphy VJ, Anders RF, *et al.* Structure of AMA1 from *Plasmodium falciparum* Reveals a Clustering of Polymorphisms that Surround a Conserved Hydrophobic Pocket. *Proceedings of the National Academy of Science U S A*. 2005 Sep 6;102(36):12736–41.
64. Coley AM, Gupta A, Murphy VJ, Bai T, Kim H, Anders RF, *et al.* Structure of the Malaria Antigen AMA1 in Complex with a Growth-Inhibitory Antibody. *PLoS Pathology*. 2007;3(9):1308–19.
65. Bozzola J, Russel L. *Electron Microscopy*. 2nd ed. McKean B, editor. Jones and bartlett Publishers; 1999.

66. Hibbs A. Confocal Microscopy for Biologists. 1st ed. Kluwer Academic/Plenum Publishers; 2004.
67. Conn P. Handbook of Proteomics Methods. 1st ed. Human Press; 2003.
68. Wagner MA, Andemariam B, Desai SA. A Two-Compartment Model of Osmotic Lysis in *Plasmodium falciparum*-Infected Erythrocytes. *Biophysiology Journal*. 2003;84(1):116–23.
69. Jensen JB, Trager W. *Plasmodium falciparum* in Culture: Use of Outdated Erythrocytes and Description of the Candle Jar Method. *Journal of Parasitology*. 1977;63(5):883–6.
70. Trager W, Jensen JB. Human Malaria Parasites in Continuous Culture. *Journal of Parasitology*. 2005;91(3):484–6.
71. Allen RJW, Kirk K. *Plasmodium falciparum* Culture: The Benefits of Shaking. *Molecular and Biochemical Parasitology*. 2010;169(1):63–5.
72. Radfar A, Méndez D, Moneriz C, Linares M, Marín-García P, Puyet A, *et al*. Synchronous Culture of *Plasmodium falciparum* at High Parasitemia Levels.. Vol. 4, *Nature Protocols*. 2009. p. 1899–915.
73. Lambros C, Vanderberg JP. Synchronization of *Plasmodium falciparum* Erythrocytic Stages in Culture. *Journal of Parasitology*. 1979;65(3):418–20.
74. Mata-Cantero L, Lafuente MJ, Sanz L, Rodriguez MS. Magnetic Isolation of *Plasmodium falciparum* Schizonts iRBCs to Generate a High Parasitaemia and Synchronized In vitro Culture. *Malaria Journal*. 2014;13(1):112–20.
75. Sanderson A, Walliker D, Molez JF. Enzyme Typing of *Plasmodium falciparum* From African and Some Other Old World Countries. *Transactions of the Royal Society of Tropical Medicine and Hygiene*. 1981;75(2):263–7.
76. Delplace P, Fortier B, Tronchin G, Dubremetz J, Vernes A. Localization, Biosynthesis, Processing and Isolation of a Major 126 kDa Antigen of the Parasitophorous Vacuole of *Plasmodium falciparum*. *Molecular and Biochemical Parasitology*. 1987;23:193–201.
77. Glauert A. Fixation, Dehydration and Embedding of Biological Specimens. 1st ed. North-Holland Publishing Company; 1975.
78. Robinson D, Ehlers U, Herken R, Herman B, Mayer F, Schurmann F. Methods of Preparation for Electron Microscopy. 1st ed. Springer-Verlag; 1987.
79. Reynolds ES. The Use of Lead Citrate Stain at High pH in Electron Microscopy. *Journal of Cell Biology*. 1963;17:208–21.
80. Moll K, Kaneko A, Scherf A, Wahlgren M. Methods in Malaria Research. 5th ed. Moll K, Kaneko A, Scherf A, Wahlgren M, editors. 2008.
81. Chazotte B. Labeling Nuclear DNA Using DAPI. *Cold Spring Harbour Protocols*. 2011;6(1):80–3.
82. Smit S, Stoychev S, Louw AI, Birkholtz L. Proteomic Profiling of *P.falciparum* Through Improved , Semi-Quantitative Two-Dimensional Gel Electrophoresis. *Journal of Proteome Research*. 2010;9:2170–81.
83. Shevchenko A, Tomas H, Havlis J, Olsen JV, Mann M. In-Gel Digestion For Mass Spectrometric Characterization of Proteins and Proteomes. *Nature Protocol*. 2006;1(6):2856–60.
84. Vaudel M, Burkhardt JM, Zahedi RP, Oveland E, Berven FS, Sickmann A, *et al*. PeptideShaker Enables Reanalysis of MS-derived Proteomics Data Sets. *Nature Biotechnology*. 2015;33(1):22–4.
85. Rayner JC. Erythrocyte Exit: Out, Damned Merozoite! Out I say! *Trends in Parasitology*. 2006;22(5):189–92.

86. Li T, Glushakova S, Zimmerberg J. A New Method for Culturing *Plasmodium falciparum* Shows Replication at the Highest Erythrocyte Densities. *Journal of Infectious Diseases*. 2003;187:159–62.
87. Solomon E, Berg L, Martin D. *Biology*. 6th ed. Thomas Learning Inc.; 2002.
88. Zolg JW, Macleod AJ, Scaife JG, Beaudoin RL. The Accumulation of Lactic Acid and Its Influence On the Growth of *Plasmodium falciparum* in Synchronised cultures. *In Vitro*. 1984;20(3):205–15.
89. Thi D, Trang X, Huy NT, Kariu T, Tajima K, Kamei K. One-Step Concentration of Malarial Parasite-Infected Red Blood Cells and Removal of Contaminating White Blood Cells. *Malaria Journal*. 2004;3(7):1–7.
90. Egan TJ. Haemozoin Formation. *Molecular and Biochemical Parasitology*. 2008;157(2):127–36.
91. Karl S, Davis TME, St Pierre TG. Parameterization of High Magnetic Field Gradient Fractionation Columns for Applications with *Plasmodium falciparum* Infected Human Erythrocytes. *Malaria Journal*. 2010;9(1):116–25.
92. Almanza A, Coronado L, Tayler N, Herrera L, Spadafora C. Automated Synchronization of *P. falciparum* Using a Temperature Cycling Incubator. *Current Trends in Biotechnology and Pharmacy*. 2011;5(2):1130–3.
93. Koster AJ, Klumperman J. Electron Microscopy in Cell Biology: Integrating Structure and Function. *Nature Review Molecular and Cell Biology*. 2003;1(4):SS6-10.
94. Adams JH, Blair PL, Kaneko O, Peterson DS. An Expanding ebl Family of *Plasmodium falciparum*. *Trends in Parasitology*. 2001;17(5):297–9.
95. Gaur D, Furuya T, Mu J, Jiang L Bin, Su XZ, Miller LH. Upregulation of Expression of the Reticulocyte Homology Gene 4 in the *Plasmodium falciparum* Clone Dd2 is Associated with a Switch in the Erythrocyte Invasion Pathway. *Molecular and Biochemical Parasitology*. 2006;145(2):205–15.
96. Stubbs J, Simpson KM, Triglia T, Plouffe D, Tonkin CJ, Duraisingh MT, *et al*. Molecular Mechanism for Switching of *P. falciparum* Invasion Pathways into Human Erythrocytes. *Science*. 2005;309:1384–7.
97. Lamarque M, Besteiro S, Papoin J, Roques M, Vulliez-Le Normand B, Morlon-Guyot J, *et al*. The RON2-AMA1 Interaction is a Critical Step in Moving Junction-Dependent Invasion by Apicomplexan Parasites. *PLoS Pathology*. 2011;7(2):e1001276.
98. Ward GE, Miller LH, Dvorak JA. The Origin of Parasitophorous Vacuole Membrane Lipids in Malaria-infected Erythrocytes. *Journal of Cell Science*. 1993;106:237–48.
99. Healer J, Crawford S, Ralph S, McFadden G, Cowman AF. Independent Translocation of Two Micronemal Proteins in Developing *Plasmodium falciparum* Merozoites. *Infection and Immunity*. 2002;70(10):5751–8.
100. Narum DL, Thomas AW. Differential Localization of Full-Length and Processed Forms of PF83/AMA-1 an Apical Membrane Antigen of *Plasmodium falciparum* Merozoites. *Molecular and Biochemical Parasitology*. 1994;67(1):59–68.
101. Wang W, Singh S, Zeng DL, King K, Nema S. Antibody Structure, Instability, and Formulation. *Journal of Pharmaceutical Science*. 2007;96(1):1–26.
102. Coley AM, Campanale NV, Casey JL, Hodder AN, Crewther PE, Anders RF, *et al*. Rapid and Precise Epitope Mapping of Monoclonal Antibodies Against *Plasmodium falciparum* AMA1 by Combined Phage Display of Fragments and Random Peptides. *Protein Engineering*. 2001;14(9):691–8.

103. Dutta S, Dlugosz LS, Drew DR, Ge X, Ababacar D, Rovira YI, *et al.* Overcoming Antigenic Diversity by Enhancing the Immunogenicity of Conserved Epitopes on the Malaria Vaccine Candidate Apical Membrane Antigen-1. *PLoS Pathology*. 2013;9(12):1–17.
104. Coley AM, Parisi K, Masciantonio R, Hoeck J, Murphy VJ, Harris KS, *et al.* The Most Polymorphic Residue on *Plasmodium falciparum* Apical Membrane Antigen 1 Determines Binding of an Invasion-Inhibitory Antibody The Most Polymorphic Residue on *Plasmodium falciparum* Apical Membrane Antigen 1 Determines Binding of an Invasion-Inhibit. Society. 2006;
105. Kabat E. The Molecular Weight of Antibodies. *Journal of Experimental Medicine*. 1939;69(1):103–18.
106. Baldwin MA. Protein Identification by Mass Spectrometry. *Molecular & Cellular Proteomics*. 2004;3(1):1–9.
107. Forero C, Wasserman M. Isolation and Identification of Actin-binding Proteins in *Plasmodium falciparum* by Affinity Chromatography. *Mem Inst Oswaldo Cruz*. 2000;95(3):329–37.
108. Arumugam TU, Takeo S, Yamasaki T, Thonkukiattkul A, Miura K, Otsuki H, *et al.* Discovery of GAMA, a *Plasmodium falciparum* Merozoite Micronemal Protein, as a Novel Blood-Stage Vaccine Candidate Antigen. *Infection and Immunity*. 2011;79(11):4523–32.
109. Pinzón CG, Curtidor H, Reyes C, Méndez D, Patarroyo ME. Identification of *Plasmodium falciparum* RhopH3 Protein Peptides that Specifically Bind to Erythrocytes and Inhibit Merozoite Invasion. *Protein Science*. 2008;17(10):1719–1730.
110. Baldi DL, Andrews KT, Waller RF, Roos DS, Howard RF, Crabb BS, *et al.* RAP1 Controls Rhoptry Targeting of RAP2 in the Malaria Parasite *Plasmodium falciparum*. *EMBO Journal*. 2000;19(11):2435–43.
111. Sahar T, Reddy KS, Bharadwaj M, Pandey AK, Singh S, Chitnis CE, *et al.* *Plasmodium falciparum* Reticulocyte Binding-Like Homologue Protein 2 (PfRH2) is a Key Adhesive Molecule Involved in Erythrocyte Invasion. *PLoS One*. 2011;6(2):e17102.
112. Agarwal S, Singh MK, Garg S, Chitnis CE, Singh S. Ca²⁺-Mediated Exocytosis of Subtilisin-Like Protease 1: A Key Step in Egress of *Plasmodium falciparum* Merozoites. *Cellular Microbiology*. 2013;15(6):910–21.
113. Holder AA, Blackman MJ, Burghaus PA, Chappel JA, Ling IT, McCallum-Deighton N, *et al.* A Malaria Merozoite Surface Protein (MSP1) Structure Processing and Function. *Mem Inst Oswaldo Cruz*. 1992;87(Supplementary III):37–42.
114. Sanders PR, Gilson PR, Cantin GT, Greenbaum DC, Nebl T, Carucci DJ, *et al.* Distinct Protein Classes Including Novel Merozoite Surface Antigens in Raft-Like Membranes of *Plasmodium falciparum*. *Journal of Biological Chemistry*. 2005;280(48):40169–76.
115. Binder EM, Kim K. Location, Location, Location: Trafficking and Function of Secreted Proteases of *Toxoplasma* and *Plasmodium*. *Traffic*. 2004;5(12):914–24.
116. Rosenthal PJ. Cysteine Proteases of Malaria Parasites. *International Journal of Parasitology*. 2004;34(13–14):1489–99.
117. Wahlgren M, Perlmann P. *Malaria: Molecular and Clinical Aspects*. Harwood Academic Publishers; 1999. 563 p.

118. Ling IT, Florens L, Dluzewski AR, Kaneko O, Grainger M, Yim Lim BYS, *et al.* The *Plasmodium falciparum* Clag9 Gene Encodes a Rhoptry Protein That is Transferred to the Host Erythrocyte Upon Invasion. *Molecular Microbiology*. 2004;52(1):107–18.
119. Culvenor JG, Day KP, Anders RF. *Plasmodium falciparum* Ring-Infected Erythrocyte Surface Antigen is Released from Merozoite Dense Granules After Erythrocyte Invasion. *Infection and Immunity*. 1991;59(3):1183–7.
120. Hustoft HK, Malerod H, Wilson SR, Reubsaet L, Lundanes E, Greibrokk T. A Critical Review of Trypsin Digestion for LC-MS Based Proteomics. In: Eastwood Leung HC, Man T-K, Flores RJ, editors. *Integrative Proteomics*. Intech; 2010. p. 73–92. Available from: <http://www.intechopen.com/books/integrative-proteomics>
121. Nilsson T, Mann M, Aebersold R, Yates JR, Bairoch A, Bergeron JJM. Mass Spectrometry in High-Throughput Proteomics: Ready for the Big Time. *Nature Methods*. Nature Publishing Group; 2010;7(9):681–5.
122. Walther TC, Mann M. Mass Spectrometry-Based Proteomics in Cell Biology. *Journal of Cellular Biology*. 2010;190(4):491–500.
123. Shilov IV, Seymour SL, Patel AA, Loboda A, Tang WH, Keating SP, *et al.* The Paragon Algorithm, a Next Generation Search Engine that Uses Sequence Temperature Values and Feature Probabilities to Identify Peptides from Tandem Mass Spectra. *Molecular & Cellular Proteomics*. 2007. Vol. 6, 1638-1655 p.
124. Shteynberg D, Nesvizhskii AI, Moritz RL, Deutsch EW. Combining Results of Multiple Search Engines in Proteomics. *Molecular & Cellular Proteomics*. 2013;12(9):2383–93.
125. Sennels L, Bukowski-Wills JC, Rappsilber J, Aebersold R, Mann M, Rappsilber J, *et al.* Improved Results in Proteomics by Use of Local and Peptide-Class Specific False Discovery Rates. *BMC Bioinformatics*. 2009;10(1):179–89.
126. Altschul S, Gish W, Miller W, Myers E, Lipman D. Basic Local Alignment Search Tool. *Journal of Molecular Biology*. 1990;215(3):403–10.
127. Bondarenko PV, Chelius D, Shaler TA, Parkway RO, Jose S. Identification and Relative Quantitation of Protein Mixtures by Enzymatic Digestion Followed by Capillary Reversed-Phase Liquid Chromatography - Tandem Mass Spectrometry. *Analytical Chemistry*. 2002;74(18):4741–9.
128. Steen H, Mann M. The abc's (and xyz's) of Peptide Sequencing. *Nature Review Molecular Cell Biology*. 2004;5:699–711.
129. Palz B, Suhail S. Fragmentation Pathways of Protonated Peptides. *Mass Spectrometry Review*. 2005;24(4):508–48.
130. Hodder AN, Crewther PE, Matthew ML, Reid GE, Moritz RL, Simpson RJ, *et al.* The Disulfide Bond Structure of *Plasmodium* Apical Membrane Antigen-1. *Journal of Biological Chemistry*. 1996;271(46):29446–52.
131. Florens L, Washburn MP, Raine JD, Anthony RM, Grainger M, Haynes JD, *et al.* A Proteomic View of the *Plasmodium falciparum* Life Cycle. *Nature*. 2002;419(6906):520–6.
132. Rivadeneira E, Wasserman M, Espinal C. Separation and Concentration of Schizonts of *Plasmodium falciparum* by Percoll Gradients. *Journal of Protozoology*. 1983;30(2):367–70.
133. Gelhaus C, Vicik R, Schirmeister T, Leippe M. Blocking Effect of a Biotinylated Protease Inhibitor on the Egress of *Plasmodium falciparum* Merozoites from Infected Red Blood Cells. *Biological Chemistry*. 2005;386(5):499–502.



Appendix I

Ethics Approval Letter

The Research Ethics Committee, Faculty Health Sciences, University of Pretoria complies with ICH-GCP guidelines and has US Federal wide Assurance.

- FWA 00002567, Approved dd 22 May 2002 and Expires 20 Oct 2016.
- IRB 0000 2235 IORG0001762 Approved dd 13/04/2011 and Expires 13/04/2014.



UNIVERSITEIT VAN PRETORIA
UNIVERSITY OF PRETORIA
YUNIBESITHI YA PRETORIA

Faculty of Health Sciences Research Ethics Committee

1/08/2013

**Approval Notice
New Application**

Ethics Reference No.: 305/2013

Title: Characterization of Plasmodium falciparum merozoite apical membrane antigen-1 protein changes prior to erythrocyte invasion

Dear Ms S.L. Downing

The **New Application** for your research received on the 1 July 2013, was approved by the Faculty of Health Sciences Research Ethics Committee on the 31/07/2013.

Please note the following about your ethics approval:

- Ethics Approval is valid for 2 years.
- Please remember to use your protocol number (305/2013) on any documents or correspondence with the Research Ethics Committee regarding your research.
- Please note that the Research Ethics Committee may ask further questions, seek additional information, require further modification, or monitor the conduct of your research.

Ethics approval is subject to the following:

Standard Conditions:

- The ethics approval is conditional on the receipt of 6 monthly written Progress Reports, and
- The ethics approval is conditional on the research being conducted as stipulated by the details of all documents submitted to the Committee. In the event that a further need arises to change who the investigators are, the methods or any other aspect, such changes must be submitted as an Amendment for approval by the Committee.

The Faculty of Health Sciences Research Ethics Committee complies with the SA National Act 61 of 2003 as it pertains to health research and the United States Code of Federal Regulations Title 45 and 46. This committee abides by the ethical norms and principles for research, established by the Declaration of Helsinki, the South African Medical Research Council Guidelines as well as the Guidelines for Ethical Research: Principles Structures and Processes 2004 (Department of Health).

We wish you the best with your research.

Yours sincerely

Professor Werdie (CW) Van Staden
MBChB MMed(Psych) MD FCPsych FTCL UPLM
Chairperson: Faculty of Health Sciences Research Ethics Committee

☎ 012 354 1677 ☎ 0866516047 ✉ deepeka.behari@up.ac.za 🌐 <http://www.healthethics-up.co.za>
✉ Private Bag X323, Arcadia, 0007 - 31 Bophelo Road, HW Snyman South Building, Level 2, Room 2.33, Gezina, Pretoria



The Research Ethics Committee, Faculty Health Sciences, University of Pretoria complies with ICH-GCP guidelines and has US Federal wide Assurance.

- FWA 00002587, Approved dd 22 May 2002 and Expires 20 Oct 2016.
- IRB 0000 2235 IORG0001762 Approved dd 13/04/2011 and Expires 13/04/2014.



Faculty of Health Sciences Research Ethics Committee

27/03/2014

**Approval Certificate
Amendment**

(to be read in conjunction with the main approval certificate)

Ethics Reference No.: 305/2013

Title: Characterization of Plasmodium falciparum merozoite apical membrane antigen-1 protein changes prior to erythrocyte invasion.

Dear Ms S.L. Downing

The **Amendment** as described in the documents received on 12/02/2014 was approved by the Faculty of Health Sciences Research Ethics Committee on the 26/03/2014.

Please note the following about your ethics amendment:

- Please remember to use your protocol number (305/2013) on any documents or correspondence with the Research Ethics Committee regarding your research.
- Please note that the Research Ethics Committee may ask further questions, seek additional information, require further modification, or monitor the conduct of your research.

Ethics amendment is subject to the following:

- The ethics approval is conditional on the receipt of 6 monthly written Progress Reports, and
- The ethics approval is conditional on the research being conducted as stipulated by the details of all documents submitted to the Committee. In the event that a further need arises to change who the investigators are, the methods or any other aspect, such changes must be submitted as an Amendment for approval by the Committee.

We wish you the best with your research.

Yours sincerely

Dr R Sommers; MBChB; MMed (Int); MPharMed.

Deputy Chairperson of the Faculty of Health Sciences Research Ethics Committee, University of Pretoria

The Faculty of Health Sciences Research Ethics Committee complies with the SA National Act 61 of 2003 as it pertains to health research and the United States Code of Federal Regulations Title 45 and 46. This committee abides by the ethical norms and principles for research, established by the Declaration of Helsinki, the South African Medical Research Council Guidelines as well as the Guidelines for Ethical Research: Principles Structures and Processes 2004 (Department of Health).

♦ Tel:012-3541330 ♦ Fax:012-3541367 Fax2Email: 0866515924 ♦ E-Mail: fhsethics@up.ac.za
♦ Web: [//www.healthethics-up.co.za](http://www.healthethics-up.co.za) ♦ H W Snyman Bld (South) Level 2-34 ♦ Private Bag x 323, Arcadia, Pta, S.A., 0007

Appendix II

Blood Donation Consent Form

INFORMATION LEAFLET AND INFORMED CONSENT FOR NON-CLINICAL RESEARCH (i.e. non-clinical operational research)

Title of the Study: Characterization of *Plasmodium falciparum* merozoite apical membrane antigen-1 protein changes prior to erythrocyte invasion

Dear Voluntary Blood Donor,

1) INTRODUCTION

We invite you to participate in a research study. This information leaflet will help you to decide if you want to participate. Before you agree to take part you should fully understand what is involved. If you have any questions that this leaflet does not fully explain, please do not hesitate to ask the study investigator, Miss Sarita Downing.

2) THE NATURE AND PURPOSE OF THIS STUDY

Malaria is a life threatening disease that kills millions of people each year, the majority of these being young children. They are infected with the malaria parasite, called *Plasmodium*, when they are bitten by a mosquito, which carries the parasite. In this study we want to isolate a specific protein (*PfAMA-1*) from the parasite, and research the role it plays in the parasites life cycle, as it is a vital candidate for a vaccine against malaria. You, as a potential healthy and voluntary blood donor, can be a very important part of this study as this study requires red blood cells, from humans like yourself, to grow these parasites in the laboratory for further research on the malaria parasite protein.

3) EXPLANATION OF PROCEDURES TO BE FOLLOWED

If you decide to help us to perform this study, the following will be required of you: 1) Your name will be placed on a donor list at the Department of Pharmacology, University of Pretoria for 2013. 2) Every 2-3 months you will be asked to donate 250 mL of blood (which is equivalent to a glass of water). 3) On a donation day an appointment will be made with the staff at the Clinical Research Unit Room 2-54 Pathology Building on Prinshof Medical Campus of the University of Pretoria. 4) The

nurse will take your blood pressure to determine whether or not you may donate blood.

5) If the nurse agrees that you are ready to donate; blood will be drawn from a vein in your left or right arm. Thereafter the blood bag with your donation will be placed in a fridge for 24 hours allowing all the red blood cells to mix with the chemicals in the bag that prevent the cells from sticking together. The following day the blood will be poured into 50 mL tubes (equivalent to three tablespoons) and allowed to settle into the three components known as plasma (yellowish), buffy coat (white thin layer) and the red blood cells we are interested in for this study. This blood will be washed to remove everything that is not red blood cells, and these cleaned red blood cells will be used to grow the malaria parasites in the laboratory.

4) RISK AND DISCOMFORT INVOLVED

There are only minimal risks involved in participating in the study, namely dizziness or light-headedness, but these can be avoided by eating a hearty meal before donating. Some of the processes may cause some discomfort, such as the needle insertion and removal. We will require about 1 hour of your time for this procedure, of which the actual blood drawing step can take anything from 10 to 15 minutes. If you agree to be on the donor list at Pharmacology you will be asked to donate every 2-3 months. You may withdraw from donating at any time.

5) POSSIBLE BENEFITS OF THIS STUDY

Although you will not benefit directly from the study, the results of the study will enable us to possibly identify the importance of the *PfAMA-1* protein as a vaccine candidate for malaria and as a result may reduce the number of deaths caused by malaria in the future.

6) WHAT ARE YOUR RIGHTS AS A PARTICIPANT?

Your participation in this study is entirely voluntary. You can refuse to participate or stop at any time during the study and/or activities at the clinic without giving any reason. Your withdrawal will not affect you in any way.

7) HAS THE STUDY RECEIVED ETHICAL APPROVAL?

This study has received written approval from the Research Ethics Committee of the Faculty of Health Sciences at the University of Pretoria and a copy of the approval letter is available if you wish to have one.

8) INFORMATION AND CONTACT PERSON

The contact person for the study is Miss Sarita Downing, if you have any questions about the study please contact her at 076 846 1751. Alternatively you may contact the project supervisor, Dr. AD Cromarty, at 012 319 2622.

9) COMPENSATION

Your participation is voluntary. No compensation will be given for your participation.

10) CONFIDENTIALITY

All information that you give will be kept strictly confidential. Research reports and articles in scientific journals will not include any information that may identify you or your health status.

CONSENT TO PARTICIPATE IN THIS STUDY

I confirm that the person asking my consent to take part in this study has told me about nature, process, risks, discomforts and benefits of the study. I have also received, read and understood the above written information (Information Leaflet and Informed Consent) regarding the study. I am aware that the results of the study, including personal details, will be anonymously processed into research reports. I am participating willingly. I have had time to ask questions and have no objection to participate in the study. I understand that there is no penalty should I wish to discontinue with the study and my withdrawal will not affect any treatment in any way.

I have received a signed copy of this informed consent agreement.

Participant's name(Please print)

Participant's signature:..... Date.....

Investigator's name.....(Please print)

Investigator's signature..... Date.....

Witness's Name.....(Please print)

Witness's signature..... Date.....

Appendix III

List of Reagents

A3.1 Culturing Reagents

A3.1.1 Sorbitol Solution

To prepare a 5% D-Sorbitol (Sigma Life Science) solution dissolve 25 g of Sorbitol in 500 mL ddH₂O and autoclave. Solution was stored at RT for 3 months.

A3.1.2 PBS

Dissolve 9.23 g of PBS salt (Becton, Dickinson & Company) in 1 L of ddH₂O and autoclave. Solution was stored at RT for 3 months.

A3.1.3 HEPES

A 1.25 M HEPES (Sigma Life Science) solution in ddH₂O was prepared by dissolving 29.8 g HEPES powder in 100 mL ddH₂O. The pH was adjusted to 7.2 – 7.5 with 1 M NaOH using the Jenway 3510 pH meter and sterile filtered with 0.20 µm sterile filter (GVS Filter technology). Stored at 4 °C.

A3.1.4 Hypoxanthine

An 80.8 mM Hypoxanthine (Sigma-Aldrich) solution was prepared in 50 mL of 0.5 M NaOH and sterile filtered with a 0.20 µm sterile filter. Stored at 4°C.

A3.1.5 Glucose

A 20% Glucose (Merck) solution was made in ddH₂O and sterile filtered with a 0.20 µm sterile filter. Stored at -20°C.

A3.1.6 RPMI Medium

A3.1.6.1 Incomplete Medium

10.4 g of RPMI (Sigma-Aldrich) and 1.8 g of NaHCO₃ (Merck) was dissolved in ~100 mL of sterile ddH₂O. Then 20 mL of 1.25 M HEPES, 10 mL of 20% Glucose, 0.48 µL of 50 mL/mg Gentamycin (Virbac Animal Health) and 2.5 mL of 80.8 mM Hypoxanthine was added. Made up to 1 L with sterile ddH₂O using a measuring cylinder and sterile filtered using a screw-on 0.20 µm sterile filter and vacuum system into sterile 500 mL glass Schott bottles. Stored at 4°C.

A3.1.6.2 AlbuMax Complete Medium

For 500 mL: 2.5 g of AlbuMax II (Life Technologies) was dissolved in 80 mL of Incomplete medium and sterile filtered with a 0.20 µm sterile filter and syringe, into the remaining ICM and mixed. The AlbuMax-complete medium was then sterile filtered using a screw-on 0.20 µm sterile filter and vacuum system into a new sterile 500 mL glass Schott bottle. Stored at 4°C for no longer than 2 weeks.

A3.1.7 E64

For a 1 mM E64 (Sigma-Aldrich) solution: 1.8 mg of E64 was dissolved in 5.04 mL of ddH₂O. This was then sterile filtered with 0.20 µm sterile filter and aliquoted into 16 Eppendorf tubes with 315 µL each. Stored at -20°C and used within 1 month.

A3.1.8 Giemsa Stain

Giemsa stain (Fluka Analytical) was diluted in dH₂O in a ratio of 1:7.

A3.1.9 Sterilising Reagents

A3.1.9.1 SDS

A 0.1% SDS (Research Organics) solution was prepared in dH₂O and poured into a spray bottle.

A3.1.9.2 Ethanol

70 mL of absolute EtOH (Merck) was added to 30 mL of dH₂O to prepare a 70% EtOH solution for sterilising work surfaces.

A3.2 TEM Reagents

A3.2.1 Buffer

The 0.15 M phosphate buffer pH 7.4 -7.6, was provided by the Laboratory of Microscopy and Microanalysis.

A3.2.2 Fixative

A 2.5 % glutaraldehyde/formaldehyde solution was prepared with 1 mL of 25 % glutaraldehyde, 1 mL of 25% formaldehyde, 5 mL of 0.15 M saline buffer and 3 mL of dH₂O.

A3.2.3 Polymerise

For a 5 g Quetol epoxy resin: 1.94 g of Quetol (SPI-CHEM Suppliers), 2.23 g of nadic methyl anhydride (NMA) (SPI-CHEM Suppliers), 0.83 g dodecenyl succinic anhydride (DDSA) (Agar Scientific) and 0.2 g of RD2 (Agar Scientific) are mixed thoroughly together. Then 0.05 g of S1 (benyldimethylamide) (Agar Scientific) was added and mixed thoroughly for 5 min. Resin solutions were prepared fresh on the day of polymerisation and the remaining resin was discarded.

A3.2.4 Staining Solutions

The 4% aqueous uranyl acetate and Reynold's lead citrate was provided by the Laboratory of Microscopy and Microanalysis.

A3.3 Confocal Microscopy Reagents

A3.3.1 Lysine Coating

A 0.1 mg/mL of poly-L-lysine (Sigma-Aldrich) solution was prepared in 5 mL of PBS. Stored at 4°C and can be reused after coating cover slips.

A3.3.2 Fixing Solution

A 5 mL solution of 0.25% (v/v) formaldehyde was prepared in PBS. Stored at 4°C.

A3.3.3 Buffer

A 50 mL PBS-T solution was prepared using 1 mL of Tween 20 in PBS. Stored at 4°C.

A3.3.4 Blocking Buffer

A 20 mL BSA-PBS-T solution was prepared by adding 200 mg BSA (Chem Cruz Santa Cruz Biotech Inc.) into the PBS-T and mixed well by gentle inversion to avoid foaming. Stored at 4°C.

A3.4 Proteomic Reagents

A3.4.1 SDS-PAGE Buffers

A3.4.1.1 Running Buffer

Dissolved 10 g of SDS, 30 g of Tris (Merck) and 144 g of glycine in 1 L of dH₂O for a 10 X concentrated buffer. For running a gel a 1X concentrated buffer was made by diluting the 10X buffer by 1/10. Stored at RT.

A3.4.1.2 Sample Buffer

For the reducing buffer: 2% SDS, 5% β-mercaptoethanol (Merck), 10% glycerine and 25 mg of bromothymol blue (Protea Lab Services Ltd.) were added to a 62.5 mM Tris buffer at pH 6.8. This made a 2X concentrated sample buffer, which was then added to the protein sample at a ratio of 1:1 [buffer: protein]. Stored at -80°C

Bio-Rad Laemmli buffer was used for non-reduced conditions.

A3.4.1.3 Fixing Solution for Gels

50% MeOH (Merck), 40% dH₂O and 10% Acetic acid (UniLab). Store in an airtight container at RT.

A3.4.1.4 Coomassie Blue Stain

Dissolved 20 mg of Coomassie Blue R250 (Polysciences Inc.) in 20 mL of Fixing solution. Stored at RT.

A3.4.2 Western Blotting Buffers

A3.4.2.1 Tris Base Tween 20 Solution (TBS-T)

For 1 L, 8 g of NaCl (Merck), 0.2 g of KCl (Prolab), 2 mL of Tween 20 and 3 g of Tris base were dissolved in 900 mL of dH₂O. The pH was adjusted to pH 8 with 1 M NaOH (Merck) or 1 M of HCl and made up to 1 L with additional dH₂O. Stored at RT.

A3.4.2.2 PBS Tween 20 Solution (PBS-T)

0.462 g of PBS was dissolved in 50 mL of dH₂O and 0.2% (v/v) of Tween 20 was added. Stored at RT.

A3.4.2.3 BSA Solution

A 2% BSA solution was made by dissolving 0.2 g of BSA in 10 mL of TBS-T or in 10 mL of PBS-T, when indicated in the method. Solution was stored at RT.

A3.4.2.4 Milk Solution

A 2% milk solution was made from dissolving 0.2 g of fat free milk powder in 10 mL of TBS-T. This was made fresh and discarded once used.

A3.4.3 BCA Assay

A3.4.3.1 Reagent A

Dissolved 1 g of Bicinchoninic acid disodium salt hydrate (BCA) (Sigma-Aldrich), 2 g of Na₂CO₃ (Merck), 1.6 g of sodium tartrate, 0.4 g of NaOH and 0.9 g of NaHCO₃ in 100 mL of dH₂O. The pH was adjusted to 11.25 with 10 M NaOH. Stored at 4°C

A3.4.3.2 Reagent B

0.4 g of CuSO₄·5H₂O (Rochelle Chemicals) was dissolved in 10 mL of dH₂O. Solutions were stored at 4°C.

A3.4.3.3 Working Solution

Mixed Reagent A with Reagent B a ratio of 50: 1 [Reagent A: Reagent B]. Solutions were stored at 4°C and stable for 1 week.

A3.4.3.4 Albumin Standards

Standards were made from 15 mg of BSA dissolved in 3 mL of dH₂O. The following concentrations were used for the BCA protein assay: 5 mg/mL, 4 mg/mL, 2.5 mg/mL, 1 mg/mL, 0.5 mg/mL, 0.4 mg/mL, 0.25 mg/mL, 0.2 mg/mL (http://web.stanford.edu/~quanw/teaching/chem184/pdf/LabManual/Appendix_4_BCA_assay.pdf). Linearity was achieved with an r^2 value of ~0.97. Standards were stored at -80°C.

A3.4.4 In-Gel Digestion Solutions

A 50 mL solution of 50 mM NH₄CO₃ (Sigma-Aldrich) in MS-H₂O (Sigma-Aldrich) was prepared with 0.2 g NH₄CO₃. The pH was measured between 7.5 and 8.5. Stored at 4°C and used within 2 weeks.

A 50 mL solution of 50 mM NH₄CO₃ in 50% MeOH (Fluka Analytical) was prepared with 0.2 g NH₄CO₃ dissolved in 25 mL of MS-H₂O and 25 mL of 100% MeOH added. Stored at 4°C and used within 2 weeks.

A 2 mL solution of 25 mM NH₄CO₃ in 50% ACN (Fluka Analytical) was prepared from 1000 µL of 50 mM NH₄CO₃ in MS-H₂O and 1000 µL of 100% ACN. Stored at 4°C and used within 2 weeks.

A 10 mL solution of 75% ACN was prepared from 7.5 mL of 100% ACN made up to 10 mL with MS- H₂O. Stored at 4°C.

The trypsin stock solution was prepared from the Promega kit, on ice, by adding 200 µL of the supplied buffer to one vial containing 20 µg of trypsin. This was vortex mixed and 20 µL aliquots in 0.5 mL microcentrifuge vials were prepared. Aliquots were stored at -20°C.

A 10 ng/µL trypsin solution was prepared fresh by diluting 20 µL of the stock trypsin in 90 µL of 50 mM NH₄CO₃ in MS-H₂O and 90 µL of MS-H₂O.

A 1 mL solution of 1M DTT (Fermentas) was prepared fresh from 0.154 g of DTT dissolved in 1000 µL of MS-H₂O.

A 1 mL solution of 10 mM DTT (Amresco) in 25 mM NH₄CO₃ was prepared from 10 µL of the 1 M DTT stock solution diluted in 495 µL of 50 mM NH₄CO₃ and 495 µL of MS-H₂O.

A 1 mL solution of 55 mM IAA (Sigma-Aldrich) in 25 mM NH₄CO₃ was prepared from 10.2 mg of IAA dissolved in 500 µL of 50 mM NH₄CO₃ and 500 µL of MS-H₂O.

A3.4.5 In-solution Digestion Solutions

A 50 mL solution of 50 mM NH₄HCO₃ was prepared by dissolving 0.197 g of NH₄HCO₃ in MS-H₂O. Stored at 4°C and used within 2 weeks.

A 4 mL solution of 100 mM NH_4HCO_3 was prepared by dissolving 32 mg of NH_4HCO_3 in MS- H_2O . Stored at 4°C and used within 2 weeks.

A 5 mL solution of 5 M Urea (Merck) was prepared by dissolving 1.5 g Urea in 50 mM NH_4HCO_3 . Stored at 4°C and used within 2 weeks.

A 2 mL solution of 8 M Urea was prepared by dissolving 0.96 g Urea in 100 mM NH_4HCO_3 . Stored at 4°C and used within 2 weeks.

A 250 μL solution of 0.2 M DTT was freshly prepared by dissolving 7.8 mg DTT in 50 mM NH_4HCO_3 .

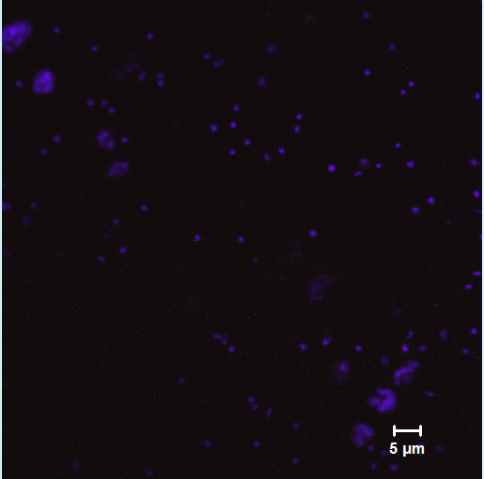
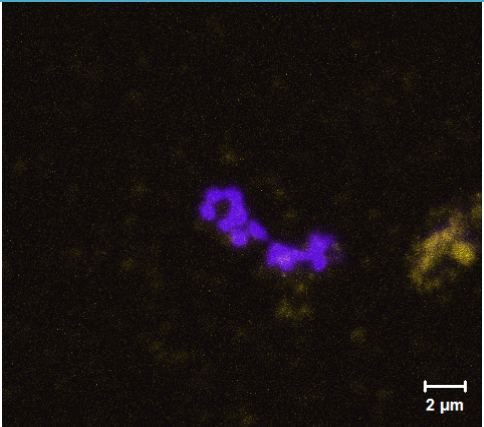
A 250 μL solution of 0.5 M IAA was freshly prepared in 50 mM NH_4HCO_3 .

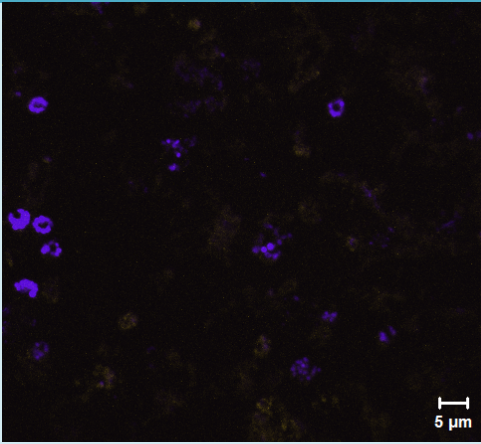
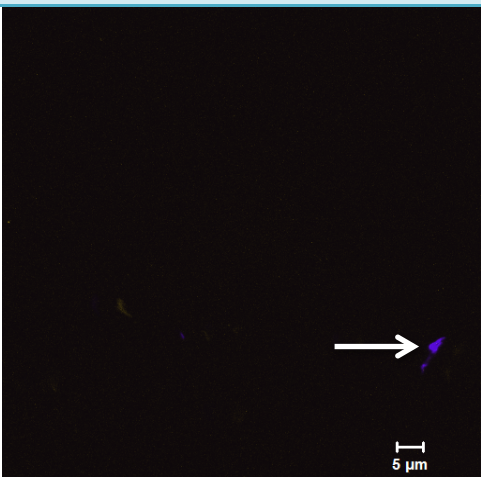
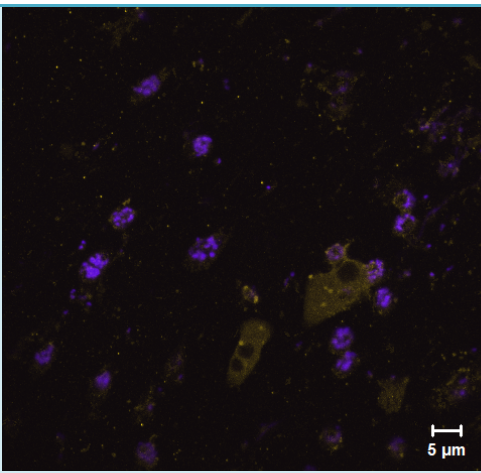
A 10 ng/ μL trypsin solution was prepared fresh by diluting 20 μL of the stock trypsin in 90 μL of 50 mM NH_4CO_3 in MS- H_2O and 90 μL of MS- H_2O .

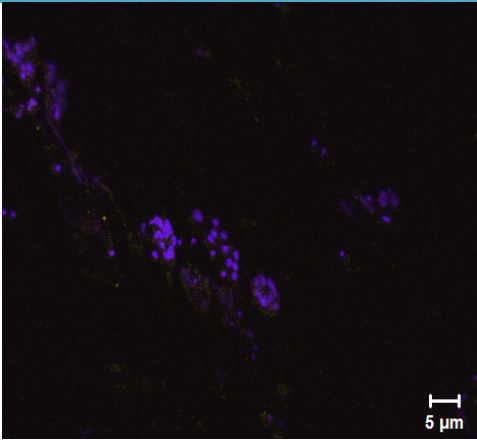
Appendix IV

Summary of Confocal Microscopy Methods

Table A1 Summary of Fixing and Blocking Methods for Confocal Microscopy

Fixative	Blocking Agent	Antibody Dilution	Results
0.25% Formaldehyde	1% BSA and 3% Human Serum	1:400 ^a	 <p>Overlay: Free mz and mz within schizont. No <i>Pf</i>AMA-1 visible.</p>
0.25% Formaldehyde	3% BSA	1:400 ^a	 <p>Overlay: Mz being released from schizont. Aggregation of Cy3-<i>Pf</i>AMA-1 dye. No co-localisation of <i>Pf</i>AMA-1.</p>

<p>0.25% Formaldehyde</p>	<p>1% Milk in PBS-T</p>	<p>1:400^a</p>	 <p>Overlay: Free mz and mz within schizonts. No <i>Pf</i>AMA-1 visible.</p>
<p>0.25% Formaldehyde</p>	<p>3% Human Serum</p>	<p>1:400^a</p>	 <p>Overlay: Free mz visible (white arrow). No <i>Pf</i>AMA-1 visible.</p>
<p>100% MeOH</p>	<p>3% Human Serum</p>	<p>1:400^a</p>	 <p>Overlay: Free mz and mz within schizonts. Aggregation of Cy3-<i>Pf</i>AMA-1 dye. No <i>Pf</i>AMA-1 visible.</p>

70% EtOH	3% Human Serum	1:400 ^a	 <p data-bbox="884 663 1362 775">Overlay: Free mZ and mZ within a schizont. No co-localisation of <i>PfAMA-1</i>.</p>
a) This is a dilution of the <i>PfAMA-1</i> antibody stock.			

Summary of *Plasmodium falciparum* Proteins

Table A2 Examples of Types of Proteins Identified

Type of Protein	Name of Protein
DNA and RNA associated	Histone (Pf3D7_1105000)
	tRNA (Pf3D7_1213800)
	Translation factor (Pf3D7_1410600)
	Helicase (Pf3D7_0320800)
Structural/cytoskeleton	Ribosomal (Pf3D7_0517000)
	Heat shock (Pf3D7_0917900)
	Actin (Pf3D7_1246200)
	Myosin (Pf3D7_1342600)
Transport	Karyopherin beta (Pf3D7_0524000)
	GTP-binding nuclear protein (Pf3D7_1117700)
Signalling	cAMP (Pf3D7_1223100)



	Calcium dependent protein kinase (Pf3D7_0217500)
	Casein kinase (Pf3D7_1136500)
Enzymes	Transketolase (Pf3D7_0610800)
	Dehydrogenase (Pf3D7_1216200)
	Inositol-3-phosphate synthase (Pf3D7_0511800)
PFV membrane	Exported protein 2 (Pf3D7_1471100)
	Skeleton binding protein (Pf3D7_0501300)
Erythrocyte adhesion proteins	CLAG 3 (Pf3D7_0302500)
	CLAG 9 (Pf3D7_0935800)
	RESA (Pf3D7_1149200)